Department of Applied Geology

Environmental Impact of Storage of Lignite and Black Shale Waste Rocks at South Jimblebar Iron Ore Mine, Western Australia

Andi Muhammad Fajrin

This thesis is presented for the Degree of
Master of Philosophy
of
Curtin University

April 2013

Declaration

This thesis contains no material which has been accepted for the award of any other degree or diploma in any university, and to the best of my knowledge and belief this thesis contains no material previously published by any other person except where due acknowledgment has been made.

Signature: ……..

Date: ……...

ABSTRACT

Exploitation of iron ore deposits at the proposed South Jimblebar mine will involve excavation of overburden and its subsequent storage in waste rock piles. Of particular interest at the South Jimblebar prospect are significant deposits of lignite, which have not been encountered at other iron ore mines in the Pilbara region of Western Australia. Additional waste rock will be generated from lithologies associated with the Banded Iron Formation (BIF) ore and sub-grade iron ore.

This study assessed the geochemical characteristics of the prospective waste rock types with regards to their capacity to generate acid mine drainage (AMD) and release potentially toxic elements to the broad environment. A total of 144 selected samples of various lithology and stratigraphic position were subjected to acid base accounting (ABA) and net acid generation (NAG) testing, as well as multi-element geochemical analysis. Results of testing and analyses indicated that non-carbonaceous mudstones were likely to be non-acid forming (NAF) material and indicated a high acid neutralizing capacity (ANC) of micritic calcareous mudstone units in the upper part of a Cenozoic sequence (CzD 2 unit).

The potentially acid forming (PAF) condition was identified in carbonaceous rocks of two different lithologies, namely lignite and black shale. The lignite occurs within the Tertiary detrital unit of the CzD 2 unit, while the black shale is interbedded with iron stone formations within the Proterozoic Namuldi Member (MU) of the Marra Mamba Formation and the Undifferentiated Jeerinah Formation. Lignite sampled from 4 of 7 available exploration cores showed low ANC (<10 kg H_2SO_4/t). Sulphur content was highly variable up to 35.1 wt % reflecting irregular distribution of pyrite mineralisation. Twenty eight percent (8 of 29) of the lignite samples investigated could be categorised as highly potentially acid forming (PAF) with net acid producing potential (NAPP) up to 941 kg H_2SO_4/t. They also showed enrichment in a number of elements of environmental significance, such as As, Be, Co, Mo, Se, Sb, and Tl, when compared to the median soil abundance.

Black shale of the Namuldi Member was moderately sulphur enriched, averaging 1.02 wt %. However, the unit also contains carbonate minerals resulting in moderate average ANC of 23.8 kg H_2SO_4/t. The balance of acid and neutralizing minerals in the 39 samples resulted in an equal number categorised as PAF and NAF. Overall they may be considered as PAF low capacity (NAPP 5.98 kg H_2SO_4/t in

average). The lowest unit at South Jimblebar, the Undifferentiated Jeerinah Formation, indicated high sulphur content (3.04 wt%) and negligible ANC, and therefore yielded appreciable PAF capacity with average NAPP of 88.9 kg H_2SO_4/t. Potentially toxic elements, As, Cd, Se, Tl and Zn, were significantly enriched in the black shale samples.

These findings clearly indicate potential for AMD generation during long-term storage of waste rocks at the South Jimblebar mine. Overall scale of possible acid generation, and acid neutralisation, will depend upon the volumes of the various lithologies reporting to the waste rock piles, and was beyond the scope of the present study. Specific waste rock management protocols are likely to be required, including selective handling of PAF material and engineered cover systems for waste rock piles containing lignite and black shale.

ACKNOWLEDGEMENT

One of the joys in completing this thesis is being able to look back over the journey past and remember all the friends and family who have helped and supported me along this long but fulfilling road.

First and foremost, I would like to express my great appreciation to my beloved Dad and Mum for their endless love and sincere prayers. My family have been a source of support and encouragement throughout the years that I devoted to this study.

My highest gratitude goes to my supervisor, Assoc. Prof. Ronald T. Watkins who is not only a mentor but a dear friend. I could not have asked for a better role model and I thank him for being helpful, kind, inspirational, supportive, and patient throughout my studies. I could not be prouder of what I have achieved in completing my masters of philosophy degree, and hope that I can pass on the research values and the dreams that he has instilled in me. Also, I would especially like to thank Deborah Watkins for providing unwavering support during my studies. I came from Indonesia alone, but Ron and Deborah welcomed me warmly and have treated like family.

It is with immense gratitude that I acknowledge the support and help of Eric Perry, Ph.D. His expertise and guidance have expanded my knowledge on environmental geochemistry exponentially. I especially thank him for his recommendation in receiving the CIPRS scholarship and his review of this thesis.

I would also like to express my gratitude to Richard Marton and Joanne Heyes from BHP Billiton Iron Ore for providing technical assistance and related data from the South Jimblebar Iron Ore Mine. This thesis has benefited greatly through earnest discussions of the geology of the Pilbara area with Richard Morris, Mal Kneeshaw and Eric Ramanaidou and general chemistry with Dr. Tutun Nugraha. These contributions are gratefully appreciated. I would also like to thank Alex Solomon for his indispensible help in reviewing the grammar in this thesis.

The informal support and encouragement of many friends has been invaluable, and I would like particularly to acknowledge the contribution of EIGG Group Members.

This research was funded by Curtin International Postgraduate Research Scholarship (CIPRS) in collaboration with BHP Billiton Iron Ore, and I would like to acknowledge both organisations for their generous support.

TABLE OF CONTENTS

LIST OF FIGURES

Chapter 1

Chapter 2

Chapter 3

Chapter 4

LIST OF TABLES

Chapter 1

Chapter 2

Chapter 3

Chapter 4

LIST OF APPENDICES

Appendix A

Appendix B

Appendix C

Appendix D

GLOSSARY

The major acronyms and specialized terms used in this thesis are explained below. Further explanation many of the terms is given in the body of the thesis where they are first introduced. The main rock types encountered in this study are also defined.

ABA	Acid base accounting (ABA) involves static laboratory procedures that evaluate the balance between acid generation and acid neutralizing process, of which NAPP is an example
AMD	Acid mine drainage
ANC Test	Acid neutralizing capacity (ANC) test quantifies the inherent acid buffering/ neutralizing potential of the rock sample. The ANC is determined by acid digestion and back titration with NaOH and expressed in kg H_2SO_4/t.
BHPBIO	BHP Billiton Iron Ore (BHPBIO), owner and operator of the South Jimblebar prospective iron ore mine, location of this study.
BIF	Banded Iron Formation (BIF) is a lithology consisting of alternation of bands composed of chert and hematite
Black Shale	The term of black shale in this case covering the carbonaceous rock lithology with fine to very fine-grained texture containing organic carbon >1 wt % and indicating dark grey to blackish colour.
GAI	Geochemical abundance index (GAI) is a numerical enrichment value of an element in a rock sample. The GAI is presented in log 2 value of comparison between measured concentrations of an element in a rock sample with referenced standard value (in this case median soil abundance by Bowen, 1979).
Lignite	The term lignite employed in this study is according to the BHPBIO usage covering a wide range of lithology comprising very fine grained mudstone containing various percentages of maceral.

MPA	Maximum potential acidity (MPA) is an estimation value of the rock to generate acid due to oxidation of its sulphide contents. The MPA value is calculated by multiplying sulphide-sulphur by 30.6 (stoichiometric value for the oxidation reaction of pyrite, FeS_2 by O_2) and reported in kg H_2SO_4/t.
Mudstone	The term of mudstone in this study broadly involve non-carbonaceous rock lithology including oxidized iron-rich shale and calcareous mudstone.
Modified ANC Test	An ANC test developed by Stewart (2005) to account for siderite effects.
NAF	Non-acid forming classification
NAG Test	Net acid generation (NAG) test is an empirical measure of the magnitude of the potential acidity that may be produced by the rock. The test involves reaction of a rock sample with a strong oxidizing agent, hydrogen peroxide (H_2O_2), to accelerate oxidation of sulphide mineral contents.
NAG pH	pH of NAG solution at room temperature after application of the standard heating step and before titration.
NAG Acidity	The quantity of acid in the final solution of the NAG test reported in kg H_2SO_4/t. The amount of acid remaining at the end of the NAG test is empirically equivalent to the total acid generated minus the acid neutralizing capacity.
NAPP	Net acid producing potential (NAPP) is the balance between acid and neutralizing capacity of the rock sample calculated by difference: MPA – ANC and reported in kg H_2SO_4/t.
Organic acid	Acidity release to a NAG solution that is due to partial oxidation of organic matter by hydrogen peroxide (H_2O_2). This organic acid can cause overestimation of NAG acidity value that are unrelated to acid mine drainage potential.
PAF	Potentially acid forming classification

Paste pH	pH of a sample slurry with a solid to water ratio of 1:2 (w/w) that can be used to indicate the inherent acidity of the rock sample.
Potentially toxic elements	Metals and metalloids categorized as potentially toxic to life form when available in elevated concentration beyond background (threshold) range or maximum permissible limit (Bhat and Khan, 2011). This term also apply for "heavy metal" definition as usage in this thesis.
Siderite	Iron (II) carbonate ($FeCO_3$) mineral where its present in a rock sample potentially rises misleadingly high neutralizing capacity value in the typical duration of standard ANC test
Sulphate-sulphur (SO_4-S)	Sulphate content (wt %) in the rock sample is determined as "readily water soluble sulphate" by extraction of powdered sample in de-ionized, de-oxygenated water at a ratio 1:20.
Sulphide-sulphur (S_2-S)	Sulphide-sulphur (wt %) is calculated by subtracting the measured sulphate-sulphur from total sulphur measurement.
Total carbon	Total carbon content of the rock sample (wt %) is measured using LECO combustion analysis.
Total sulphur	Total sulphur content of the rock sample (wt %) is measured using LECO combustion analysis.

1. INTRODUCTION

1.1. Background to Study

BHP Billiton Iron Ore (BHPBIO) proposes the development of a new iron ore mine at the South Jimblebar site in the Pilbara region of Western Australia, as phase 2 of the Jimblebar Iron Ore Project. This development of a large-scale open pit mine will increase the installed ore production from the Jimblebar area from approximately 45 million tonnes per annum (Mtpa) to 75 Mtpa (SKM, 2009). Extraction of the mineral target from the South Jimblebar prospect involves the excavation of significant quantities of Tertiary lignite and Archean black shale. Whereas the storage of low-grade ironstone and associated siliclastic rock wastes normally poses little or no appreciable risk of pollution to the local groundwater and the broader environment, interbedded black shale units frequently cause environmental problems due to the oxidation of contained sulphide minerals, giving rise to the generation of acid mine drainage (AMD).

Tertiary lignite (young, immature, low rank coal) is not widely encountered in iron ore mining in the Pilbara region, but may pose similar risks of AMD formation if it contains pyrite or other metal sulphide minerals. Heavy metals, such as Hg and Cd, and metalloids (As and Se) may be associated with the sulphide and organic matter, and are thus potential components of leachate formation when the waste is stored in sub-aerial waste rock piles. As the occurrence of lignite in the Pilbara area is unusual, its geochemical characteristics, in particular its influence on the environment during long-term storage, are not well understood.

Groundwater investigations at the South Jimblebar prospect have identified two types of aquifer, namely the unconsolidated sedimentary aquifer of the Tertiary detrital unit and the fractured rock aquifer of the Marra Mamba Formation. Both aquifers were reported to be alkaline (Garnett and Bolton, 2004). However, the Tertiary detrital aquifer lies in the upper part of the detrital unit comprising gravel and carbonate mudstones that contribute to the alkalinity of the groundwater. Lignite bearing clay within the lower part of the Tertiary detrital sequence is of low permeability (Garnett and Bolton, 2004), and therefore may have very limited influence on the groundwater composition. Thus, the current groundwater quality

data may not reflect the interaction between the groundwater and lignite unit, which has the potential to give rise to acidity.

It is vital that the geochemical nature of the lignite and black shales, their capacity to release acid and metal laden drainage during weathering, be fully determined during the early stage of mine planning. In addition, for comprehensive environmental impact assessment, it is necessary to examine the geochemical characteristics of other rock types from various units in the South Jimblebar stratigraphy. This information will be important in the timely implementation of mine waste management to avoid any environmental risk related to acid mine drainage formation and metal/metalloid pollution.

1.2. Purpose and Significance of Study

This research project assesses the potential environmental impact of future storage of waste rock at the South Jimblebar mine. The current study will focus primarily on two waste rock types: lignite and carbonaceous ("black") shale, with the aim of:

- quantifying the overall acid generating potential of each rock type in order to predict the possible extent of future acid mine drainage production; and
- geochemically characterising each of the rock types with respect to their content of metals and metalloids (e.g. As, Se) of environmental importance.

The geochemical characterization of the prospective mine site is a fundamental aspect considered in mine planning and operation in order to minimize and mitigate the negative impacts of mining activities on the environment. The outcomes of this study provide baseline information regarding the geochemical nature of future waste rock at the South Jimblebar mine, including new knowledge of the geochemical characteristics of rare lignite encountered in the Jimblebar area.

1.3. Location of Study Area

The prospective South Jimblebar iron ore mine is a part of BHPBIO's Jimblebar Iron Ore Project in the Pilbara region of Western Australia. The site is located at 23° 21. 7 S, 119° 44.8 E, approximately 40 km east of the town of Newman, and 1,100 km north of Perth (Figure 1.1).

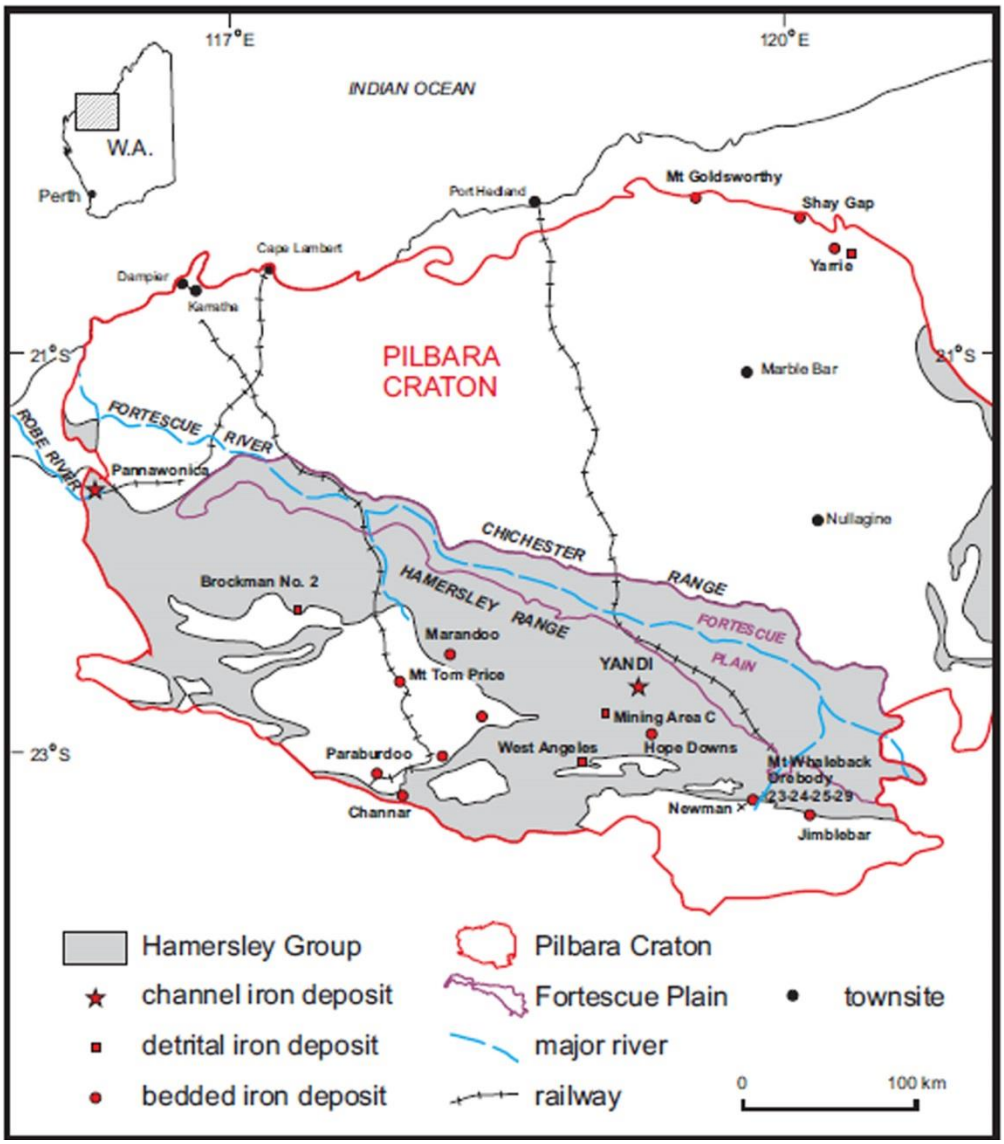

Figure 1.1. Location of Jimblebar Iron Ore Project in the Southeast of the Pilbara region adapted from Stone (2004). The map also showing the distribution of channel, detrital, and banded iron deposits in the region

1.4. Climate

Climate has a major influence on the water quality in the prospective mine area. Climatic factors, such as temperature and precipitation, are key variables determining the reaction kinetics of waste rock weathering and the distribution of mobilized geochemical contaminants.

The Pilbara region is characterized by an arid subtropical climate resulting from the influence of two air masses, namely the Indian tropical maritime air mass moving in from the west or north-west, and the tropical continental air from inland Australia (ANRA, 2012). Climatic data from South Jimblebar was obtained from the

decommissioned Newman climate station (site number 007151) that recorded data during the period of 1965 to 2003 (Table 1.1 and 1.2 (Bureau of Meteorology, 2012).

Table 1.1. Average monthly temperatures 1965-2003 of Jimblebar area

Average (°C)	Jan	Feb	Mar	Apr	May	Jun	Jul	Aug	Sept	Oct	Nov	Dec
Maximum	39	37.2	35.8	31.6	26	22.4	22.3	24.8	29.2	33.6	36.6	38.3
Minimum	25.3	24.4	22.4	18.4	13	9.6	8.1	10.1	13.7	17.9	21.4	23.9

Table 1.2. Average monthly rainfall and evaporation 1965-2003 of Jimblebar area

Average (mm)	Jan	Feb	Mar	Apr	May	Jun	Jul	Aug	Sep	Oct	Nov	Dec
Rainfall	51.4	80.1	38.6	25.3	23.2	25	12.6	10.5	4.1	3.9	9.8	27
Evaporation	461	369	343	290	174	173	199	193	264	377	424	466

Table 1.1 indicates that Newman experiences a very hot summer season, with average maximum temperatures exceeding 30°C from October through to April, while experiencing milder winter temperatures, with average minimum temperatures below 15°C from May to September. According to data presented in Table 1.2, the Pilbara region has low precipitation and high evaporation rates, with an average annual value of 26.0 mm and 311 mm, respectively. Owing to the occurrence of tropical cyclones, the region receives maximum rainfall during the late summer (January to March) of up to 80.1 mm. For example, Johnson and Wright (2001) reported cyclone Joan in 1975 produced up to 600 mm of rainfall during its passage over the region. Consequently, the regional precipitation is characterized by fluctuation between summer and winter, and also occasional extreme rainfall events. Such a pattern potentially both accelerates rock weathering and provides rapid transport of dissolved weathering products into the broader environment.

1.5. Geological Background

1.5.1. Regional Geology of the Pilbara

The Hamersley Province is an area of about 80,000 km^2 covering the southern half of the Pilbara Craton of Western Australia (Morris and Kneeshaw,

2011). It contains late Archean to early Proterozoic age (2800-2300 Ma) meta-sedimentary rocks of the Mount Bruce Supergroup which lie unconformably on the mid-Archean granitoid and greenstone cratonic basement (Fig. 1.2) (Pickard, Barley and Krapež, 2004; Kneeshaw 2008).

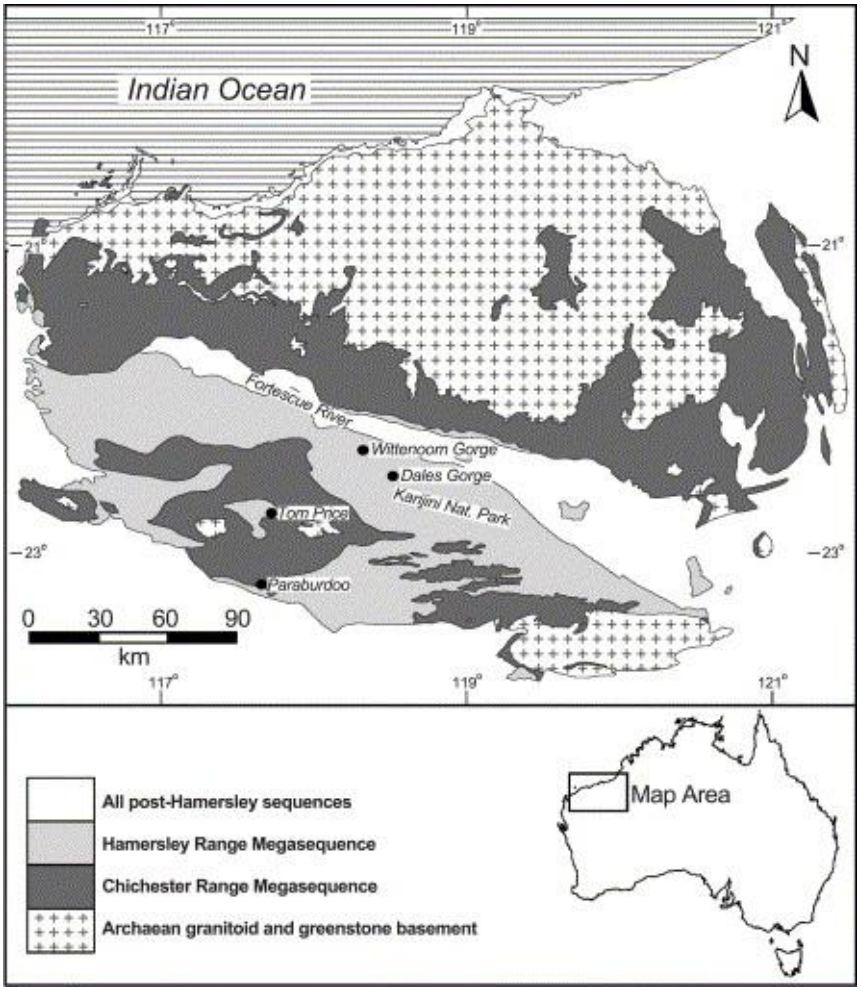

Figure 1.2. Geological map of the Hamersley Province (adapted from Pickard *et al*., 2004)

The Mount Bruce Supergroup is a platformal cover sequence of weakly metamorphosed (mainly prehnite-pumpellyite to lower greenschist facies) sedimentary and volcanic rocks. Within the Supergroup are three sub-groups: the basal Fortescue Group, the overlying Banded Iron Formation (BIF)-rich Hamersley Group, and the southern remnant of the uppermost Turee Creek Group (Morris and Kneeshaw, 2011).

Of the three groups, the Hamersley Group is the most relevant to the present study. It is a 2.5 km thick sequence of dominantly deep water chemical sediments, with subordinate turbiditic sediments and various intrusive and extrusive igneous

rocks. It is regionally conformable with both the underlying Fortescue Group and overlying Turee Creek Group. The sedimentary units include, in approximate order of decreasing abundance, BIF, hemi-pelagic shale, dolomite derived from peri-platformal ooze, chert, pyroclastic shale and tuff, turbiditic carbonate and turbiditic volcanic sediments. Figure 1.3 shows the regional stratigraphy of the Hamersley Group. The enriched iron ore deposits forming the exploitable iron ore reserves generally occur within the Brockman and Marra Mamba Iron Formations (Kneeshaw, 2008; BHPBIO, 2011).

1.5.2. Local Geology of South Jimblebar

The Jimblebar Iron Ore Project involves both the Brockman Iron Formation and Marra Mamba Iron Formation. BHPBIO divides the operational mine area into three mine blocks that are Wheelarra Hill, Hashimoto, and South Jimblebar block.

Wheelarra Hill and Hashimoto blocks contain the Brockman Iron Formation, while the South Jimblebar block targets the Marra Mamba Iron Formation (BHPBIO, 2009). Wheelarra Hill is an operating open-pit mine at Jimblebar, while Hashimoto and South Jimblebar sites are planned to be exploited in the financial year 2014 (BHPBIO, personal communication, August 17, 2012). A project overview at full development indicating the open pit and waste rock pile is presented in Figure 1.4.

The focus of the present study is the geochemical characterization of potential waste rock from mining of the South Jimblebar block. Based on core log and nomenclature provided by BHPBIO, the rock succession at South Jimblebar consists of conformable sequences of the following:

1. Tertiary Detritus
2. Lower members of the Wittenoom Formation
    - Paraburdoo Member
    - West Angela Member
3. All members of the Marra Mamba Formation
    - Mount Newman Member
    - MacLeod Member
    - Nammuldi Member
4. Undifferentiated Jeerinah Formation, Fortescue Group.

Extended periods of erosion have incised deep valleys into the Archean and Proterozoic basement rocks, which have subsequently been infilled with Tertiary aged sediments formed during periods of fluvial and lacustrine sedimentation. The resulting discontinuous Tertiary detrital sequences occupy the palaeovalley between Wheelarra Hill in the north and the South Jimblebar site in the south, largely overlying the lower member of the Wittenoom Formation. Figure 1.5 shows the schematic geological setting through the Jimblebar Iron Ore Project area.

Transported Tertiary detrital rocks at South Jimblebar are recognized in three different stratigraphic units, from the base upwards as follows (BHPBIO, 2011):

- Tertiary Detrital 1 (TD 1), characterized by red haematitic silt with clay matrix, known as "red ochre detritus". These materials are derived from rock weathering of Marra Mamba Iron Formation.
- Tertiary Detrital 2 (TD 2), characterized by bleached and mottled clays and micritic limestone. Lignitic claystone (clay containing fragmented lignite macerals) is also typically present at the base of TD 2 and has associated pyrite mineralization.
- Tertiary Detrital 3 (TD 3), characterized by fine grained alluvium and colluvium with elevated TiO_2 and Al_2O_3. These materials are the youngest debris eroded from outcrops on both sides of the palaeovalley.

It can be seen from Fig. 1.4 that the South Jimblebar mine will be developed as two elongate (E-W) open cast pits with combined length of around 15 km, while waste rock will be stored in three separate overburden storage areas (OSA).

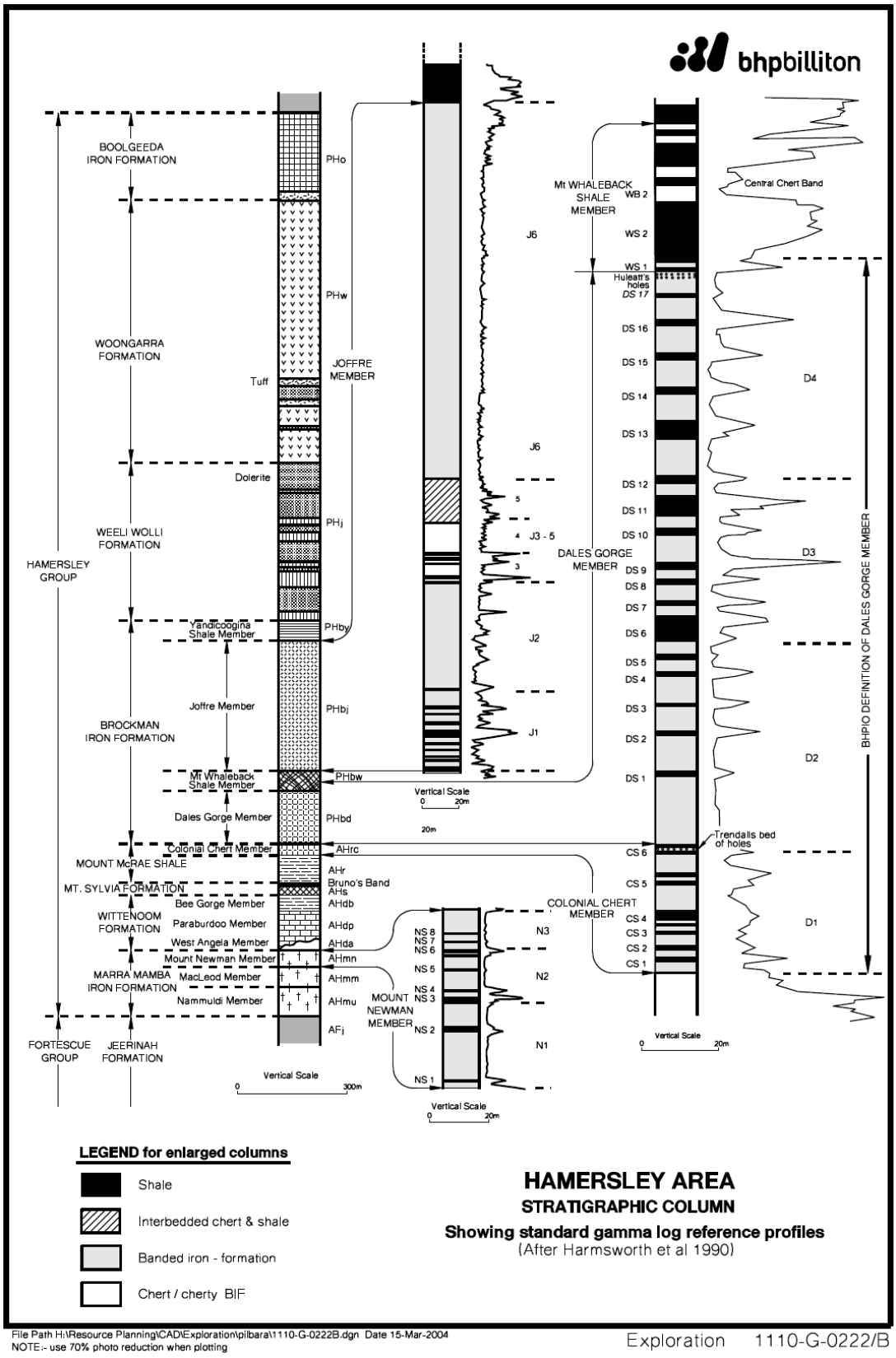

Figure 1.3. Stratigraphic column of the Hamersley Province (adapted from BHPBIO, 2011 after Harmsworth *et al*., 1990)

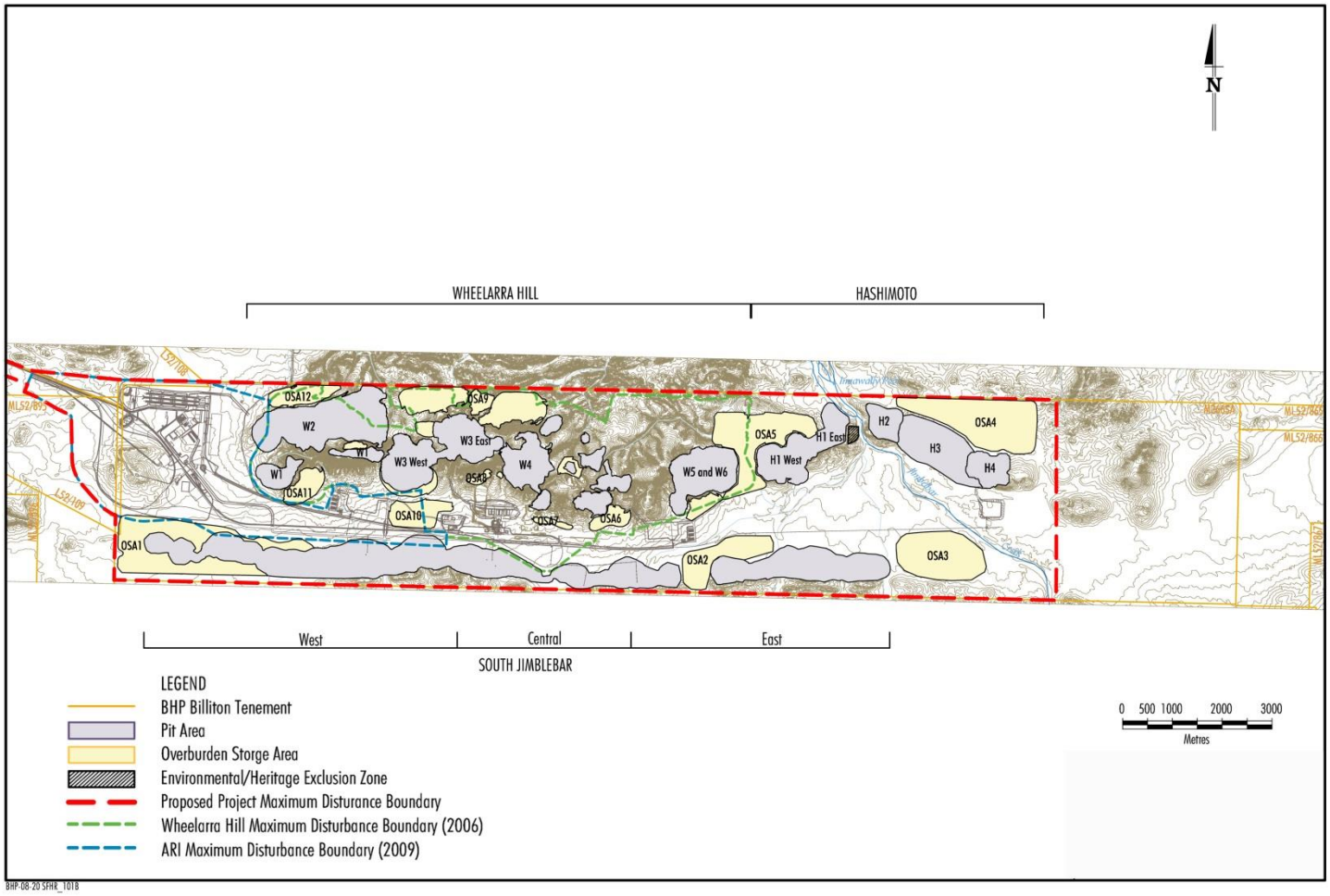

Figure 1.4. Proposed mine development areas and waste rock piles at the Jimblebar Iron Ore Project (adapted from BHPBIO, 2009).

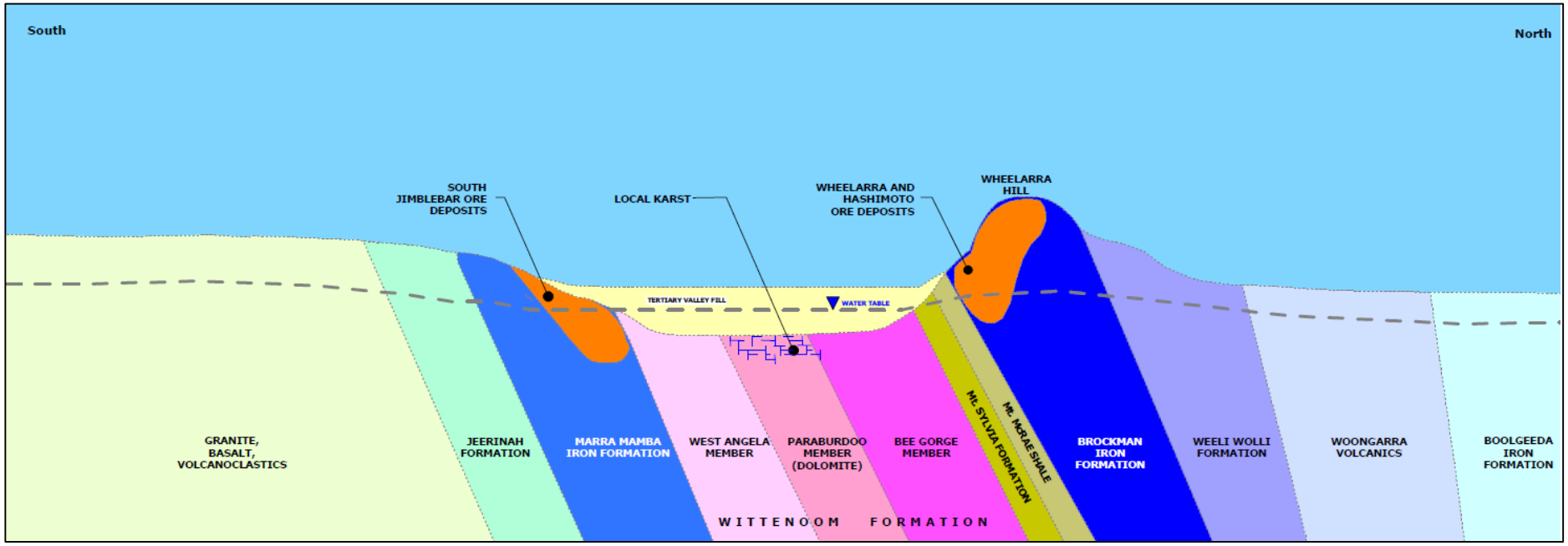

Figure 1.5. Schematic geological section through the BHPBIO's Iron Ore Jimblebar Project (adapted from Strong and Hall, 2009)

1.5.3. Hydrogeology

Groundwater constrains the depth of the oxidized zone. Through water-rock interaction, the rock sequence above the water table is usually more weathered and leached than rock in the saturated zone below. Groundwater investigation by Johnson and Wright (2001) identified three major aquifer groups in the Central Pilbara as summarized in Table 1.3.

Table 1.3. Summary of prospective aquifer in the Central Pilbara

Aquifer Type	Aquifer	Geological Unit	Saturated thickness (m)	Bore yield (kL/day)	Aquifer Potential
Unconsolidated Sedimentary aquifer	Valley fill	Alluvium	15	<1000	Major
		Colluvium	30	<1500	Major
Chemically deposited aquifer	Calcrete	Calcrete	15	5000	Major
	Pisolitic limonite	Robe Pisolite	10	1500	Major
Fractured-rock aquifer	Fracture sedimentary	Hamersley Basin			
	BIF	Brockman Iron Formation	20	<500	Local
		Marra Mamba Iron Formation			
	Dolomitic	Wittenoom Dolomite	25	2000	Major
	Sandstone	Hardey Sandstone	30	<250	Local

Specifically, Strong and Hall (2009) reported two aquifers at South Jimblebar: an unconsolidated-sedimentary aquifer and a fracture-BIF rock aquifer. The former comprises a valley fill sequence developed in the broad Copper Creek palaeo-valley between Wheelarra Hill and South Jimblebar with a range in depth from 82 m to 162 m. Groundwater contained in the palaeovalley fill sediment is associated with primary permeability and porosity within deep alluvial and colluvial deposits, and with secondary weathering-induced permeability in calcrete horizons. The deeper aquifer in banded iron formation (BIF) is typically associated with fractures and ore mineralization (Johnson and Wright, 2001). At South Jimblebar, the mineralized Marra Mamba Formation provides an elongated east to west trending aquifer system which forms the southern margin of the Copper Creek valley. This aquifer is largely continuous over its 15 km strike length, although the base of the ore body (and thus the saturated thickness of the aquifer) varies along strike (Strong

and Hall, 2009). The upper sedimentary aquifer is recharged by infiltration of rainfall and run-off and the deeper fractured-rock aquifer by subsequent vertical infiltration.

There is some hydraulic connection between the fractured-aquifer of the Marra Mamba Formation and the Paraburdoo Member dolomite via faults. The connections also occur in areas where significant mineralization extends through the West Angela Member and to the valley fill sediments where the valley has eroded into the ore body (Fig. 1.6) (BHPBIO, 2009). The similarity of water quality, characterized by alkaline pH of the groundwater, found in the Marra Mamba Formation, Paraburdoo Member dolomite and Tertiary valley fill sediment suggests a degree of hydraulic connection (Strong and Hall, 2009).

The water table at the South Jimblebar mine is on average approximately 70 m below the topographical surface as reported by BHPBIO (2011). It appears deeper to the south of the deposit with raised topography, in comparison to a shallower profile on the northern side of the deposit where the topography is relatively flat. Approximately 53 % of the resource estimate of iron ore at South Jimblebar is located below the water table.

1.6.Previous Work

1.6.1. Occurrence of Lignite in the Pilbara Region

Fragments of carbonaceous fossilized wood have been identified in the Cenozoic Detrital (CzD) 2 unit associated with the channel iron deposit (CID) in the Pilbara Region. CID deposition occurs extensively in both upland-fluvial (e.g. Yandi CID mine, Marillana Formation) and lowland-estuarine (Robe Formation) environments (Ramanaidou, Morris, and Horwitz, 2003; Kneeshaw, 2008). In contrast to the CzD 2 sequence, such preserved wood is very sparingly present in the earlier (CzD 1) and later detrital (CzD 3) units as reported by Morris (1994).

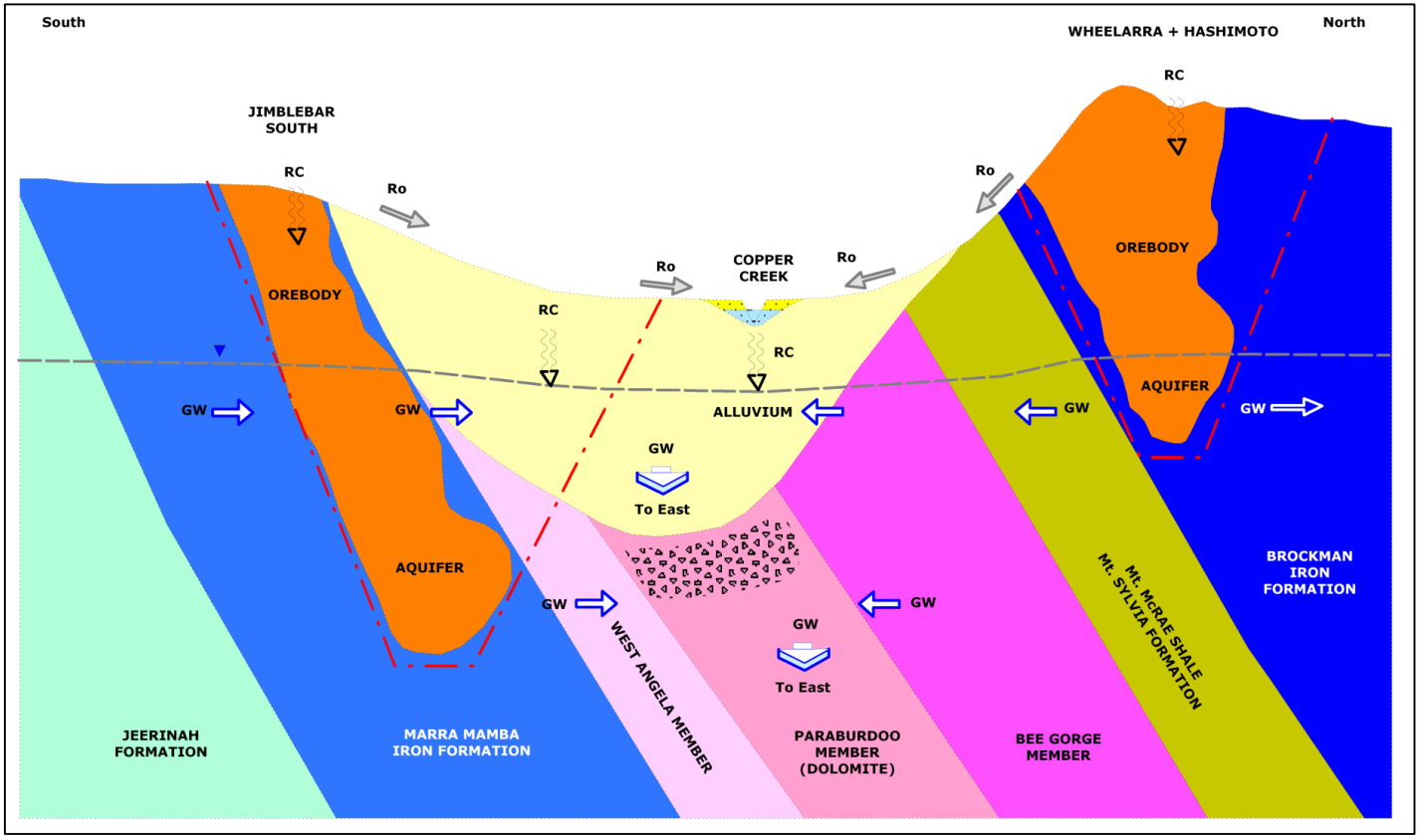

Figure 1.6.a. Schematic diagram of north to south cross section of the hydrogeological model, South Jimblebar (GW: ground water; RO: runoff; RC: recharge) (adapted from Strong and Hall, 2009)

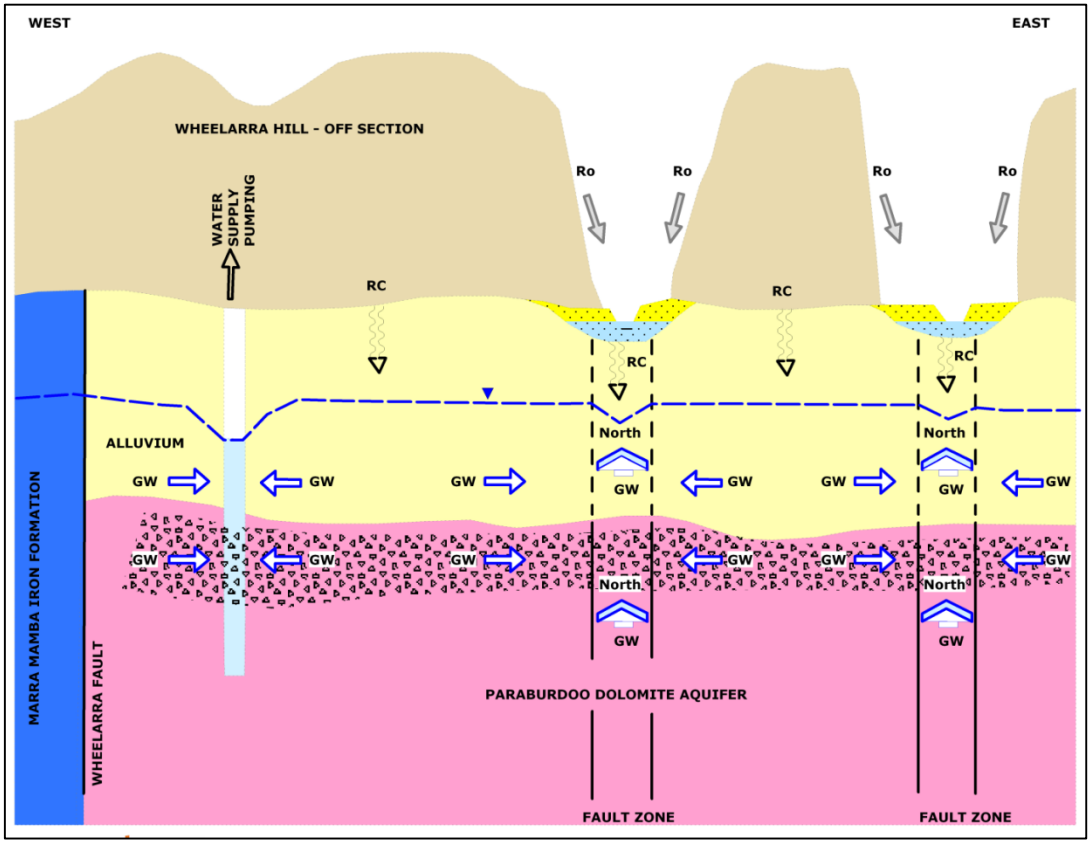

Figure 1.6.b. Schematic diagram of east to west cross section of the hydrogeological Model, South Jimblebar (GW: Ground water; RO: Runoff; RC: Recharge) (adapted from Strong and Hall, 2009)

Note that the term “Cenozoic Detrital” is employed by BHPBIO personnel, and is developed from the nomenclature of Tertiary Detrital (1-3) that is used by BHPBIO (see section 1.5.2). Ramanaidou and Morris (2007) broadened the term Tertiary to include the Quaternary and used the general term Cenozoic Detritals 1, 2, and 3 for rocks of Paleocene to Recent age.

The lower part of the CzD 2 sequence is composed of organic-rich claystone, while the middle to upper part of the CzD 2 sequence is a CID deposit with well-preserved fragments of goethitised fossil wood (Morris and Ramanaidou, 2007). Morris and Ramanaidou (2007) and Kneeshaw (2008) reported that conglomerate and clay with lignitic (organic fossil) material associated with siderite and pyrite are common at the base of CzD 2 horizon.

Palynological study of organic-rich claystone in the Munjina Member at the Yandi CID mine has revealed the presence of plant tissues, fungal spores, semifusinite particle and fossil pollen grains with ages ranging from Early Oligocene to Early Miocene (Stone, 2004; Macphail and Stone,2004). Furthermore, it is concluded that environmental deposition of CzD 2 was from deep, but not necessarily permanent, water within the paleochannel. On the other hand, Morris (1991) reported that the age of the preserved wood to be late Oligocene to middle Miocene. The sediments are probably of freshwater lacustrine and paludal origin, possibly deposited in a system of flood-plain swamps.

Although there is a similarity in the occurrence of lignitic material within the CzD 2 sequences at South Jimblebar and Yandi CID mine (Munjina Member of Marillana Formation), there has been no published (or BHPBIO unpublished) account of the nature and depositional history of the lignite-bearing units from South Jimblebar, as sampled in this study from exploration cores. One might presume that the absence of CID at Jimblebar suggests that rocks exposed to erosion at that time were mainly shales, rather than a deep regolith (weathered surface material including soil) on iron-rich rocks that were likely present at Yandi (R. C. Morris, personal communication, December 4, 2012).

1.6.2. Geochemical Characterizations of Marra Mamba Iron Formation

The mineralogical investigation of the Marra Mamba Formation by Klein and Gole (1981) concluded that the uppermost part of the Marra Mamba Formation is

magnetite-rich, whereas the lowermost part is sulphide-rich. Furthermore, Klein and Gole (1981) noted that various carbonate minerals are also abundant in all parts of the Marra Mamba Formation. Calcite and dolomite (or ankerites) are commonly major constituents in the upper section, while siderite and dolomite (or ankerites) are abundant in the lower section. Pyrite in the Marra Mamba Formation formed in an anoxic deep water environment (Partridge, Golding, and Young, 2008).

1.6.3. Environmental Geochemical Analysis of Waste Rock at Pilbara Iron Ore Mines

Investigations of the geochemical characteristics of rocks in the Pilbara region, particularly related to their potential to generate acid drainage and release heavy metals, have included several previous studies. Rocks of acid forming potential were identified at Mt. Whaleback iron ore mine by Graeme Campbell and Associates Pty Ltd (GCA) (1996). Samples of Mt. McRae Shale, Mt. Whaleback Fault Shale and Jeerinah Formation were shown to have moderate to high potential acidity resulting in net acid potentials ranging from 50-970 kg H_2SO_4/t, whereas samples of Wittenoom dolomite, Mt.Whaleback shale, Jeerinah dolerite, and shale and chert/ BIF of the Sylvia Formation were reported as non-acid forming. Dolomite rock from the Wittenoom Formation yielded a neutralizing capacity up to 150 kg H_2SO_4/t; however, the carbonate content was found to react very slowly to buffer acid.

Furthermore, GCA (2005) reported results pertaining to the geochemical characterization of the Cloud Break deposit belonging to Fortescue Metal Group Ltd. A total of 17 samples were collected from the Tertiary Detrital sequence, Nammuldi Member of the Marra Mamba Formation, and Roy-Hill Shale Member of the Jeerinah Formation. It was concluded that, with the exception of the Roy Hill Shale samples, the regolith (detrital) and another waste-bedrock were non-acid forming materials. Some samples were also identified to have slight enrichment of As, Bi, Sb and Se.

As a rule of thumb, based on extensive geochemical analysis of the rocks in their Pilbara iron ore mines, Rio Tinto Iron Ore adopts a conservative approach of 0.1 wt% total sulphur as a boundary between non-acid forming and potentially acid

forming black shale and 0.3 wt % total sulphur for other lithologies such as BIF and detrital rocks (Green and Borden, 2011).

1.7. Outcomes of Present Study

The current study represents the first detailed evaluation of the geochemical character and acid generating potential of lignite encountered in iron ore operation in the Pilbara Region of Western Australia. It utilizes the presently only known occurrence of major thickness of lignite in the overburden of an iron ore mine. It assessed the geochemical characteristics of lignite and other waste rock of the future South Jimblebar Iron Ore Mine in Western Australia. Well-developed but locally impersistent lignite deposits have been revealed as potentially acid-forming. Archean black shale which will also report to future waste rock piles at the South Jimblebar mine have acid forming capacities and are relatively enriched in certain elements of environmental significance. In contrast, non-carbonaceous mudstones are classified as non-acid forming and therefore may be of use as cover materials on long-term waste rock storage facilities.

The findings of this research are of importance for implementation of waste rock management to minimize the environmental risk of future mining of iron ore at South Jimblebar. They also will provide a better understanding of the environmental risk associated with the presence of Tertiary lignite where this may be encountered elsewhere at future mines in the region.

2. METHODOLOGY

This chapter discusses the protocols employed in characterizing rock samples that represent future waste materials to be stored at the South Jimblebar Iron Ore Mine.

2.1. Sampling and Sample Preparation

2.1.1. Rock Sampling

Selection of representative samples of the prospective mine area is a fundamental step in predictive waste rock characterisation. Ideally, the number and location of drill core sampling points must be arranged as closely as possible to describe the overall geochemical characteristics of the area to be mined. In the current study, lignite samples were available from seven diamond rock cores (60 mm diameter) provided by BHPBIO from the South Jimblebar prospect. Sampling of the cores was undertaken at the drill core library of the Australian Laboratory Service (ALS), BHPBIO's contractor for metallurgical analyses, at Balcatta, Perth.

The seven drill cores were distributed across the planned mine area, and thus are considered capable of representing the general stratigraphy and lithology of the prospective mine site. However, the irregular distribution of lignite deposits resulted in very different thickness of the rock type within individual cores, with its absence from three cores. The drill core ID and locations of sampling points are given in Table 2.1 and Figure 2.1.

Table 2.1. Drill cores ID and depth

Drill core ID	Depth of core (m)
SJ11022D	299.3
SJ0785D	297.0
SJ0772D	216.4
SJ0845RDT	366.3
SJ0847D	267.9
SJ0848D	216.2
SJ0849D	166.3

The full drill core SJ0772D contained only the Tertiary detrital sequence, while drill cores SJ0845RDT, SJ0847D, SJ0848D, and SJ0849D presented a

relatively complete stratigraphy of South Jimblebar. In the case of drill cores SJ0785D and SJ1102D, BHPBIO provided only the part containing the lignite units to be sampled.

Samples for geochemical analysis and testing were obtained from each of the cores, with focus upon:

- suspected potentially acid forming rocks (lignite and black shale), recognized visually and frequently containing sulphide mineral crystals, (e.g. pyrite);
- suspected potentially acid neutralizing rocks (e.g. limestone);
- volumetrically significant rock types.

These rocks were selected to best constrain the overall character of material forming future waste rock piles. Prior to removal from the drill cores, the sampled units were described for several parameters including rock type, colour, grain size, presence of bedding or lamination, presence of sulphides, and weathering condition.

2.1.2. Sample Preparation

Individual samples selected from the rock cores were crushed to gravel size (<5 mm) using a hydraulic press. The complete resulting sample was homogenized and placed in a stainless steel splitter. A representative sub-sample of approximately 250 g was pulverized to approximately 200 Mesh (<75μm) in a Ni-carbide Tema® swing mill. The apparatus was pre-cleaned using unmineralized quartz prior to use. To prevent contamination between samples, the apparatus was cleaned thoroughly with water and acetone after each use.

The powdered sample was placed in a screw-capped plastic container prior to analysis. The remaining crushed material was placed in a sealable plastic bag and archived in the Environmental Inorganic Geochemistry Group (EIGG) sample store, Department of Applied Geology, Curtin University.

2.2. Waste Rock Characterisation

Geochemical characterization of prospective waste rocks in this study included assessment of the acid generating potential and elemental composition of a total of 144 rock samples. The analytical procedures provided an estimation of the potential for a rock to produce and to neutralise acid solutions, and the extent of

possible geochemical contamination arising from the future weathering and decomposition of the rock.

2.2.1. Assessment of the Acid Forming Potential

Assessment of the overall acid generating potential of prospective waste rock samples in this study involved application of acid-base accounting (ABA). This approach involved determination of the following:

- Paste pH
- Total carbon and sulphur
- Acid neutralisation capacity (ANC)
- Readily (water) soluble sulphate
- Maximum potential acidity (MPA)
- Net acid producing potential (NAPP)

In addition, the following parameters were also determined:

- Net acid generation (NAG) test
- Carbonate (reactable)

2.2.1.1 Paste pH

Paste pH is a simple test to indicate whether the sample contains readily available acidity and alkalinity. A paste pH > 7 suggests the presence of reactive carbonate, whereas paste pH < 5 may indicate the presence of highly soluble acidic salts, i.e. jarosite ($KFe_3(SO_4)_2(OH)_6$) and melanterite ($FeS\text{-}O)_4.7H_2O$). Minerals such as these represent a source of stored sulphate acidity in the sample (Weber *et al*., 2004; Garvey and Taylor, 2000; Lengke, Davis, and Bucknam, 2009).

Paste pH was performed according to the procedure of AMIRA (2002). The slurry was made by mixing powdered sample with deionised water at a solid to water ratio of 1:2 (w/w). The slurry was agitated on a vortex mixer for 30 seconds and allowed to stand for 12 hours before recording pH. The pH was recorded using a Schott ProLab 3000 benchtop pH meter fitted with a ScienceLine pH combination electrode-A 7780.

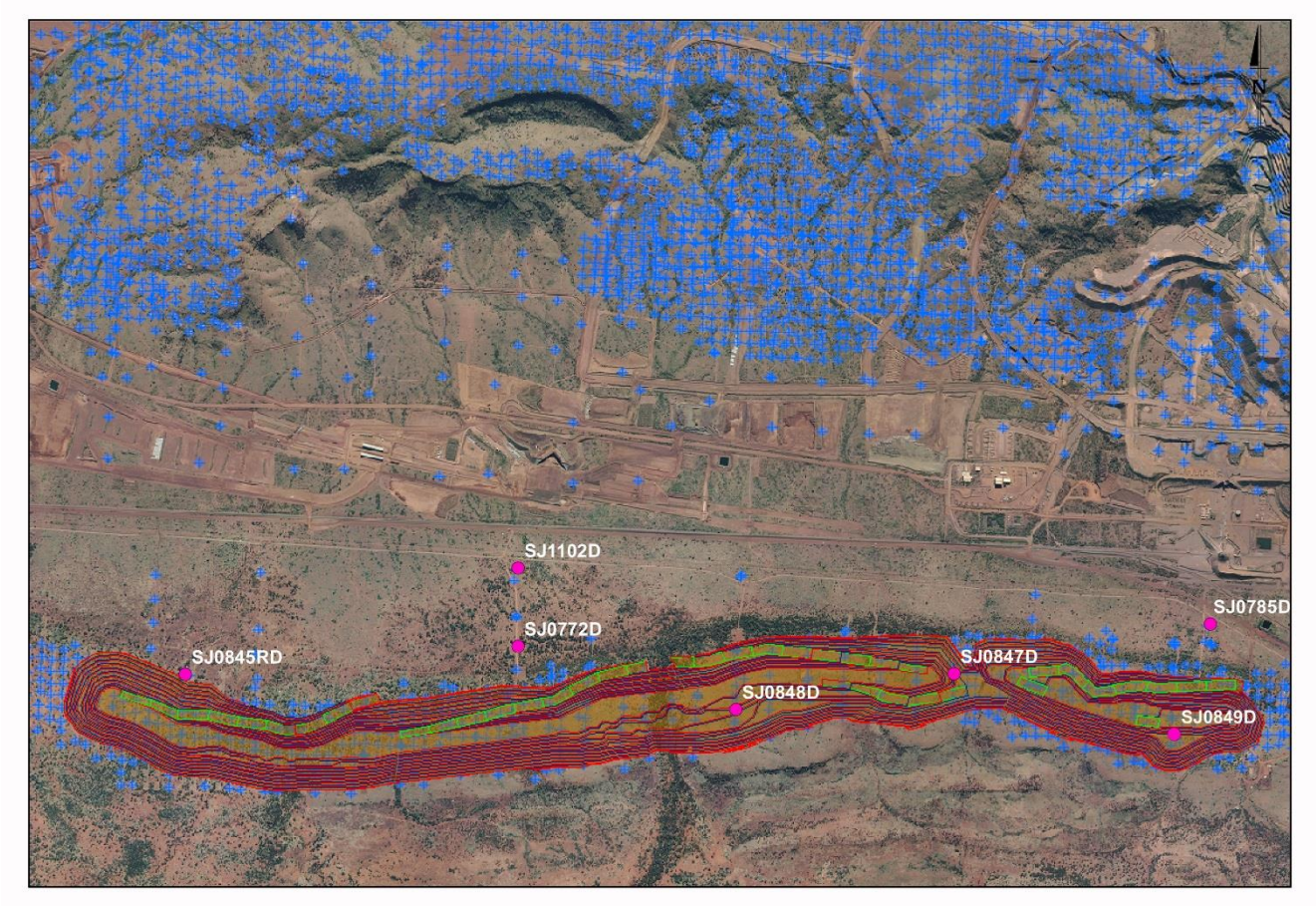

Figure 2.1. General location of drill cores with respect to proposed area of planned pit. Information provided by BHPBIO (Mine Closure Group).

2.2.1.2. Total Carbon and Sulphur

The total carbon (wt %) and sulphur (wt %) determination was conducted using an ELTRA® CS-4000 Carbon/Sulphur Determinator fitted with a resistance furnace and an induction furnace (Fig. 2.2). The resistance furnace was used for lignite samples with their high organic carbon content, generally identified by their blackish colour and carbonaceous texture. The induction furnace was employed for all other samples, including "black shale" samples which generally contained less than 1 wt % carbon despite their often very dark colouration. Both furnaces work similarly, combusting the powdered samples in a stream of oxygen to convert the carbon and sulphur in the sample to carbon dioxide (CO_2) and sulphur dioxide (SO_2), respectively.

For low carbon content samples, approximately 150 mg of powdered sample was accurately weighed into a ceramic crucible that had been tarred on a chemical balance. This was mixed with 0.7 g of pure iron (Fe) and 2.2 g of pure tungsten (W) which act as "accelerants" in the oxidation/combustion. The crucible was then loaded into the induction furnace that rapidly heated the sample to ~2200 ºC in a stream of pure O_2. The evolved gaseous oxides (CO_2 and SO_2) passed through a series of filters to remove moisture and halogens and ensure all carbon and sulphur are in the dioxide state. The concentration of each gas was measured by infrared (IR) spectrometry.

In the case of samples containing a high concentration of organic carbon, 300 mg of powdered sample was weighed into a ceramic boat without metal accelerant. The boat was then pushed into the combustion tube of the resistance furnace where it was heated more slowly to 1350 ºC.

The carbon-sulphur determinator was calibrated using appropriate certified international reference materials, normally RTS-1 containing 1.66 wt % S and JSI-2 containing 1.25 wt% C. Instrument calibration was checked throughout sample runs to assure it was within the expected limits (<2%). In addition, for quality control, one of every ten samples was analysed in duplicate to ensure the reproducibility of the measurement to an acceptable level (<5 % relative percent difference).

Figure 2.2. ELTRA-CS 4000 Carbon/ Sulphur Determinator. Left to right: Computer (control and recorder), main housing containing the IR spectrometers with in-line filters (front left) and induction furnace (front right), resistance furnace, weighing balance.

2.2.1.3. Acid Neutralization Capacity

The acid neutralisation capacity (ANC) describes the inherent ability of a sample to buffer or neutralise acid that may be produced by the oxidation of sulphide minerals or organic material during the weathering process. The ANC was determined by adding a known quantity and molarity of HCl followed by back-titration of NaOH to determine the quantity of acid consumed by the sample according to the Modified Sobek ANC Test (AMIRA, 2002).

Prior to ANC determination, a few drops of 25% HCl were added to a small quantity of powdered sample on a spotting dish. The intensity of reaction, or "fizz rating", was indicated by the formation of bubbles or audible fizz (effervescence). Based on the fizz rating, sample weight, volume and molarity of HCl and NaOH, to be used in the ANC test, were determined using Table 2.2.

A prescribed weight of the powdered sample was reacted with a given volume and molarity of HCl. When the initial reaction had ceased, the sample was heated on a hot-plate (80-90 °C) for one to two hours or until reaction was complete. It was then back-titrated to pH 4.5 using an appropriate molarity of NaOH. The titration was then recommenced and taken to pH 7.0. The volumes of NaOH recorded were used to calculate value for each pH expressed in kg H_2SO_4/t according to equation 2.1.

Table 2.2. Acid and base quantities used in ANC determination according to the sample's fizz rating

Reaction	Fizz Rating	Molarity HCl (moles/L)	Volume HCl (mL)	Molarity NaOH (moles/L)	Sample Weight (g)
No Reaction	0	0.1	25.0	0.1	5.0
Slight Reaction	1	0.1	25.0	0.1	5.0
Moderate Reaction	2	0.5	25.0	0.5	2.0
Strong Reaction	3	0.5	40.0	0.5	2.0
Very Strong Reaction	4	0.5	40.0	0.5	1.0

$$ANC = \frac{49 \times \{(V_{HCl} \times M_{HCl}) - (V_{NaOH} \times M_{NaOH})\}}{W} \qquad \text{Equation 2.1}$$

Where:

ANC = Acid neutralizing capacity (kg H_2SO_4/t)

V = volume of HCl or NaOH (mL)

M = Molarity of HCl or NaOH (moles/liter)

W = weight of sample reacted (g)

2.2.1.4. Readily (water) Soluble Sulphate

Sulphur in the rock may occur in three main forms: sulphide, sulphate and organic sulphur. Sulphur may also rarely occur in the form of elemental sulphur and rare phases like thiosulphate. However, sulphate and organically bound sulphur, due to their stable condition, will not undergo further oxidation to generate significant acidity (Jenning *et al.*, 2000). According to Perry (1998) sulphate minerals are usually present in significant quantities only in weathered rock as intermediate products of metal sulphide oxidation; and otherwise absent from fresh rock.

To determine the amount of readily available soluble sulphate present in the sample, 5 g of powdered sample was mixed with 100 ml of deoxygenated (He sparged) 18 Ω deionised "Millipore" water in a 120 ml plastic container. The container was then shaken on a reciprocal shaker for 6 hours at room temperature and left to stand. Where the settling process was incomplete, the sample was centrifuged at 4500 rpm for 15 minutes. The supernatant solution was analyzed for sulphate using a Dionex® ICS-1000 High Performance Ion Chromatography (HPIC) equipped with a Dionex AS-4 and AG-4 column set (Fig. 2.3).

The soluble sulphate (SO_4^{2-}) concentration (ppm) was converted to wt %S as follows:

$$\text{wt \% S as } SO_4 = \frac{[SO_4^{2-} \text{ (ppm)} \times 0.33]}{10{,}000} \qquad \text{Equation 2.2}$$

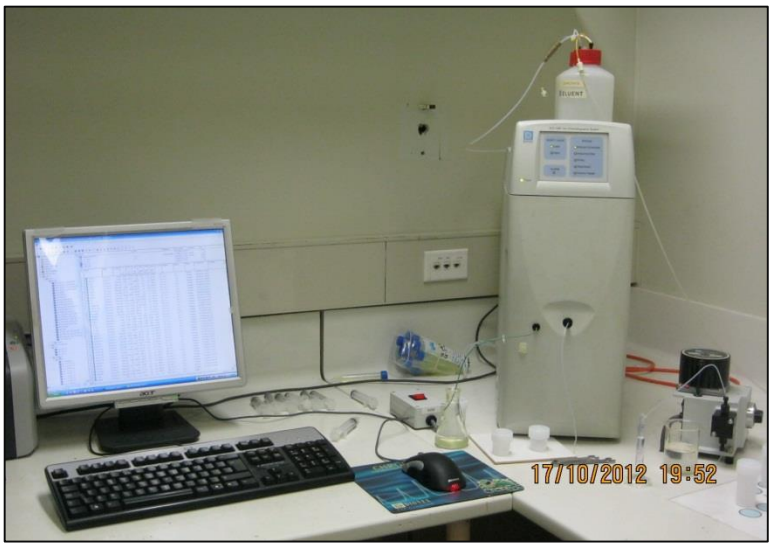

Figure 2.3. Dionex® ICS-1000 high-performance ion chromatograph (HPIC).

2.2.1.5. Maximum Potential Acidity (MPA)

The principal acid generating component in mined waste rock is reactive sulphide sulphur, chiefly in the form of pyrite (FeS_2) and pyrrhotite ($Fe_{1-x}S$) (Moncur *et al.,* 2009). The calculation of maximum potential acidity (MPA) assumes that the measured total sulphur (wt %) content of a rock sample is present wholly as pyrite, and the oxidation to generate acid proceeds according to the reaction:

$$FeS_2 + \frac{15}{2} O_2 + \frac{7}{2} H_2O \rightarrow Fe(OH)_3 + 2H_2SO_4 \qquad \text{Equation 2.3}$$

Based on the stoichiometry of this reaction, the MPA of a sample containing 1 %S as pyrite is 30.6 kilograms of H_2SO_4 per ton of material (i.e. kg H_2SO_4/t) (AMIRA, 2002). Hence the total sulphur (TS) value is converted to MPA of a sample as follows:

$$\text{MPA (kg } H_2SO_4/\text{t)} = \text{wt \% TS x } 30.6 \qquad \text{Equation 2.4}$$

However, that proportion of original pyrite that has experienced oxidation to sulphate is no longer available to produce acid through the oxidation reaction (2.3). Therefore, for greater accuracy, the amount of sulphur occurring as sulphate must be deducted from total sulphur before calculation of MPA (Watkins, 2010).

$$\text{MPA } (\text{kg } H_2SO_4/\text{t}) = (\text{wt \% TS - wt \% S as } SO_4) \text{ x } 30.6 \qquad \text{Equation 2.5}$$

2.2.1.6. Net Acid Producing Potential (NAPP)

The net acid producing potential (NAPP) is the quantitative balance between the propensity of the rock to generate acid due to oxidation of reactive sulphide, and its capacity to neutralize the acid produced. Hence, NAPP is calculated by subtraction of the ANC from MPA of a sample expressed in units of kg H_2SO_4/ t, following the equation below:

$$\text{NAPP } (\text{ kg } H_2SO_4/\text{t }) = \text{MPA - ANC} \qquad \text{Equation 2.6}$$

If the MPA is less than the ANC then the NAPP is negative, which indicates that the sample may have sufficient ANC to neutralise any acid generated. Conversely, if the MPA exceeds the ANC then the NAPP is positive, which indicates that the material may be acid generating (AMIRA, 2002). Miller *et al.* (1991) proposed an interpretation for rock classification based on the NAPP value in which materials are considered non-acid-forming if the NAPP is less than -20 kg H_2SO_4/ tonne, while a NAPP above 20 kg H_2SO_4/t is considered to be acid forming. NAPP values between -20 and 20 kg H_2SO_4/t are considered uncertain.

2.2.1.7. Net Acid Generation (NAG) test

The net acid generation (NAG) test is an empirical measure of the magnitude of the potential acidity that may be produced by the rock sample. It is a “static” test involving reaction of a sample with a strong oxidizing agent, hydrogen peroxide (H_2O_2), to effect oxidation of sulphide minerals. During the same procedure, acid may be consumed by acid-neutralizing minerals in the rock sample. Consequently, the amount of acid remaining at the end of the test procedure is empirically equivalent to the total acid generated minus the acid-neutralizing capacity. The results of the NAG test are recorded in terms of NAG pH (the pH of the final

solution after reaction with excess H_2O_2 is complete) and the NAG acidity (quantity of acid in the final solution).

The NAG test procedure employed in the present study was adapted from that proposed by AMIRA (2002). 2.50 g of powdered rock sample was reacted in a tall form glass beaker with 250 mL of 15% H_2O_2 (pH adjusted to 5.5). The oxidation reaction was allowed to proceed overnight, with care taken to avoid heat generated by the exothermic reaction causing the sample to boil over. On the following day the sample was gently heated on a hotplate to accelerate the oxidation of any remaining sulphide for a minimum of 2 hours or until all effervescence ceased. The sample was then vigorously boiled for several minutes to decompose any residual H_2O_2.

When cool, the pH of the liquor was recorded as the NAG pH. Subsequently, the solution was titrated with NaOH solution of known molarity to pH 4.5 and then to pH 7, to give the NAG acidity via the equation:

$$\text{NAG acidity} = \frac{49 \text{ x } V \text{ x } M}{W} \qquad \text{Equation 2.7}$$

Where:

NAG = net acid generation (kg H_2SO_4/tonne)

V = volume of NaOH used in titration (mL)

M = Molarity of NaOH used in titration (moles/liter)

W = weight of sample reacted (g)

NAG acidity to pH 4.5 mainly indicates the amount of strong mineral acidity due to Fe, Al and most of the hydrogen ions, whereas NAG acidity to pH 7 involves additional acidity derived from hydrolysis of soluble metals such us Cu and Zn (AMIRA, 2002).

A potential difficulty arises in the NAG test in assuring sufficient H_2O_2 is present to fully oxidize all sulphide in the rock sample. The peroxide may be consumed by reaction with sulphide and also through oxidation of organic matter. Caution must be taken in the case of samples containing total sulphur >1 wt % assumed as pyrite (note that the total sulphur content is known through the earlier carbon and sulphur analysis). To ensure the complete oxidation of all the sulphide minerals in such samples, the sample weight was reduced to 1.25 g and, where necessary, further additions of peroxide were made. Depletion in reactive H_2O_2 was recognized by presence of a clear solution with all solid material settled and no

emanation of fine bubble streams. In this case, a further addition of 125 mL of peroxide was made where the sample was known to contain high sulphide content.

A second cause of H_2O_2 exhaustion in the NAG test may arise when testing samples with high carbonaceous content, since the peroxide will be spent in oxidizing the chemically-reduced carbon. Furthermore, the NAG acidity may be increased significantly by the production of large amount of weak organic acid. For carbonaceous rock samples with total carbon > 5 wt %, 125 mL of additional 15% H_2O_2 was added after two hours heating on the hotplate. Then, the vigorous boiling step was continued for four hours until the NAG solution turned slightly transparent.

To ensure the adequacy of peroxide used in the multi sequential addition NAG test (for samples with >1% total sulphur), the pH and EC were regularly checked to see whether or not a change occurred in pH and EC values. Stable pH and EC values indicated that the oxidation of sulphide minerals had ceased. Duplicates of every 10 sample analyses were performed as a quality control measure.

Garvey and Taylor (2000) and AMIRA (2002) suggest a general indication of the acid potential of a sample based on the NAG pH and NAG acidity as shown in Table 2.3.

Table 2.3. Interpretation of the NAG test results

NAG pH	NAG Acidity (kg H_2SO_4/t)	Acid Potential of Sample
≥ 4.5	0	Non Acid Forming
< 4.5	≤ 5	Potentially Acid Forming-Lower Capacity
< 4.5	> 5	Potentially Acid Forming

2.2.1.8. Carbonate (Reactable)

Practically all major rock-forming minerals, with the exception of quartz, offer some degree of neutralization of AMD-derived sulphuric acid. However, it is the carbonate component, particularly calcite that offers the most rapid acid neutralization. As a consequence, the carbonate content of the waste rock can have a significant effect on the rate of evolution of AMD in rocks with potential for acid generation.

The content of reactable carbonate was determined by use a *Carbonate Bombe* (Muller and Gastner, 1971). This technique involves measuring the CO_2

pressure generated by reaction of a known weight of powdered rock samples with an excess of (hydrochloric) acid in a closed vessel. The CO_2 pressure is proportional to the $CaCO_3$ content of sample (Siesser and Rogers, 1971; Muller and Gastner, 1971; Birch, 1981) and the *Bombe* is calibrated using pure $CaCO_3$.

The carbonate analysis was only performed for samples with slight to very strong-fizz reaction with HCl during the ANC "fizz test". One gram of powdered sample was placed in the chamber of bombe and 5 mL of 25% HCl was placed in an open receptacle by means of an "A" grade bulb pipette (± 0.05 mL). The top of bombe was screwed onto the cylinder and the acid was poured to the powdered sample by inverting the acid receptacle. The bombe was swilled gently to ensure complete wetting of the sample and then left until all effervescent reaction had ceased. A further swill of the bombe was performed and the pressure, which should be constant, recorded. Calcite and aragonite react immediately by effervescing strongly: after 10 second or so the reaction is completed. The dolomite reaction sets in more slowly, and complete reaction may take 10-15 minutes (Muller and Gastner, 1971).

Since the volume of a gas is dependent on the temperature and atmospheric pressure, the pressure gauge must be calibrated for each batch of analyses. This was achieved by recording the pressure produced using 0.25 g, 0.50 g, and 0.10 g of pure $CaCO_3$ to produce a calibration curve. The calibration was checked by analysis of in-house standards produced by accurate mixing of analytical grade, anhydrous $CaCO_3$ and quartz powder. The pressure readings were recalculated using the linear regression equation of the calibration to give a wt % carbonate content of the rock samples as presented at Fig.2.4.

Furthermore, carbonate (wt %) is converted into carbon as carbonate (C as $CaCO_3$) (wt %) and then to (carbonate) neutralization potential (CO_3-NP) using the equations below:

$$\text{C as } CaCO_3 \text{ (wt \%)} = \text{wt \% } CaCO_3 \times 0.12 \qquad \text{Equation 2.8}$$

$$CO_3\text{-NP (kg } CaCO_3/t) = \text{wt \% C as } CaCO_3 \times 81.6 \qquad \text{Equation 2.9}$$

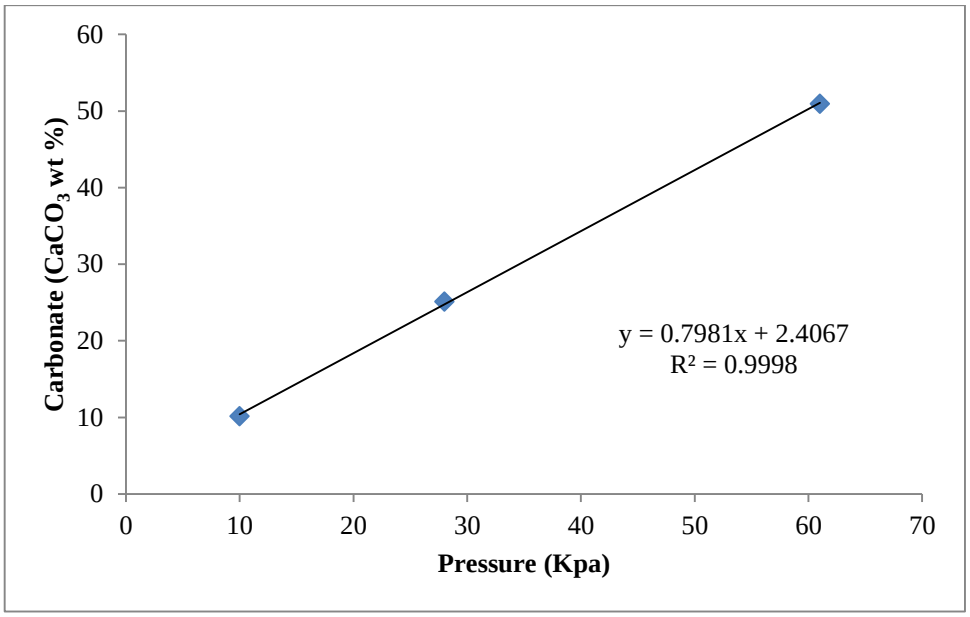

Figure 2.4. Typical calibration curve of the carbonate bombe

2.2.2. Elemental Composition

The concentrations of metals and metalloids of environmental significance were determined in samples of prospective waste rock after dissolution in a hot mixture of concentrated nitric and perchloric acid. This aggressive acid digestion was considered to reflect the absolute maximum amount of the elements that could potentially be released through the most comprehensive, long-term weathering of the rock waste. Typically, the resulting sample solution contained only quartz and very small numbers of crystals of the most resilient silicate and oxide minerals.

The concentrations of elements in the solution were measured using inductively coupled plasma mass-spectrometry (ICP-MS) and atomic emission spectrometry (ICP-AES) at the Forensic Science Laboratory at the University of Western Australia.

2.2.2.1. Acid Wet Digestion Analysis

The acid wet digestion technique involved sample dissolution using a hot mixture of distilled nitric acid (HNO_3) and distilled perchloric acid ($HClO_4$) in a ratio of 3 to 1. This process is capable of dissolving most of silicate, sulphide and carbonate minerals contained in the rock samples.

An accurately weighed 1.000 g of powdered sample was placed in an acid washed 100 ml Erlenmeyer flask. Subsequently, 10 mL of ultrapure HNO_3 were poured into the flask and the flask was covered by a watch glass and allowed to reflux overnight at 90^oC on a hot plate. The watch glass was then removed to allow evaporation of the solution. Prior to full dryness, 9 mL ultrapure HNO_3 and 3 mL ultrapure $HClO_4$ were added and the solution allowed to reflux for a further 8 hours before being evaporated to incipient dryness.

2 ml of concentrated ultrapure HNO_3 was added to redissolve the salts and the solution transferred to a 50 ml A-grade volumetric flask and made up to the mark (~4 % HNO_3).

2.2.2.2. Geochemical Abundance Index (GAI)

The Geochemical Abundance Index (GAI) was calculated for each sample to evaluate the relative degree of elemental enrichment. The GAI (Muller, G (1979) as cited in Forstner, Ahlf, and Calmano, 1993) indicates which elements are enriched in the sample with respect to the referenced standard, in this case median soil abundance documented by Bowen (1979). The GAI was calculated using the following formula:

$$GAI=\text{Log}_2\left(\frac{\text{measured concentration}}{1.5 \text{ x average abundance}}\right) \qquad \text{Equation 2.10}$$

The index value reflects the fold of enrichment of element in the rocks as presented in Table 2.4.

Table 2.4. Element enrichment for GAI integers
(Thomas and Evans, 1998)

GAI	Enrichment Factor
0	0 – 2 fold
1	3 - 6 fold
2	6 -12 fold
3	12 – 24 fold
4	24 - 48 fold
5	48 - 97 fold
6	> 97 fold

3. RESULTS

The first part of this chapter addresses rock character including stratigraphy and rock sample description. Results of geochemical analysis of the rock samples, including of acid base accounting and trace element contents, will be presented in the second part.

3.1. Lithology and Stratigraphic Relations

A total of 144 samples were collected from 7 drill cores. The rocks in this study were classified according to broad lithology, with particular regards to their potential to produce acid mine drainage (AMD). The rock samples were divided simply into two main groups: carbonaceous and non-carbonaceous rock (Table 3.1). Carbonaceous rocks frequently exhibit pyrite mineralisation as a result of complex reactions of sulphate reduction and organic decomposition in iron-abundant and oxygen-deficient environments (Tucker, 1981; Nichols, 2009), so that they likely have potential to generate AMD.

Carbonaceous samples associated with the Proterozoic Banded Iron Formation (BIF) include shale and mudstones. The fissile property distinguishing between shale and mudstone was variably developed within each rock core and, for simplicity, carbonaceous shale and carbonaceous mudstone are collectively referred to in this thesis as black shale. Additionally, a main focus of this study was Tertiary lignite and associated organic-rich mudstone occurring in the Cenozoic Detrital (CzD) 2 stratigraphic unit.

The main examples of non-carbonaceous rocks were shales and mudstones, although a few samples of siliceous (cherty) Banded Iron Formation (BIF), not suspected of posing any environment risk as waste rocks, were included in the studied sample suite. Again, shale and mudstone of non-carbonaceous nature were simply termed mudstone in this thesis.

Thus, the samples in the current study were classified into four main lithologies: lignite, black shale, mudstone, and BIF. Explanation of the sample description is presented in subsection 3.1.2.

Table 3.1. Category and lithology of rock samples

Group	Lithology
Carbonaceous	Lignite
	Carbonaceous shale
	Carbonaceous mudstone
Non-carbonaceous	Shale
	Mudstone
	Cherty BIF

Beside the preoccupancy with carbonaceous character, the suite of samples was also selected to represent the full stratigraphic sequence at the South Jimblebar site and reflected in the 7 drill cores (sub section 1.5.2). The stratigraphy of 5 drill cores is represented schematically in Figure 3.1. Note that the full cores SJ1102D and SJ0785D were not provided by BHPBIO and, accordingly, lignite samples only were taken from the CzD 2 unit. Stratigraphic codes of selected samples from the 7 drill cores are presented in Table 3.2.

Table 3.2. BHPBIO's stratigraphic codes of South Jimblebar Area

Stratigraphy Formation	Stratigraphy Member	Code
Cenozoic Detrital	Cenozoic Detrital 3	CzD 3
	Cenozoic Detrital 2	CzD 2
	Cenozoic Detrital 1	CzD 1
Wittenoom Formation	Undifferentiated West Angela Member	OA
	West Angela Member 1	WA 1
Marra Mamba Formation	Mount Newman Member 3	MN 3
	Mount Newman Member 2	MN 2
	Mount Newman Member 1	MN 1
	MacLeod Member	MM
	Nammuldi Member	MU
Jeerinah Formation	Undifferentiated Jeerinah Formation	N

Figure 3.1. Stratigraphic units present in studied drill cores from South Jimblebar

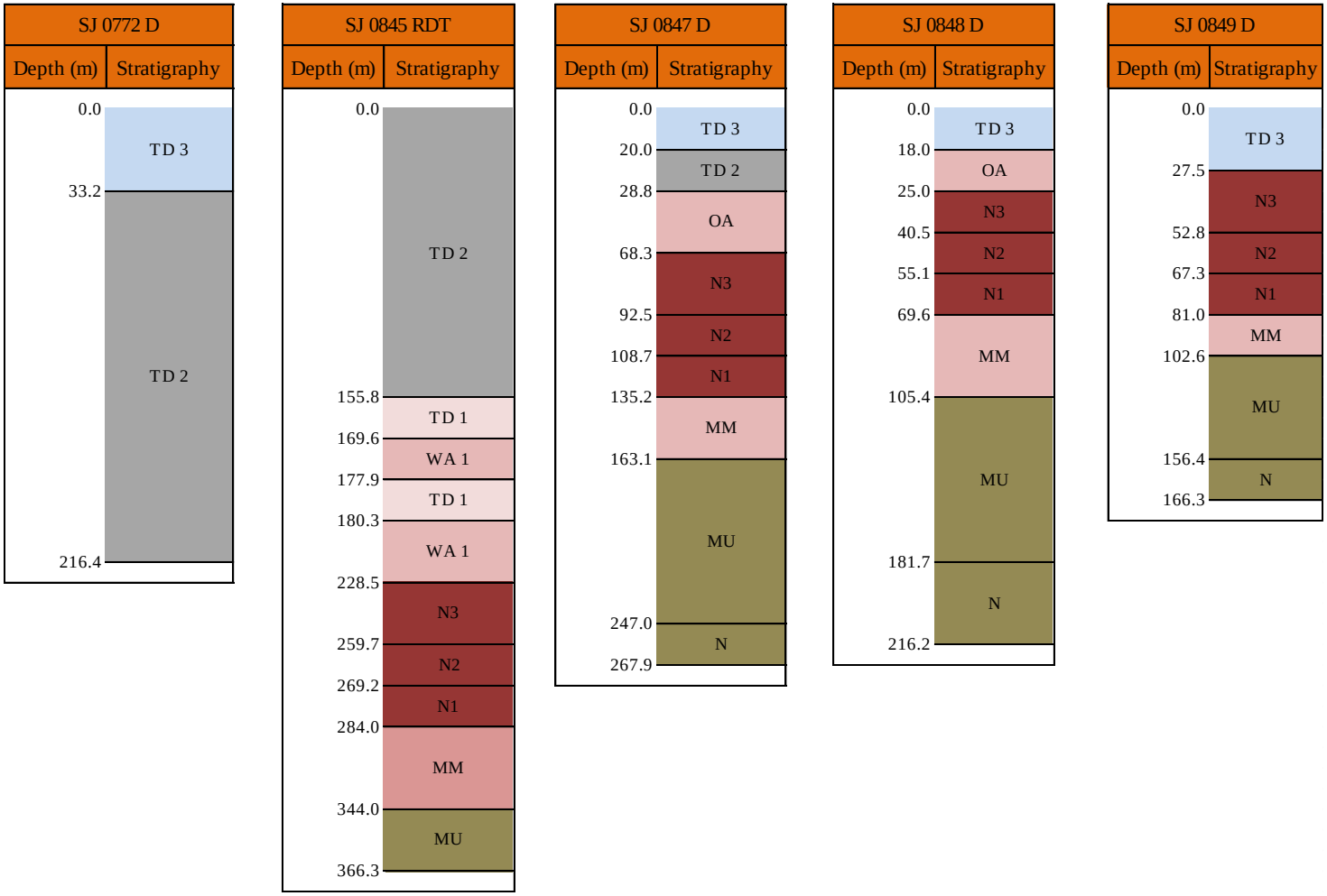

The numbers of samples representing each lithology and stratigraphic unit are shown in Table 3.3. A fully detailed listing is provided in Appendix A.

Table 3.3. Distribution of samples amongst different lithologies and stratigraphic units

Startigraphy Code	Lithology	SJ0772D	SJ0785D	SJ0845RDT	SJ0847D	SJ0848D	SJ0849D	SJ1102D
CzD 3	Mudstone	2			2	1	1	
CzD 2	Mudstone	9		5	1			
	Lignite	11	3	12				3
OA	BIF				1			
	Mudstone				4	1		
WA 1	Mudstone			8				
N 3	Mudstone					3		
N 2	BIF				1			
	Mudstone			1			1	
N 1	BIF				1			
	Mudstone			1		1		
MM	Mudstone				1	1	1	
MU	BIF				1			
	Mudstone				1	3	1	
	Black shale				25	11		
N	Black shale				8	10	8	

Based on the information provide in Table 3.3, the total of 144 selected samples consisted of 29 lignite, 62 black shale, 49 mudstone, and 4 BIF samples. Lignite occurred in the Tertiary detrital unit of the CzD 2 unit. Pyritic black shale was present in the Nammuldi Member (MU) that is the lower part of the Marra Mamba Formation, and the Undifferentiated Jeerinah Formation (N). Non-carbonaceous mudstones were sampled from all the stratigraphic units, whereas BIF samples were taken from the Undifferentiated West Angela Member (OA) of Wittenoom Formation and the Mount Newman Member (MN) of Marra Mamba Formation.

Thus, samples in this study represent the predominant lithogies and stratigraphy units within the South Jimblebar prospect. The sampled drill cores were well-spaced horizontally across the planned mine area (Fig. 2.2), therefore, it is considered that this preliminary sampling encompassed all significant rock types in the studied area. However, it should be noted that modelling the volume and spatial distribution of each rock type is beyond the scope of this study. A fully comprehensive assessment of geochemical characteristics of the whole extent of the

overburden in the future South Jimblebar mine requires more systematic and detailed coring than was available for the present study from resource exploration.

3.2. Rock Sample Description

The following section provides brief description of different lithological types comprising the waste rock sample suite. See also Appendix A.

3.2.1. Lignite

The term "lignite" is normally employed to describe young carbonaceous rocks with carbon content between 50 - 60 wt %, and high inherent moisture content Stow, 2005). When occurring massively, it is the lowest rank of coal, commonly termed "brown coal". When used in the current study, the term is derived from the BHPBIO usage and covers a wide range of lithology comprising very fine grained mudstone containing macroscopic plant fragments (maceral) of Tertiary age within the CzD 2 sequence at South Jimblebar. Specifically, BHPBIO initially confined lignite to rocks with low clay mineral (AlOH group) content and low spectral reflectance as shown on the hyperspectral logs of HyLogger™ instrument. Based on the drill logs provided by BHPBIO, lignite and lignite-bearing claystones occurred in units ranging in thickness from 46.5 m to 169 m.

The various percentages of macerals found in the samples are of the vitrain and fusain types. Vitrain as described by Stow (2005) is bright and glassy, brittle, with conchoidal fracture, while fusain is charcoal-like, soft and powdery, and soils the fingers. Figure 3.2 shows five selected samples of lignite rock from the present study.

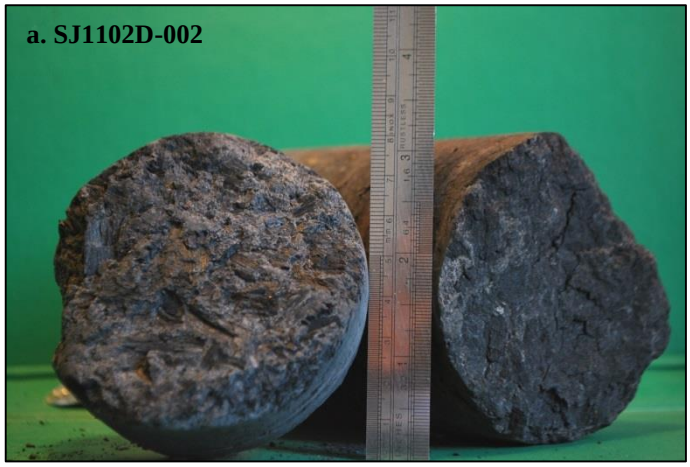

Figure 3.2. Typical lignite samples collected from Tertiary detrital of the CzD 2 unit, South Jimblebar.

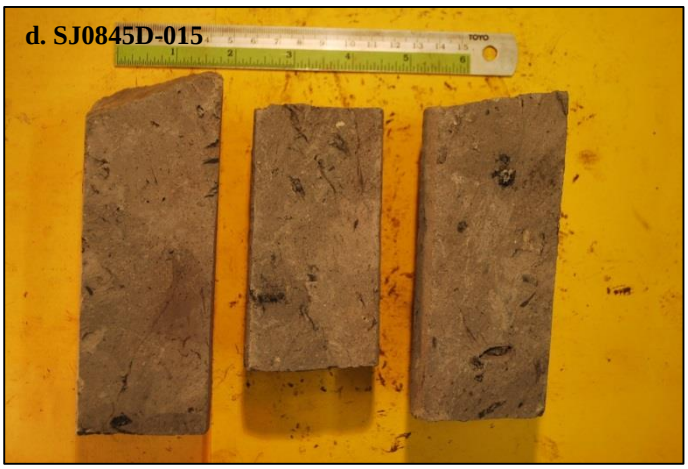

Figure 3.2. (Continued).

Figure 3.2. (Continued).

The rock cores shown in Figure 3.2 illustrate the range in appearance displayed by Tertiary lignite within the CzD 2 unit. Figures 3.2.a-c display varying proportions of dark macerals contained in fine-grained clay matrix. The matrix weathers pale in colour compared to the black colour of the macerals. Angular macerals show depositional bedding structure. In contrast, Figure 3.2.d shows a massive, greyish, fine-grained mudstone with few discrete organic fragments. Figure 3.2.e shows a mineralised, micritic carbonaceous rock with a distinctly higher density than the previous samples. Fine crystal pyrite and secondary minerals, predominantly sulphates, are evident in some samples of lignite, as in Figure 3.2.c and e. Light-coloured alteration products are seen on the exterior of some cores indicating oxidation occurring after core recovery.

3.2.2. Black Shale

Black shale is defined in this study as any carbonaceous rock with fine to very fine-grained texture containing organic carbon >1 wt %. There was no specific measurement for organic carbon in the present study, but in the absence of major carbonate, it was assumed that total carbon approximated organic carbon in the samples. Recognition of samples was on the basis of a dark grey to blackish colour indicative of organic carbon content. Examples of black shale are shown in Figure 3.3.

Figure 3.3. Typical black shale samples collected from the Nammuldi Member and the Undifferentiated Jeerinah Formation, South Jimblebar.

Figure 3.3. (Continued)

As mentioned in the previous section, black shales were sampled from the Nammuldi Member of Marra Mamba Formation (Figure 3.3. a-c) and the Undifferentiated Jeerinah Formation (Figure 3.3.d). The core samples in Figure 3.3.a and b are characterised by dark grey, uniformly very fine-grained, light weight, friable texture and weak shaley parting. Also, black shale samples from the Nammuldi Member frequently contain veinlets of powdery, white, carbonate minerals as seen in Figure 3.3.b.

However, another sample of Nammuldi Member (Figure 3.3.c) is massive, very fine-grained black shale, more dense, with a regular strongly-developed shaley parting. Some parts are variagated, with dark bands and lighter-coloured (chert or quartz) bands. Pyritic mineralisation occurs in this sample. The sample of black shale from the Undifferentiated Jeerinah Formation (Figure 3.3.d) is characterised by high density, high hardness, and also contains secondary veins of pyrite mineralisation.

3.2.3. Mudstone

Mudstone (non-carbonaceous) occurring in the upper part of the detrital sequence (CzD 3) is typified by a brecciated texture with red haematitic silt and clay matrix as shown at Fig.3.4.a. Micritic calcareous iron-rich mudstone (Fig.3.4.b) is also present in the upper part of the CzD 2 sequence.

Mudstone was also sampled from massive units in the Undifferentiated West Angela Member (OA), West Angela Member (WA), Mount Newman Member (MN) and MacLeod Member (MM). Figures 3.4 (c) to (e) are typical examples from those units. Oxidised iron-rich shale with obvious fissility (Figure 3.4.c) is a sample from

the Undifferentiated West Angela Member, while uniformly very fine rock with faint shaley parting character (Figure 3.4.d) was selected from the West Angela Member.

Figure 3.4. Typical mudstone samples collected from various stratigraphies in South Jimblebar.

Figure 3.4. (Continued).

Figure 3.4.e shows a limonitic altered mudstone with resulting high density. This rock type occurs massively within the Mount Newman Member, while an extremely very fine, kaolinite mudstone (Figure 3.4.f) was sampled from the MacLeod Member.

3.2.4. Banded Iron Formation (BIF)

BIF is a lithology consisting of alternation of bands composed of chert and hematite. It has an overall dense texture, is hard and brittle, with colour ranging through shades of white, grey, brown, yellow, and red. It is heavy, with density increasing with the proportion of hematite. Figure 3.5 shows samples of BIF rock. Sample (a) is BIF collected from the Undifferentiated West Angela Member (OA) of Wittenoom Formation and sample (b) from the Mount Newman (MN) Member of Marra Mamba Formation.

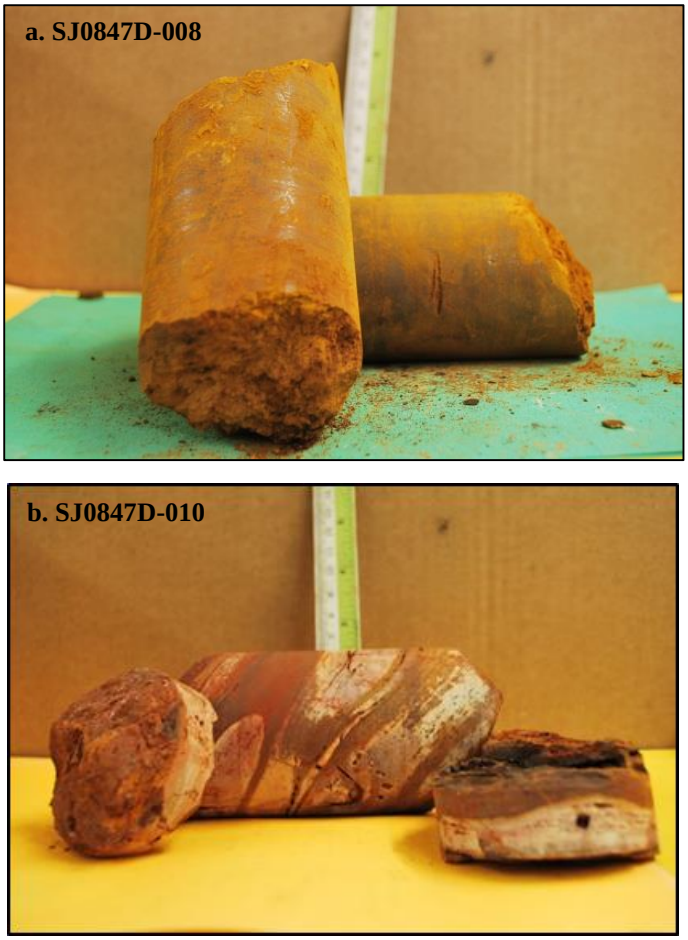

Figure 3.5. Typical BIF samples collected from various stratigraphies in South Jimblebar.

3.3. Geochemical Characterisation

A variety of geochemical analyses and static tests has been carried out on the rock samples to elucidate their potential impact on the environment during future storage in waste rock piles at the South Jimblebar mine. These analyses and tests were to assess the acid generating potential of the rocks and the quantity of the trace

elements of environmental importance that might be released during future weathering and decomposition of the rock.

3.3.1. Acid Mine Drainage (AMD) Assessments

All 144 samples were subjected to a typical regime of AMD test work required for acid-base accounting (ABA). This consisted of standing paste pH, total sulphur, total carbon, sulphate-sulphur, and acid neutralizing capacity (ANC). A net acid generation (NAG) test was also performed. In the ABA, the value of sulphate-sulphur was subtracted from the total sulphur to calculate maximum potential acidity (MPA). The net acid producing potential (NAPP) was calculated according to formula in Eq. 2.6. The results of acid base accounting are tabulated in Appendix B.

3.3.1.1. Paste pH

Paste pH is an indication of the existing inherent acidity of a rock sample, i.e. the acidity that is derived through the dissolution of all readily water-soluble mineral phases. The results of paste pH (Table 3.4) in total indicated an average value of pH >5, for all four main classes of rock samples. The average was lowest for lignite (pH 5.17) and was close to neutral for mudstone and BIF.

Table 3.4. Results summary of paste pH of the four main waste rock types from the South Jimblebar prospect.

Variable	Black Shale		Lignite	Mudstone	BIF
	MU	N			
n	36	26	29	49	4
Max	8.94	8.02	7.49	8.03	7.38
Min	3.78	2.17	1.39	5.13	6.51
Average	6.75	5.09	5.17	6.89	6.94
Median	7.59	4.37	5.41	6.99	6.94

Note. MU: black shale of the Nammuldi Member; N: black shale of the Jeerinah Formation.

However, 22 % of black shale samples (8 of 36) from the Nammuldi Member, 54 % of black shale (14 of 26) from the Undifferentiated Jeerinah Formation, and 24% of Tertiary lignite samples (7 of 29) resulted in paste pH $\leq$ 5,

with the lowest pH being 1.39 for a lignite sample. The paste pH <5 of lignite and black shale provides an initial indication of the presence of stored acidity resulting from previous sulphide oxidation and acid formation.

3.3.1.2. Total Carbon

As expected, the total carbon content of the 29 lignite samples was significant, averaging 14.3 wt %, although a wide range from 0.93 wt % to 36 wt % was represented. The highest values of total carbon were attributable to the maceral content of the lignite that consisted of organic carbon. The carbonaceous shales were characterised by a dark grey to black colour, the maximum carbon content was 9.47 wt % and the average for the 62 samples was >3 wt %.

Samples of mudstone and BIF generally had very low total carbon content with an average <1 wt % in both cases. However, two samples of calcareous mudstone from the upper part of the CzD 2 sequence in drill core SJ0772D (Fig.3.6) had total carbon up to 12.6 wt % principally on account of their carbonate content. As a quality control, a total 40 of 144 samples were analysed for carbon in duplicate with a resultant 1.47 % relative difference (see Appendix D).

Table 3.5. Results summary of total carbon analysis of the four main waste rock types from the South Jimblebar prospect.

Variable	Black Shale		Lignite	Mudstone	BIF
	MU	N			
	wt %				
n	36	26	29	49	4
Max	9.47	7.78	36.0	12.6	0.24
Min	0.05	0.60	0.93	<0.01	<0.01
Average	3.21	3.87	14.3	0.60	0.08
Median	3.28	3.46	13.4	0.06	0.04

Figure 3.6. Samples of calcareous mudstone collected from CzD 2 unit, South Jimblebar.

3.3.1.3. Reactive Carbonate

A slight to very strong fizz reaction (effervescence) was observed for 22 of 144 samples. Of these, five were collected from the CzD 2 unit, where they included two calcareous mudstone and three lignite samples. The remainder were samples of black shale from the Nammuldi Member of Marra Mamba Formation which commonly exhibited strong effervescence.

The results for carbon as carbonate (wt %) and calculated carbonate neutralizing potential (CO_3-NP) (kg $CaCO_3$/t) are given in Table 3.6. The highest CO_3-NP of up to 883 kg $CaCO_3$/t belonged to the two samples of Tertiary calcareous mudstone, while black shale of the Nammuldi Member and the three lignite samples of the CzD 2 sequence yielded an average of 107 kg $CaCO_3$/t and 28.8 kg $CaCO_3$/t, respectively.

Table 3.6. Carbonate and carbonate neutralizing potential of 22 samples of future waste rock from the South Jimblebar prospect

No	Sample ID	Rock Type	Stratigraphy	C as $CaCO_3$ (wt %)	CO_3-NP (kg $CaCO_3$/t)
1	SJ0772D-004	Calcareous mudstone	CzD 2	72.6	711
2	SJ0772D-005	Calcareous mudstone	CzD 3	90.2	883
3	SJ0772D-018	Lignite	CzD 4	2.8	27.5
4	SJ0772D-019	Lignite	CzD 5	2.8	27.5
5	SJ1102D-002	Lignite	CzD 6	3.2	31.4
6	SJ0847D-024	Black shale	MU	7.2	70.5
7	SJ0847D-025	Black shale	MU	31.1	305
8	SJ0847D-026	Black shale	MU	8.8	86.1
9	SJ0847D-027	Black shale	MU	5.6	54.8
10	SJ0847D-028	Black shale	MU	23.2	227
11	SJ0847D-031	Black shale	MU	24.8	242
12	SJ0847D-032	Black shale	MU	5.6	54.8
13	SJ0847D-033	Black shale	MU	5.6	54.8
14	SJ0847D-034	Black shale	MU	8.8	86.1
15	SJ0847D-035	Black shale	MU	13.6	133
16	SJ0848D-021	Black shale	MU	9.9	97
17	SJ0848D-024	Black shale	MU	3.2	31.4
18	SJ0848D-028	Black shale	MU	9.3	90.8
19	SJ0848D-029	Black shale	MU	14.7	144
20	SJ0848D-030A	Black shale	MU	8.2	79.8
21	SJ0848D-030B	Black shale	MU	2.8	27.5
22	SJ0848D-031	Black shale	MU	4.1	40

3.3.1.4. Total Sulphur

Results of the total sulphur, sulphate-sulphur, and calculated sulphide-sulphur are summarised in Table 3.7. The relative percent difference for 40 duplicate analyses was an acceptable value 3.04 % as presented in Appendix D. Overall, mudstone and BIF were characterised by low concentrations of sulphur with

averages of 0.04 wt % and 0.03 wt %, respectively, whereas lignite and black shale had significantly higher concentrations.

Tertiary lignite from the CzD 2 sequence contained total sulphur with an average of 2.33 wt % total sulphur. The lowest total sulphur in a sample of lignite was 0.00 wt %. Conversely, a maximum sulphur content of 35.1 wt % was measured for a very fine mineralised micritic carbonaceous rock (considered as a lignite) containing discrete finely crystalline pyrite taken from drill core SJ0785D (Fig 3.7.a). The large range in total sulphur content clearly reflects irregular and sporadic degrees of pyrite mineralisation within the CzD 2 unit of the drill cores. Other samples of Tertiary detrital contain secondary sulphate minerals, most obviously seen as jarosite (yellowish crystals) and melanterite (white crystal) in sample of mineralised micritic carbonaceous mudstone of SJ0785D-007.

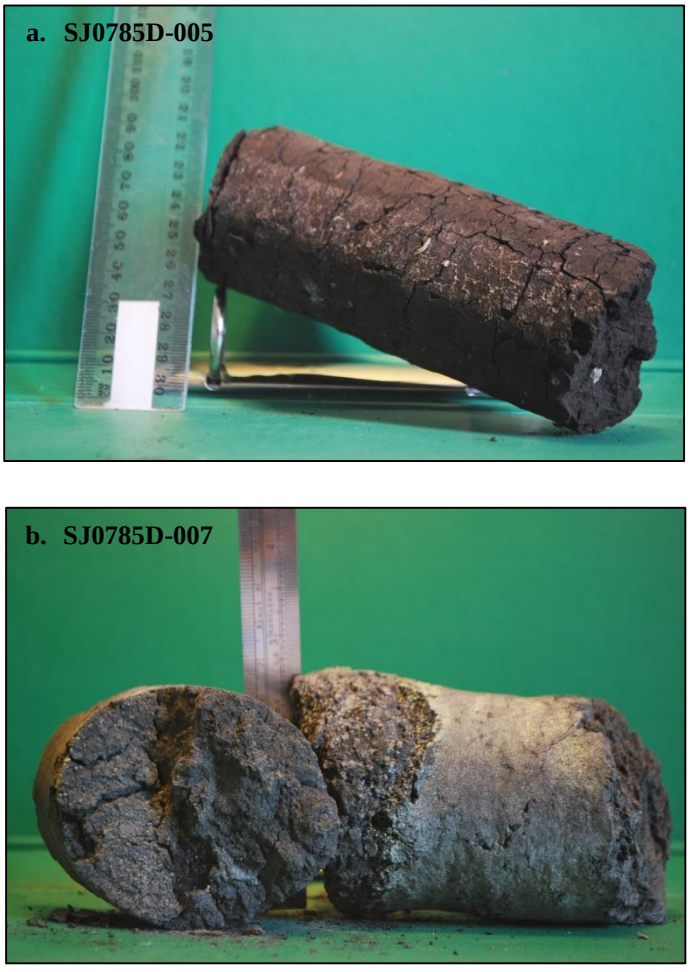

Figure 3.7. Mineralised micritic carbonaceous rock at the CzD 2 unit

Black shale, like lignite, showed considerable range in sulphur content. A total of 36 black shale samples from the Nammuldi Member indicated average total

sulphur content of 1.02 wt %. Whereas, 26 samples of black shale collected from the Undifferentiated Jeerinah Formation yielded a significantly higher average of 3.04 wt % and a maximum value of 19.9 wt % total sulphur.

Localised abundance of pyrite was observed on mineralised secondary veins pyrite in black shale of the Nammuldi Member of Marra Mamba Formation and the Undifferentiated Jeerinah Formation in drill core SJ0847D, SJ0848D, and SJ0849D. Figure 3.8 shows selected black shale sample with obvious metallic-sulphide mineralisation aligned with bedding from the Undifferentiated Jeerinah Formation of drill core SJ0847D.

Figure 3.8. Fine grained metallic sulphide (pyrite) aligned along bedding in samples of black shale from the Undifferentiated Jeerinah Formation.

3.3.1.5. Sulphate-Sulphur (SO_4-S)

Concentrations of sulphate-sulphur in all four categories of waste rock were very low, with the average ranging from <0.01-0.33 wt %, as shown in Table 3.7. However, considerably greater concentrations of sulphate-sulphur, of up to 4.36 wt %, were recorded in a few samples of mineralised lignite and mineralised black shale having high total sulphur content. In general, the amount of sulphur occurring as sulphide could be assumed to approximate the total S content, on account of the low recorded sulphate-sulphur concentrations.

Table 3.7. Result summary of sulphur analysis of the four main waste rock types from the South Jimblebar prospect

Variable	Black Shale						Lignite			Mudstone			BIF		
	MU			N											
	TS	SO_4-S	S_2-S	TS	SO_4-S	S_2-S	TS	SO_4-S	S_2-S	TS	SO_4-S	S_2-S	TS	SO_4-S	S_2-S
				wt %			wt %			wt %			wt %		
n	36			26			29			49			4		
Max	4.08	0.16	3.99	19.9	0.81	19.5	35.1	4.36	30.7	0.45	0.02	0.45	0.05	0.01	0.04
Min	0.01	<0.01	0.01	0.02	<0.01	0.02	<0.01	<0.01	<0.01	<0.01	<0.01	<0.01	0.01	<0.01	0.01
Average	1.02	0.05	0.97	3.04	0.12	2.93	2.33	0.33	2.01	0.04	<0.01	0.04	0.03	<0.01	0.02
Median	0.35	0.02	0.33	2.01	0.08	1.92	0.13	0.02	0.12	0.02	<0.01	0.02	0.02	<0.01	0.02

Note:
TS : total sulphur
SO_4-S: sulphate sulphur
S_2-S : sulphide sulphur

3.3.1.6. Maximum Potential Acidity (MPA)

Since sulphate-sulphur does not undergo further oxidation to generate acid, the calculation of potential acidity must be corrected by deducting the initial sulphate-sulphur content from the total sulphur and the result is assumed as reactive sulphide-sulphur. This value may then be used to calculate the potential acidity based on the stoichiometry of the pyrite oxidation reaction in Eq. 2.3.

The sulphate-sulphur results (Table 3.7) indicated that all the rock had very low concentrations with exceptions for a few samples of high sulphur lignite and black shale samples. The content of organic sulphur is normally very small in silicate rocks. However, lignite samples are suspected of retaining some degree of organic sulphur.

Samples of black shale of the Undifferentiated Jeerinah Formation, and Tertiary lignite showed significant MPA with average values of >60 kg H_2SO_4/t, while black shale of the Nammuldi Member resulted in a lower value of 29.8 kg H_2SO_4/t. In contrast, mudstone and BIF generally produced a very low acid potential with a median <1 kg H_2SO_4/t.

Table 3.8. Result summary of MPA calculation of the four main waste rock types from the South Jimblebar prospect

Variable	Black Shale		Lignite	Mudstone	BIF
	MU	N			
	kg H_2SO_4/t				
n	36	26	29	49	4
Max	122	598	941	13.7	1.35
Min	0.32	0.48	0.02	0.03	0.40
Average	29.8	89.6	61.4	1.11	0.71
Median	10.2	58.8	3.67	0.61	0.54

3.3.1.5. Acid Neutralizing Capacity (ANC)

Overall, the acid neutralizing capacities of the rock samples were low. The average ANC for each of the rock types was <2 kg H_2SO_4/t, except black shale of the Nammuldi Member, and mudstone with averages of 23.8 kg H_2SO_4/t and 34.2 kg H_2SO_4/t, respectively. It should be noted that the higher average ANC of mudstone

was contributed by two samples of Tertiary detrital of calcareous mudstone (SJ0772D-004 and SJ0772D-005) that were taken from the upper part of the CzD 2 and yielded ANC up to 849 kg H_2SO_4/t.

Appreciable ANC values were also recorded for some black shale samples from the Nammuldi Member present in cores SJ0847D and SJ0848D (Figure 3.9). It is suspected, however, that these rocks contain non-acid neutralizing carbonate minerals, such as siderite ($FeCO_3$). Further explanation of this will be presented in Chapter 4. Duplication of 41 of 144 samples in ANC test resulted in 3.1% of relative percent difference (see Appendix D).

Table 3.9. Result summary of ANC analysis of the four main waste rock types from the South Jimblebar prospect.

Variable	Black Shale		Lignite	Mudstone	BIF
	MU	N			
	kg H_2SO_4/t				
n	36	26	29	49	4
Max	127	2.93	12.3	849	2.79
Min	<0.01	<0.01	<0.01	<0.01	<0.01
Mean	23.8	0.67	1.93	34.2	0.94
Median	9.74	0.00	0.00	2.45	0.49

Figure 3.9. Sample of black shale samples of the Nammuldi Member with secondary white carbonate veins yielding significant neutralizing capacity.

Figure 3.9. (Continued).

3.3.1.8. Net Acid Production Potential (NAPP)

Calculation of NAPP showed that the lignite and black shale of the Undifferentiated Jeerinah Formation were generally high capacity acid forming rocks with average acid potential of 59.5 and 88.9 kg H_2SO_4/t, respectively. However, a few samples of lignite and black shale had very high NAPP values, with potential to generate acid up to 941 kg H_2SO_4/t. Black shale samples from the Nammuldi Member indicated low acid forming capacity with an average of 5.98 kg H_2SO_4/t. Mudstone and BIF, in contrast, were acid neutralizing or had negligible acid potential with average NAPP of -33.1 kg H_2SO_4/t and -0.24 kg H_2SO_4/t, respectively. Again, caution must be taken for mudstone due to its high negative NAPP is more influenced by two samples of calcareous mudstone of the CzD 2 unit. Median value of NAPP for mudstone is only -1.49 kg H_2SO_4/t.

Table 3.10. Result summary of calculated NAPP of the four main waste rock types from the South Jimblebar prospect.

Variable	Black Shale		Lignite	Mudstone	BIF
	MU	N			
	kg H_2SO_4/t				
n	36	26	29	49	4
Max	105	598	941	11.4	0.64
Min	-125	-0.25	-11.0	-845	-2.39
Average	5.98	88.9	59.5	-33.1	-0.24
Median	2.88	58.4	2.25	-1.49	0.40

3.3.1.9. Net Acid Generation (NAG) Test

The NAG testing of 144 samples yielded NAG_{pH} between 1.96 and 10.12 with $NAG_{pH\ 7.00}$ acidities ranging from 0.00 to 1004 kg H_2SO_4/t. A summary of the NAG test results based on the rock types is presented in Table 3.11 and Table 3.12. The values of relative percent different of 58 duplicates of 144 samples were 0.81% and 3.23% for NAGpH and NAG acidity, respectively (see Appendix D).

Table 3.11. Result summary of NAG pH of the four main waste rock types from the South Jimblebar prospect.

Variable	Black Shale		Lignite	Mudstone	BIF
	MU	N			
n	36	26	29	49	4
Max	8.46	6.18	9.61	10.1	7.53
Min	2.18	1.96	1.98	3.34	4.49
Average	5.04	2.79	6.56	7.09	6.5
Median	4.40	2.45	7.5	7.41	6.99

Table 3.12. Result summary of $NAG_{pH\ 7.0}$ acidity of the four main waste rock types from the South Jimblebar prospect.

Variable	Black Shale		Lignite	Mudstone	BIF
	MU	N			
	kg H_2SO_4/t				
n	36	26	29	49	4
Max	91.5	566	1004	7.96	0.86
Min	0.00	1.76	0.00	0.00	0.00
Average	21.5	82.2	62.4	1.03	0.22
Median	5.09	53.4	0.00	0.00	0.00

Samples of black shale from the Undifferentiated Jeerinah Formation may generally be classified as high capacity acid generating with average NAG pH and NAG acidities 2.79 and 82.2 kg H_2SO_4/t. This NAG acidity corresponds reasonably closely with the calculated NAPP. Black shale of the Nammuldi Member overall had low acid forming capacity with slightly acid NAG pH of 5.04 and moderate NAG acidity 21.5 kg H_2SO_4/t. NAG results for samples of mudstone and BIF similarly

were consistent the low calculated NAPP values, indicating a non-acid forming status.

Interestingly, the NAG test results of lignite samples categorised the rocks predominantly as non-acid forming. Only 8 of 29 samples yielded NAGpH <4.5. These results contrasted with the NAPP calculations that gave positive NAPP (average of 62.4 kg H_2SO_4/t) indicating significant potential to generate acid. The $NAG_{pH\ 7.0}$ acidity of these 8 samples of lignite ranged between 2.45 kg H_2SO_4/t and extremely up to 1004 kg H_2SO_4/t.

3.3.2. Major and Trace Element Geochemistry

Multi-element analysis was conducted on a sub-suite of 31 selected waste rock samples. The analysed suite was predominantly composed of lignite and black shale, which were the main subject of the study, and were suspected of containing the greatest amounts of trace metals and metalloids on account of their carbonaceous composition and potential sulphide mineral content. The selected samples comprised 7 lignite samples (Tertiary detrital), 10 black shales samples of the Nammuldi Member, and 8 black shale samples of Undifferentiated Jeerinah Formation. In addition, 6 mudstone samples were collected from various stratigraphic horizons.

A broad scan analysis of 9 major and 55 trace elements was performed using ICP-AES and ICP MS, respectively. The summarized contents of strong acid leachable element of environmental importance in lignite, black shale of the Nammuldi Member, black shale of the Undifferentiated Jeerinah Formation, and mudstone are respectively presented in Table 3.13, Table 3.14, Table 3.15, and Table 3.16. Full results including those of strong acid leachable major and non-toxic elements are given in Appendix C. In addition, 3 of 31 samples were analysed in duplicate and resulted in 4.29% average of relative precent difference (see results in Appendix D).

A total of 21 elements listed in Tables 3.13 – 3.16 are potentially toxic metals and metalloids. The results show that on average lignite had the highest concentration of 12 potentially toxic elements, namely: Be, Sc, V, Cr, Co, Ni, As, Mo, Sb, Tl, Pb, and U. Black shale samples from the Nammuldi member signalled noticeable amounts of Cu and Ag, while for black shales from the Undifferentiated

Jeerinah Formation show relative enrichment in Zn, Se, and Cd. The highest concentrations of Ti, Mn, Hg, and Th were recorded from Mudstone.

To assess the numerical enrichment value, the assay results were, subsequently, compared to median soil abundance (Bowen, 1979) and presented in log 2 values as geochemical abundance index (GAI). This is further discussed in Chapter 4.

Table 3.13. Concentration of elements of environmental importance in Tertiary lignite samples (n = 7) from the CzD 2 unit, the South Jimblebar prospect.

Elements	Be	Sc	Ti	V	Cr	Mn	Co	Ni	Cu	Zn
	ppm									
Min	0.85	0.32	40.6	0.08	0.82	8.47	9.66	26.8	2.15	<0.02
Max	25.0	30.6	342	252	304	468	83.5	392	117	175
Average	5.86	11.3	204	77.8	89.3	102	35.7	137	45.4	73.2
Median	1.63	5.88	244	47.7	76.9	34.3	32.9	102	42.7	62.0

Elements	As	Se	Ag	Mo	Cd	Sb	Hg	Tl	Pb	Th	U
	ppm										
Min	2.04	1.14	<0.02	0.10	0.02	<0.02	0.03	0.08	0.16	0.17	0.49
Max	558	4.76	0.06	14.5	0.26	17.3	1.79	27.9	126	14.2	16.6
Average	127	2.30	0.03	3.56	0.10	3.82	0.47	6.11	35.0	6.56	6.80
Median	6.93	1.95	0.04	0.56	0.05	0.06	0.14	0.19	14.1	5.12	7.06

Table 3.14. Concentration of elements of environmental importance in black shale samples (n = 10) from the Nammuldi Member of the Marra Mamba Formation, the South Jimblebar prospect.

Elements	Be	Sc	Ti	V	Cr	Mn	Co	Ni	Cu	Zn
	ppm									
Min	0.10	2.79	2.15	9.48	10.5	0.16	4.37	8.67	8.39	25.1
Max	1.58	9.38	147	27.4	78.6	2929	43.0	90.3	207	935
Average	0.57	4.80	60.8	17.5	42.4	295	16.7	34.4	134	190
Median	0.42	4.31	66.7	17.0	38.7	1.21	13.4	27.7	169	82.9

Elements	As	Se	Ag	Mo	Cd	Sb	Hg	Tl	Pb	Th	U
	ppm										
Min	<0.02	0.14	0.01	<0.02	0.01	<0.02	0.02	<0.02	2.59	1.60	0.30
Max	14.3	0.6	4.52	0.63	0.20	0.05	1.07	1.29	24.3	11.9	1.01
Average	4.12	0.41	0.68	0.09	0.06	0.02	0.31	0.15	11.0	5.21	0.69
Median	3.62	0.41	0.22	0.03	0.03	0.01	0.15	0.02	7.8	3.41	0.74

Table 3.15. Concentration of elements of environmental importance in black shale samples (n = 8) from the Undifferentiated Jeerinah Formation, the South Jimblebar prospect.

Elements	Be	Sc	Ti	V	Cr	Mn	Co	Ni	Cu	Zn
	ppm									
Min	0.23	0.94	8.14	13.2	17.5	0.56	4.56	11.8	38.9	16.4
Max	1.51	8.25	274	42.6	86.9	346	42.2	74.0	186	3674
Average	0.53	3.05	76.1	27.2	39.3	44.0	20.2	40.2	102	581
Median	0.39	2.46	54.1	26.9	30.1	0.91	14.3	33.8	105	37.1

Elements	As	Se	Ag	Mo	Cd	Sb	Hg	Tl	Pb	Th	U
	ppm										
Min	1.53	1.01	0.04	0.17	0.10	<0.02	0.04	0.05	8.47	1.04	0.55
Max	72.5	28.5	0.48	1.41	32.3	0.06	0.89	3.05	84.0	4.10	2.75
Average	14.5	5.20	0.22	0.57	4.67	0.03	0.32	0.76	29.7	2.31	1.47
Median	5.55	1.69	0.19	0.47	0.16	0.03	0.17	0.28	17.3	2.19	1.34

Table 3.16. Concentration of elements of environmental importance in mudstone samples (n = 6) from various stratigraphy of the South Jimblebar prospect.

Elements	Be	Sc	Ti	V	Cr	Mn	Co	Ni	Cu	Zn
	ppm									
Min	0.44	1.73	21.4	2.73	3.92	2.62	4.08	1.74	4.46	2.97
Max	2.81	12.5	679	131	221	12290	34.8	101	90.1	102
Average	1.22	8.59	233	51.2	62.5	2645	13.5	31.0	45.3	45.4
Median	0.76	9.93	105	46.0	29.1	891	7.86	16.3	44.0	26.6

Elements	As	Se	Ag	Mo	Cd	Sb	Hg	Tl	Pb	Th	U
	ppm										
Min	0.80	0.12	0.01	0.02	<0.02	<0.02	0.01	<0.02	0.79	0.32	0.07
Max	23.2	0.87	0.14	2.04	0.13	0.08	3.17	0.11	26.1	13.9	4.10
Average	10.9	0.48	0.06	0.68	0.05	0.04	0.60	0.05	12.3	6.70	1.73
Median	10.6	0.45	0.04	0.41	0.04	0.03	0.13	0.03	12.8	7.02	1.72

4. DISCUSSION

The first section of this chapter briefly describe the proposed development of the South Jimblebar Mine to give an understanding of mine plan and waster rock removal during mining operation. Subsequently, the second section presents an interpretation of the results of geochemical testing and analyses of prospective waste rock samples from the South Jimblebar mine site. A major aim is to classify the rocks sampled from South Jimblebar exploration cores according to their acid generating capacities and their content of elements of environmental importance. The implications of geochemical characteristics on waste rock management will be discussed in the last section.

4.1. Project Development Overview

Development of the South Jimblebar Mine of BHPBIO targets the high grade iron deposit of the Marra Mamba Formation, mainly mineralized within the Mount Newman Member. Figure 4.1 shows the project overview of the South Jimblebar Mine. It can be seen that the project stretches from west to east divided into three open mine pits, namely: Western, Central, and Eastern Mine Pits. In addition, during the mining operation, waste rocks will be placed into overburden storage area (OSA) in two different locations, out-mine pit and in-mine pit (backfilling method). As indicated in Figure 4.1, there are three out-pit waste rock piles that are:

- the OSA 1 : located at further western of the Western Pit
- the OSA 2 : located between the Central and the Eastern Pits
- the OSA 3 : located at further eastern of the Eastern Pit

Note that the location of in-pit waste rock pile has not been disclosed by BHPBIO.

Cross sections from south to north of the South Jimblebar deposits are presented in Figs 4.2.a-c involving all lithologies and stratigraphic units intersected within the Central and the Eastern Pits. Cross section for the Western Pit is not fully represented in Figure 4.2.

Based on the Figure 4.2, overburden excavation will involve removal of relatively significant quantities of the Cenozoic detrital sequence, including Tertiary calcareous mudstone and Tertiary lignite within the CzD 2 strata. Subsequently, the overburden removal involves excavation of the Wittenoom Formation, the MacLeod

Member and the Nammuldi Member of the Marra Mamba Formation. As a simplification, all the body of the Mount Newman Member of the Marra Mamba Formation is assumed as mineral deposit target, therefore not will be a concern in waste rock management.

It should be noted that sampling of rocks of the Wittenoom Formation was only possible for the West Angela Member, while the dolomite-rich Paraburdoo Member was not found within the sampled drill cores. Furthermore, removal of a small portion of the Jeerinah Formation only occurs in the Western Pit of the South Jimblebar Mine (Richard Marton, personal communication, December 4, 2012).

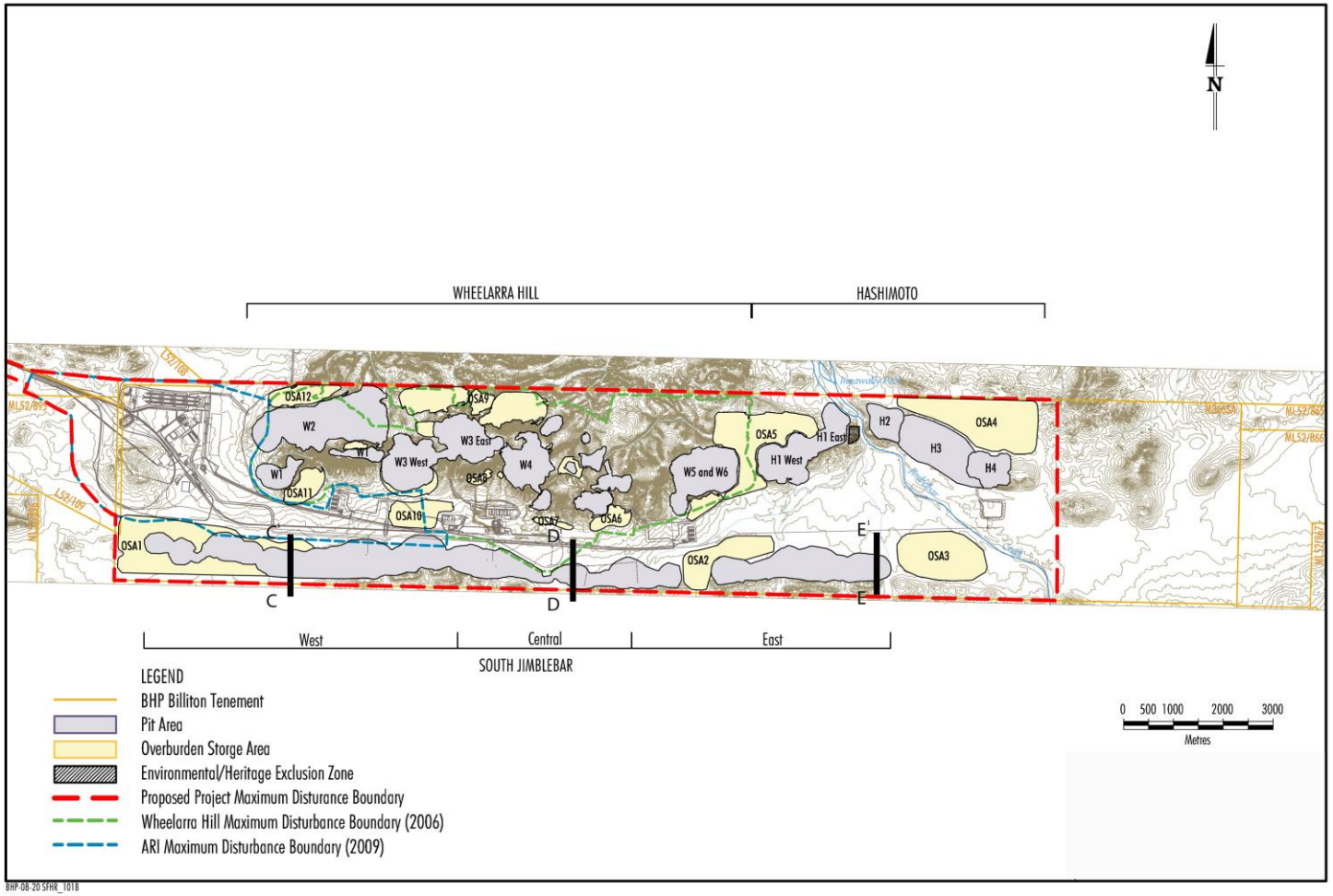

Figure 4.1. Plan view of the proposed South Jimblebar mine with cross section indicated (after BHPBIO, 2009)

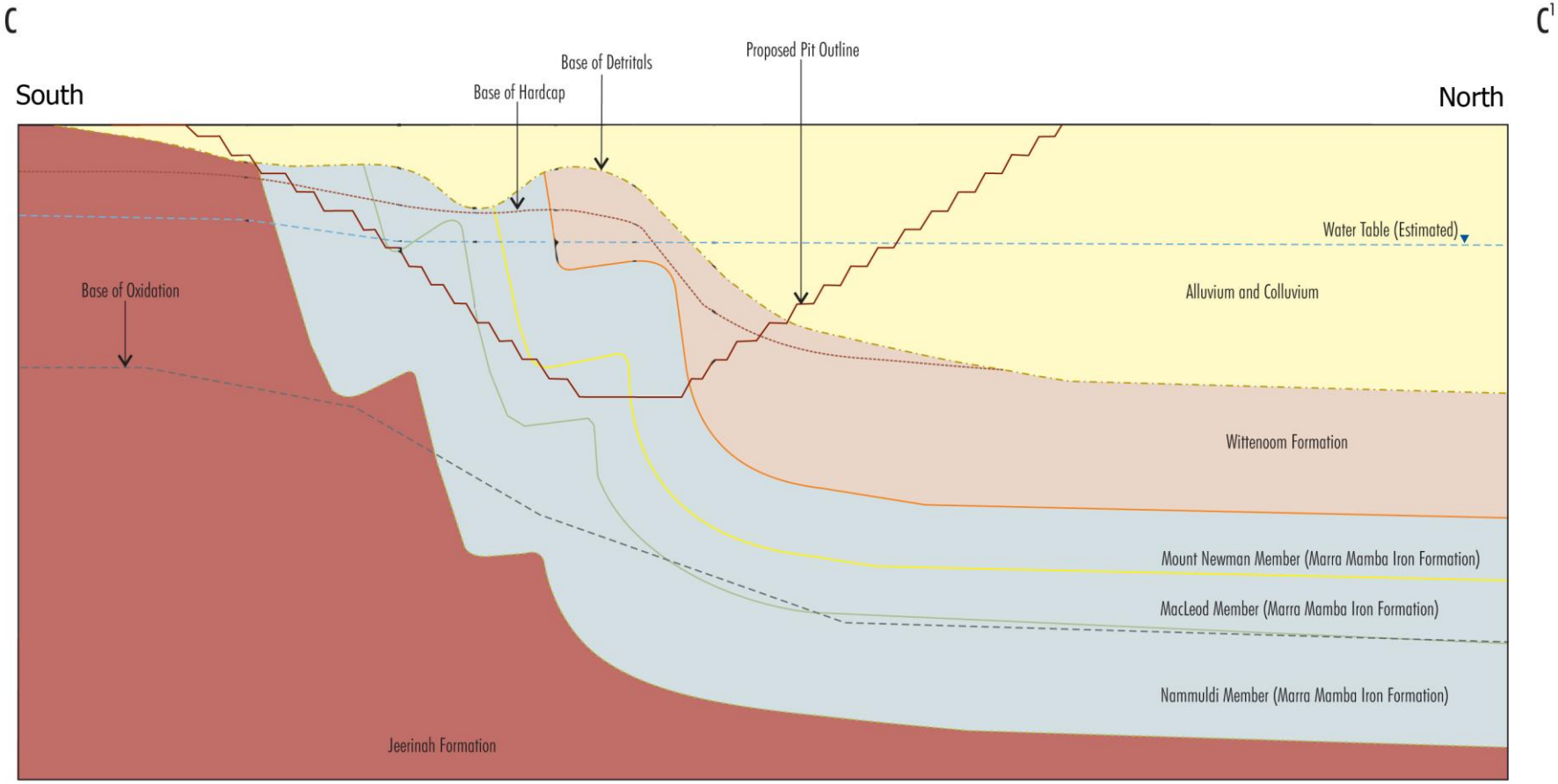

Figure 4.2. a. Schematic diagram of south to north cross section of western part of the planned Central Pit of the South Jimblebar mine (refer to Fig. 4.1 for location of section line)

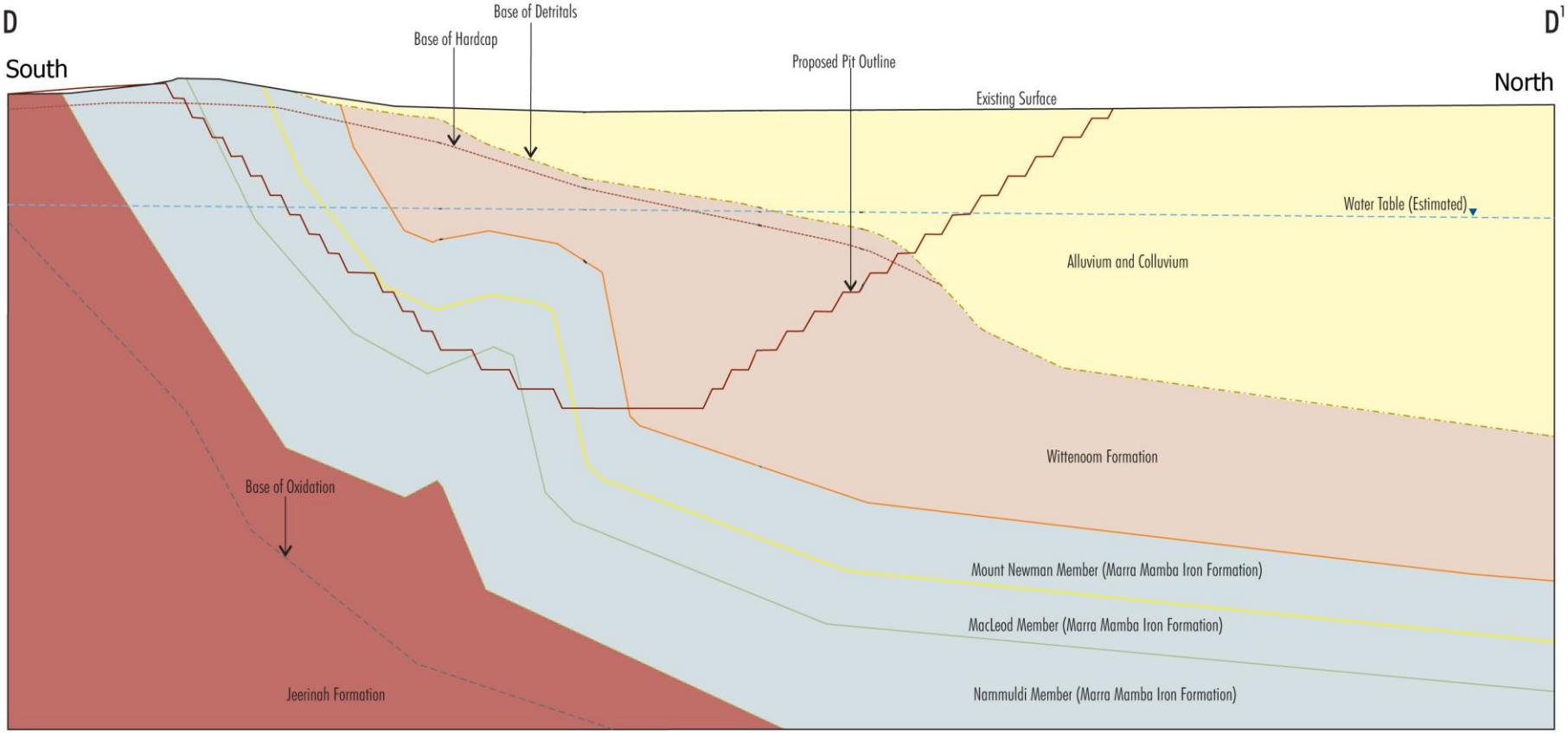

Figure 4.2.b. Schematic diagram of south to north cross section of eastern part of the planned Central Pit of the South Jimblebar mine (refer to Fig. 4.1 for location of section line)

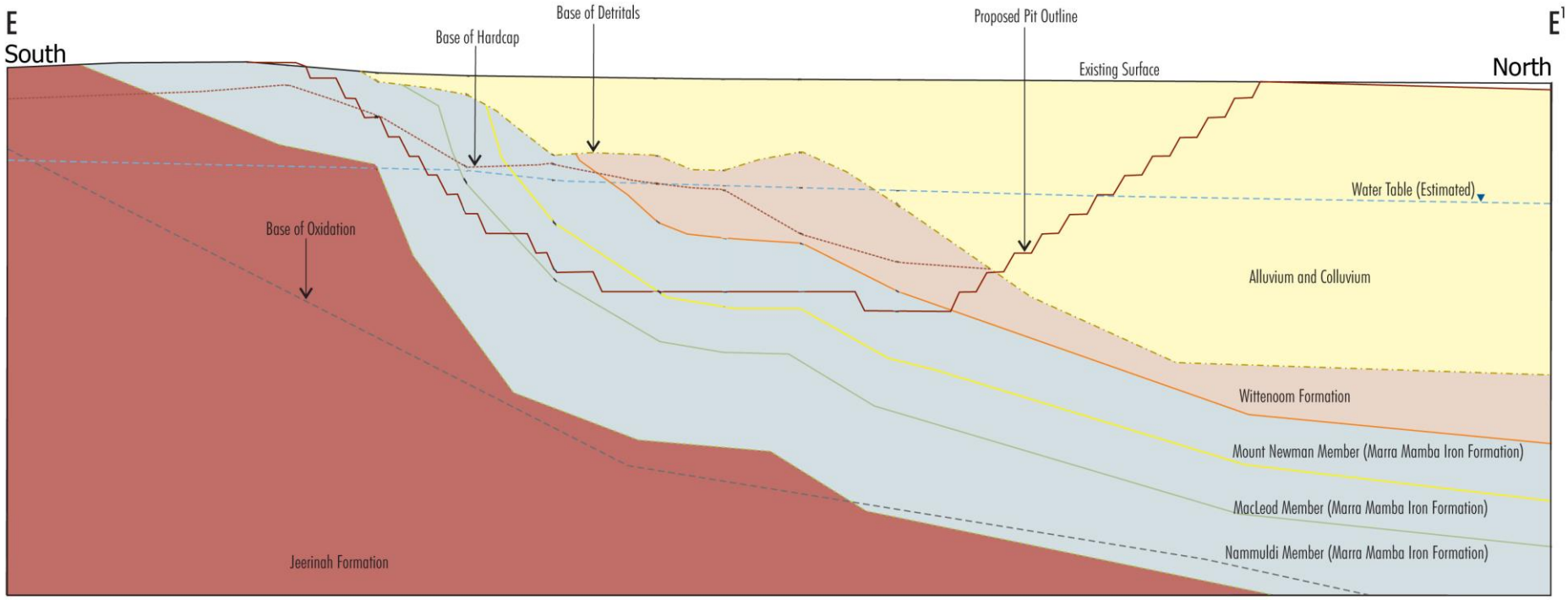

Figure 4.2.c. Schematic diagram of south to north cross section of eastern part of the planned Eastern Pit of the South Jimblebar mine (refer to Fig. 4.1 for location of section line)

4.2. Siderite Effect on Acid Neutralizing Capacity (ANC)

Carbonate minerals provide the greatest and most immediate acid neutralization of acid mine drainage. Calcite, $CaCO_3$, and dolomite, $CaMg(CO_3)_2$, for example, are both widely abundant carbonate minerals with considerable acid neutralizing capability. However, an issue arising in the measurement of acid neutralizing capacity (ANC) of a rock is overestimation of the effective ANC value due to the presence of siderite ($FeCO_3$) (Skousen *et al*., 1997; Paktunc, 1999; Weber *et al*., 2003).

Siderite, $FeCO_3$, is commonly present as a diagenetic mineral in shales and sandstone as well as in hydrothermal veins. When in contact with acidic solutions generated by sulphide oxidation (AMD), siderite provides initial acid neutralization. However, as a result of the increasing pH, Fe^{2+} is hydrolyzed and releases H^+ ions, thereby increasing the acidity of the solution through the reaction in Eq. 4.1-4.3. Three moles of H^+ are consumed in Eq. 4.1 and 4.2, while three moles are produced in Eq. 4.3. Therefore, in an ANC test, where iron follows the full sequence of Eq. 4.1 to 4.3, siderite has no net contribution to acid neutralizing capacity.

$$FeCO_3 + 2H^+ \rightarrow Fe^{2+} + CO_2 + H_2O \qquad \text{(Equation 4.1)}$$

$$Fe^{2+} + \frac{1}{4}O_2 + H^+ \rightarrow Fe^{3+} + \frac{1}{2}H_2O \qquad \text{(Equation 4.2)}$$

$$Fe^{3+} + 3H_2O \rightarrow FeOH_3 + 3H^+ \qquad \text{(Equation 4.3)}$$

In the current study, the samples that were collected from the lower part of Nammuldi Member may contain abundant siderite and dolomite as reported by Klein and Gole (1981). Based on the core log provided by BHPBIO, black shale was identified within the Nammuldi Member sequence in the lower part of drill cores SJ0847D and SJ0848D. The precise quantity of siderite in those samples was not determined. Nevertheless, the presence of significant siderite is apparent through the conflict between the calculated net acid production potential (NAPP) and the net acid generation (NAG) test results.

It can be seen from Fig. 4.3 that two samples (SJ0847D-024 and SJ0847D-035) in quadrant IV show conflict between negative NAPP and low NAGpH (<4.5). Such condition is one indication of the effect of siderite. In these cases, re-analyses of the ANC of anomalous samples was undertaken using a modified H_2O_2 ANC test

(Stewart, Miller, and Smart, 2006). Such analysis was also conducted on further samples selected from the lower part of Nammuldi Member.

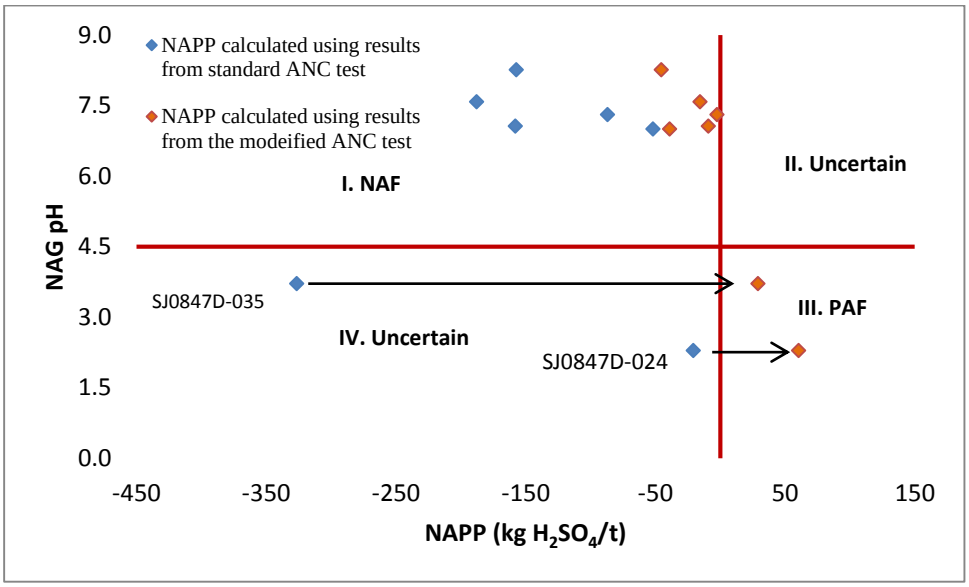

Figure 4.3. Comparison between NAG pH and NAPP of black shale from Nammuldi Member of Marra Mamba Formation.

Stewart (2005) investigated the effect of siderite on ANC measurement and concluded that a siderite content >15 wt % resulted in a significantly overestimate of ANC when using the standard ANC test. Stewart (2005) proposed a modified ANC test using hydrogen peroxide (H_2O_2) to ensure complete oxidation and hydrolysis of all iron. In the modified ANC test, H_2O_2 is added as a strong oxidation agent and the reaction time is extended, so that a true net-acid neutralizing capacity is measured.

The addition of H_2O_2 during the NaOH back titration accelerates the process of ferrous iron (Fe^{2+}) oxidation to ferric iron (Fe^{3+}). The hydrolysis of Fe^{3+} to ferric hydroxide ($Fe(OH)_3$) then proceeds rapidly. These processes will decrease the pH and precipitate of $Fe(OH)_3$ as shown in Figure 4.4. The titration is continued until reaching stable pH 7.0. The comparison of ANC results between standard ANC and modified ANC is given in Table 4.1.

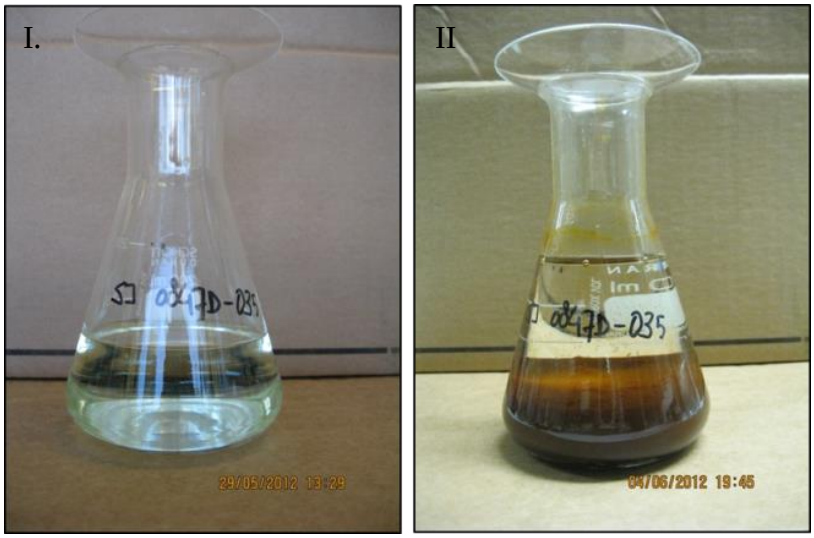

Figure 4.4. (I) ANC solution before titrating; (II) $Fe(OH)_3$ precipitate formation after adding H_2O_2 and titrating to pH 7.0.

Table 4.1. Comparison of ANC results of suspected siderite-enriched samples between standard ANC test and modified H_2O_2 ANC test

Sample ID	**Standard ANC**	**Modified H_2O_2 ANC**
	kg H_2SO_4/t	
SJ 0847 D-024	137	55.7
SJ 0847 D-026	161	49.3
SJ 0847 D-027	61.1	48.1
SJ 0847 D-028	91.5	6.98
SJ 0847 D-031	257	85.0
SJ 0847 D-034	204	55.1
SJ 0847 D-035	417	60.9

Data in Table 4.1 show notable differences where the modified ANC test significantly reduced the ANC value compared to the standard ANC test. If not recognized, this effect potentially leads to misclassification of samples in the NAPP calculation. Figure 4.3 demonstrates that recalculation of NAPP on two samples (SJ0847D-024 and SJ0847D-035) has redefined them from uncertain Quadrant IV to PAF material (Quadrant III). The remaining samples, despite having significantly reduced values of ANC, are classified as NAF material by both the standard and

modified ANC test. This is probably accounted for by abundance of other neutralizing-carbonate minerals, such as calcite and dolomite.

4.3. Organic Acid Effect on Net Acid Generation Test

The presence of organic acid on the net acid generation (NAG) test may have affected the results obtained from black shale and lignite samples with their high organic carbon contents. As reported previously, samples of black shale and lignite contained total carbon up to 9.47 wt % and 36.0 wt %, respectively. Partial oxidation of organic matter will increase the abundance of organic acid and subsequently cause overestimation of sulphide-derived acidity in the NAG result.

Garvie and Taylor (2000) suggested adding additional H_2O_2 aliquots into the NAG solution prior to titration when testing coal and carbonaceous material. Furthermore, Stewart (2005) proposed a modified organic carbon NAG test. This involved more a complicated procedure of filtering the initial 250 ml NAG solution and dividing into three separate portions. A 100 ml aliquot was treated in a normal way. A second 100 ml was subjected to extended boiling for 4 hours. Subsequently, a further 50 ml aliquot was used to determine the content of soluble sulphur, total organic carbon, Ca^{2+}, and Mg^{2+} to calculate the acid base balance in the solution. The detail of this procedure can be found in Stewart (2005).

In the current study, a combination of peroxide addition and extended boiling to decompose the organic acid in the NAG solution was performed on samples with total carbon >5 wt %. During the reaction and boiling steps, a distinctive frothing occurred in the solution indicating decomposition of the organic emulsion. The froth and black solids particles in the solution gradually disappeared during the boiling process. The samples were cooled after two hours of boiling, the NAG pH was recorded; an additional 125 ml hydrogen peroxide was added and boiling continued for four hours. Fig.4.5 shows the alteration of solution during the NAG test process.

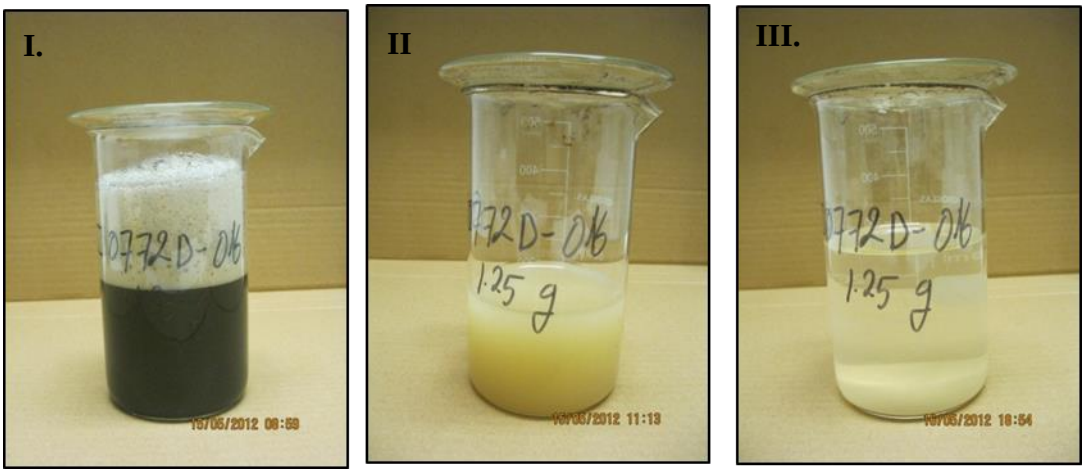

Figure 4.5. Alteration of solution during extended boiling NAG test for high carbonaceous rock. (I) Frothing after several minutes heating; (II) NAG solution after two hours boiling; (III) NAG solution after six hours boiling.

The aggressive degradation of organic matter during the NAG test most probably relates to an advance oxidation process called the *Fenton reaction* that is widely applied for treatment of various organic wastes. The reaction will generate hydroxyl radicals through the catalytic reaction of Fe^{2+} or Fe^{3+} in the presence of hydrogen peroxide as described in Eq. 4.4 – 4.5 (Ramírez, Theng, Mora, 2010)

$$Fe^{2+} + H_2O_2 \rightarrow Fe^{3+} + OH\bullet + OH^- \qquad \text{Equation 4.4}$$

$$Fe^{3+} + H_2O_2 \rightarrow Fe^{2+} + OOH\bullet + H^+ \qquad \text{Equation 4.5}$$

Subsequently, the hydroxyl radicals are highly reactive oxidants that aggressively degrade the organic content producing carbon dioxide (CO_2) and water (H_2O).

Comparisons of results of standard and extended boiling NAG tests were performed for 12 selected lignite samples (Table 4.2). In general, the extended boiling treatment resulted in higher NAG pH and lower NAG acidity to various degrees for different samples. Based on the results in Table 4.2, the effect of extended boiling and additional H_2O_2 on high organic carbon samples can be divided into three categories, which are:

1. NAGpH and NAG acidity changed significantly from acid to base condition
2. NAGpH and NAG acidity changed slightly and remained in basic condition
3. NAGpH and NAG acidity changed slightly and remained in acidic condition

Table 4.2. Standard and extended boil NAG test results

Category	Sample ID	Total Carbon	Total Sulphur	NAPP	Standard NAG Test		Extended Boiling NAG Test	
		wt %		kg H_2SO_4/t	NAG pH	NAGpH 7.0 Acidity (kg H_2SO_4/t)	NAG pH	NAGpH 7.0 Acidity (kg H_2SO_4/t)
1	SJ 0772 D-016	36.0	0.72	21.5	3.59		8.45	-
	SJ 0772 D-020	22.0	0.13	3.67	3.56		8.65	-
	SJ 1102 D-004	30.3	0.15	3.98	2.75	133	8.24	-
	SJ 1102 D-006	18.6	0.03	0.51	4.32	37	8.33	-
2	SJ 0772 D-010	20.7	0.43	11.7	8.12	-	8.27	-
	SJ 0772 D-014	29.2	0.65	18.9	8.61	-	8.77	-
	SJ 1102 D-002	22.0	0.22	0.05	6.20	5.19	7.50	-
3	SJ 0772 D-012	5.2	0.96	26.8	2.84		2.93	21.6
	SJ 0772 D-019	35.8	1.41	31.6	2.87		3.56	19.0
	SJ 0785 D-003	27.7	21.4	539	2.06	589	2.11	599
	SJ 0785 D-005	13.9	35.1	941	2.08	1016	1.98	1004
	SJ 0785 D-010	29.1	4.33	112	2.24	129	2.35	129

The first category indicated a significant influence of high organic matter content on the standard NAG test for samples with low sulphur content. Owing to the excess of H_2O_2 when oxidizing a small quantity of pyrite, residual H_2O_2 in the NAG solution partially oxidized the organic matter resulting in release of organic acid. Stewart (2005) reported that organic acid has a remarkable interference on the standard NAG test for rock with low sulphide-sulphur (<0.7 wt %) and total organic carbon >5 wt %. The effects of high organic carbon, beside the appearance of a blackish colored solution and frothing during the NAG process, can also be indicated by the standard-NAG acidity greatly exceeding calculated NAPP (e.g. in samples SJ1102D-004 and SJ1102D-006). These cases reflect the contributions from organic acid giving overestimation of NAG acidity up to 133 kg H_2SO_4/ t.

In the second category, samples have low sulphur content, but their NAG pH in both treatments was slightly neutral to basic. This may result from the sulphur being in non-reactive form (e.g. organic sulphur); whence the peroxide was enough to fully convert the organic matter to CO_2 and H_2O.

In contrast, the third category indicated an insignificant effect of organic carbon on samples with high sulphur ($\geq$ 0.96 wt %) contents that mainly present as reactive sulphide. The H_2O_2 oxidizes pyrite in preference to the organic carbon (Stewart 2005) and therefore the H_2O_2 will be depleted after oxidizing high sulphide-sulphur, leaving little or no peroxide to decompose the organic matter. Thus, generation of organic acid will be negligible level when calculating NAG acidity.

Interestingly, all the samples in the first and second category, with the exception of sample SJ1102D-002, yielded a zero ANC value, but had a basic pH condition after the extended boiling. This probably arose from the presence of unmeasured neutralizing capacity by the standard ANC test. Boiling in an oxidizing environment for a long time may cause alteration of resistant silicate minerals which consume acidity (Weber, 2003; Stewart, 2005).

4.4. Net Acid Generation (NAG) Test

The net acid generation (NAG) test is an empirical determination of the balance between acid potential and acid neutralization capacity of the rock exposed to strong oxidation. The rapid oxidation of reactive sulphide in the rock generates acid, while neutralization is affected by carbonate and or silicate dissolution. Since

the acid generation and acid neutralization reactions occur essentially simultaneously during the NAG test, the final results obtained describe the net actual potential acidity.

As a general rule, NAG pH 4.50 is used as a convenient reference point for distinguishing acid and non-acid forming rock. Rock with NAG pH ≤4.5 is considered as potential acid forming (PAF), whereas NAG pH ≥4.5 is considered as non-acid forming (NAF) (AMIRA, 2002; Price, 2009). In the context of water quality, water with pH <4.5 indicates no alkalinity (Benjamin, 2002).

Among 144 samples tested, 53 samples (37%) yielded NAG pH <4.5 and are categorized as PAF, and the other 91 samples (63%) yielded NAG pH > 4.5 and are categorized as (NAF) material. Specifically, the results demonstrate that carbonaceous rocks make a significant contribution to the PAF category with more than 50% having NAG pH <4.5. In contrast, most of the non-carbonaceous rocks (> 90%) had NAG pH >4.5 (Table 4.3).

Table 4.3. NAG pH of rocks of carbonaceous and non-carbonaceous character

Rock Grouping	**NAG pH <4.5 (PAF Category)**		**NAG pH >4.5 (NAF Category)**	
	n	**%**	**n**	**%**
Carbonaceous rocks	50	55	41	45
Non-carbonaceous rocks	3	6	50	94

The relation between NAG_{pH} and titrated NAG acidity to pH 7 ($NAG_{pH\ 7.00}$ acidity) is presented in Fig. 4.4. NaOH titration to pH 7 broadly involves not only sulphide-derived strong mineral acidity but also various weaker components of acidities. Titration to pH 7 was only performed on samples yielding NAG_{pH} <7.0. Samples giving NAG pH >7 are considered to have no acid potential (0.0 kg H_2SO_4/t). Figure 4.6 shows that the 144 samples in the current study may be divided into two main categories as below:

- NAG pH > 4.5 and $NAG_{pH\ 7.0}$ acidity < 5 kg H_2SO_4/t (Quadrant I in Fig. 4.6.b)
- NAG pH <4.5 and $NAG_{pH\ 7.0}$ acidity > 5 kg H_2SO_4/t (Quadrant III in Fig. 4.6.b)

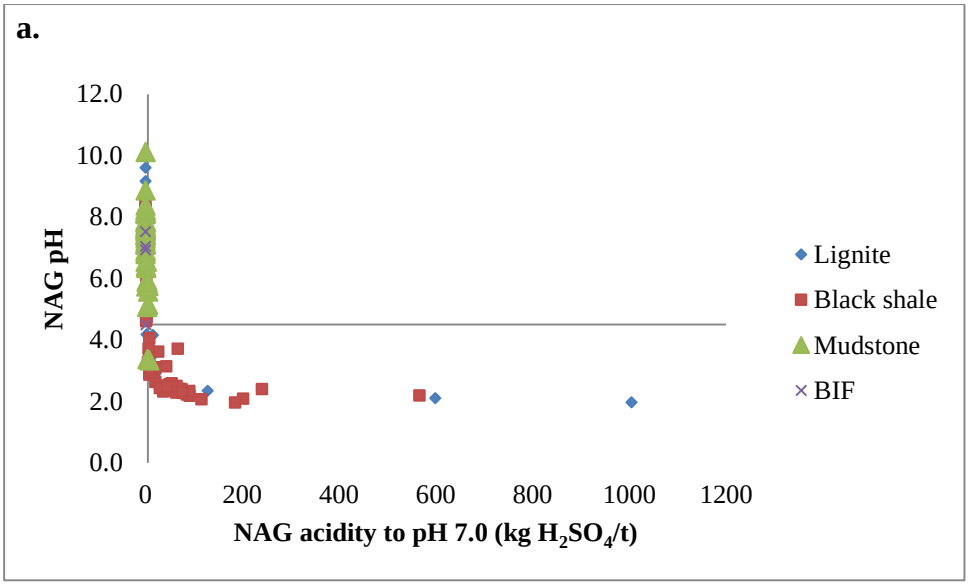

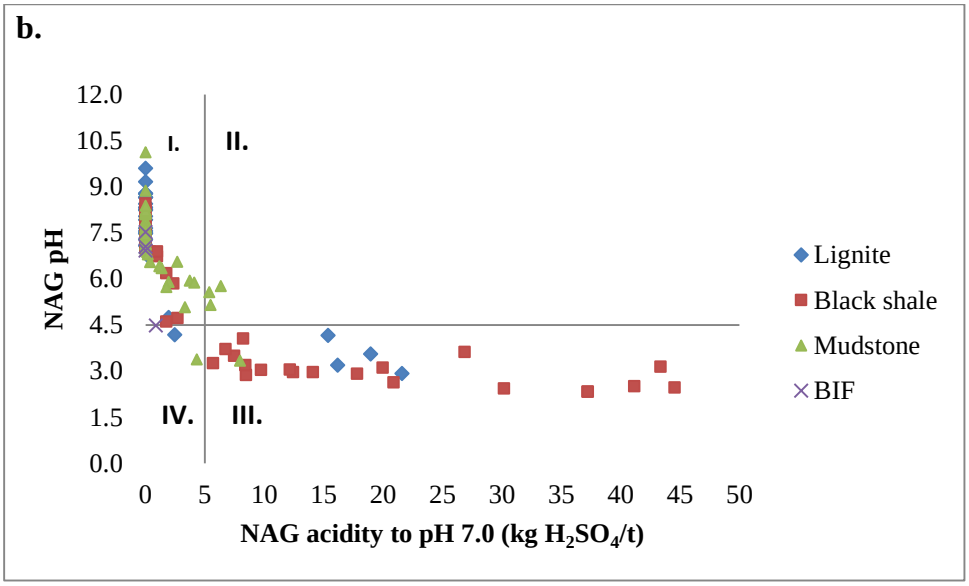

Figure 4.6. (a). Correlation of NAG pH to $NAG_{pH\ 7.00}$ acidity; (b). Enlarged view of axis region of Fig. 4.4.a.

Only five samples plotted out of these ranges: three samples in Quadrant II (NAG pH >4.5, NAG acidity >5.0 kg H_2SO_4/t) and two samples in Quadrant IV (NAG pH <4.5, NAG acidity <5.0 kg H_2SO_4/t). However, each case is plotted very close to the quadrant boundary. Therefore, NAG pH 4.5 well defines the category boundary between potentially acid and non-acid potential rock.

Since the acidity in the rock derives from oxidation of reactive sulphide minerals, it was expected that total sulphur will have a positive correlation with acidity production. Figures 4.7 show a general pattern that higher total sulphur (based on log (10) values) related to lower NAG pH. There is a good linear relation

for acid samples where there is little or no neutralization. More scatter occurs amongst the high NAG pH samples, probably because of the effects of neutralization.

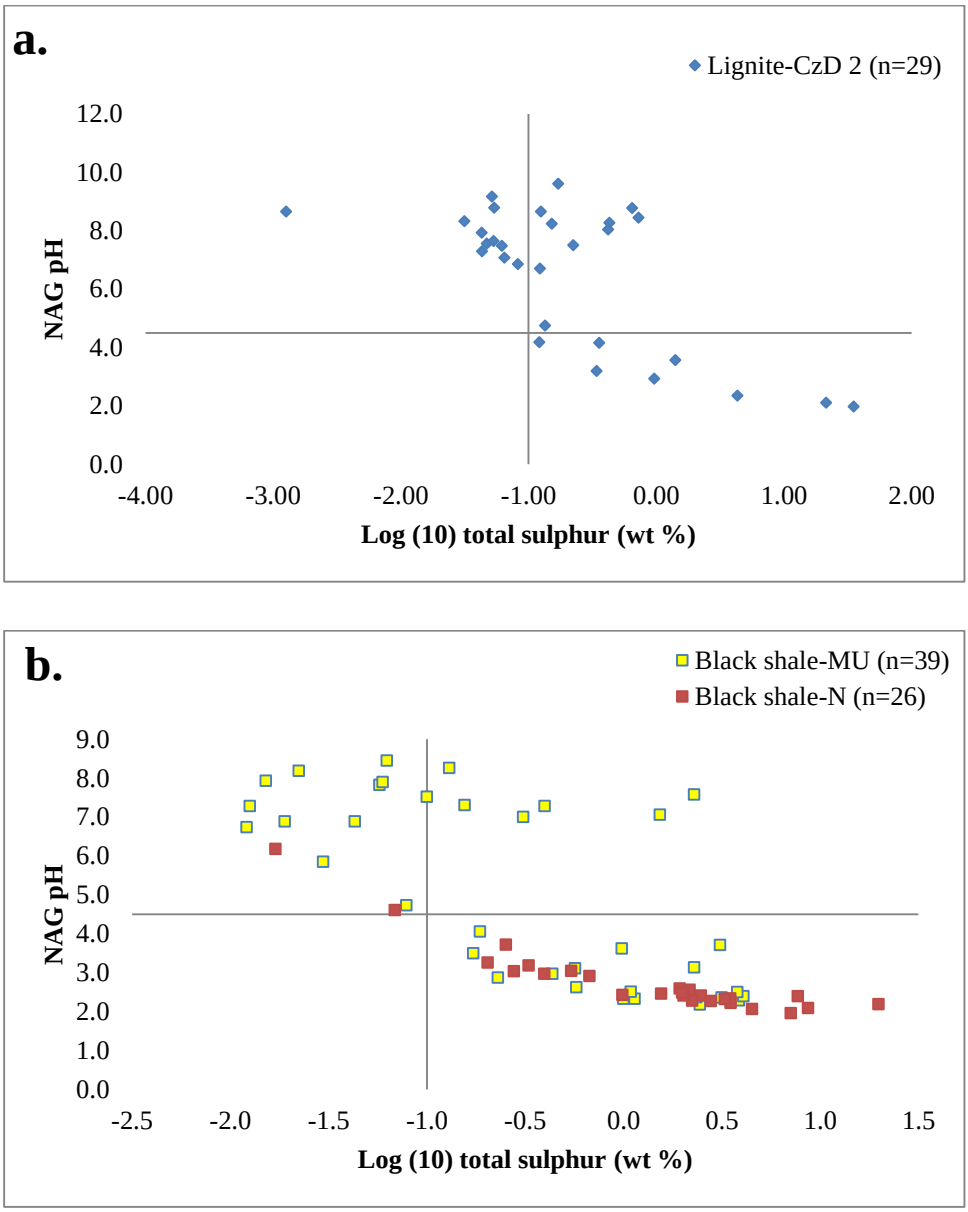

Figure 4.7. Correlation of NAG pH and total sulphur of 144 samples of potential waste rock from the South Jimblebar prospect.

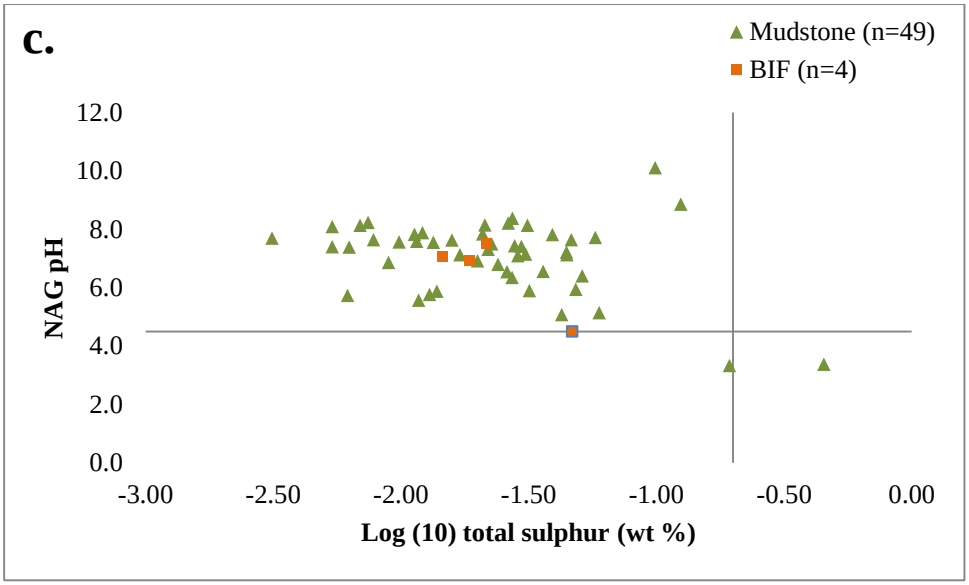

Figure 4.7. (Continued)

The relation between NAG pH and total sulphur in Fig. 4.7 indicates the potential to use total sulphur as a criterion for the identification of acid potential of the rock. A cut off of 0.1 wt % total sulphur (-1 wt % in log (10) value) reasonably defines the potential of the lignite and black shale rocks to generate AMD. Carbonaceous rock containing sulphur >0.1 wt % yielded NAG pH< 4.5 and categorized as PAF material. This indicates that 0.1 wt % total sulphur probably could be used as a reference point for distinguishing acid and non-acid forming for lignite and black shale. In the case of non-carbonaceous rocks, 0.2 wt % of total sulphur (-0.69 wt % in log (10) value) is, in the case of the rock suite in the present study, a good reference point for identifying acid and non-acid forming rocks.

Similar findings have been previously reported by Green and Borden (2011) in the Pilbara region, where 0.1 wt % total sulphur is potentially used as a boundary to classify non-acid forming (NAF) and potentially acid forming(PAF) black shale, while 0.3 wt % total sulphur is used for other lithologies such as BIF and detrital rocks. Li (2000) concluded, excepting extremely rare occasions, a fresh mine waste containing < 0.1 wt % sulphide-sulphur will not generate AMD, regardless of the neutralization potential value. Price, Morin and Hutt (1997), however, used a screening criterion of 0.3 wt % sulphide-sulphur to identify potentially acid generating mine waste. Rock with sulphide-sulphur content < 0.3 wt % is considered unlikely to generate acid.

However, 10 of 29 Tertiary lignite samples of the Cenozoic Detrital (CzD) 2 strata having between >0.1 wt % and 0.9 wt % total sulphur had NAG pH > 4.5 as can be seen in the upper right quadrant of Figure 4.7.a. Also, 7 of 62 black shale samples of the Nammuldi Member of Marra Mamba Formation with total sulphur ≥0.1 wt % had NAG_{pH} >4.5 (in the upper right quadrant of Figure 4.7.b).

Details of these 17 samples including their stratigraphy and their acid base accounting and NAG test data are presented in Table 4.4. These discrepancies can be attributed to:

- total sulphur partly or totally presented as non-acid forms
- concentration of minerals capable of neutralizing the acidity generated during the sulphide oxidation.

Neutral NAG pH of black shale samples from the Nammuldi Member can be explained from their quite high ANC values, since these rocks are characterized by enrichment of both sulphide and carbonate minerals. By contrast, for 10 of the Tertiary lignite-bearing clay samples collected from the sequence of CzD 2, their low ANC values cannot explain a neutral NAG pH. One possible explanation is that the sulphur mainly occurs in unreactive sulphur form, such as organically bounded sulphur associated with the organic matter (maceral).). Casagrande, Finkelman, and Caruccio (1989) observed that coal organic sulphur is unreactive even in strongly oxidising conditions of peroxide and thus concluded that organic sulphur is a non-participant in acid generation.

In addition, the extreme conditions of the NAG test; oxidation at high temperature for some hours, probably caused dissolution of normally resistant silicate minerals releasing additional alkalinity (Weber, 2003; Stewart, 2005). Nevertheless, it is important to note that the result of the NAG test does not precisely reflect the equivalent acid neutralizing capacity of the rock samples, as the ANC test provides.

Table 4.4. Detail of the black shale samples with TS >0.1wt % and NAG pH >4.5

No	Sample ID	Stratigraphy	Rock Type	Acid Base Accounting						NAG Test Data	
				Total S	S- SO_4	S-Sulfide	MPA	ANC	NAPP	NAG pH	NAG Acidity to pH 7.00
				wt %			(kg H_2SO_4/t)				(kg H_2SO_4/t)
1	SJ1102D-002	TD 2	Lignite	0.22	0.02	0.20	6.18	6.13	0.05	7.50	0.00
2	SJ1102D-004	TD 2	Lignite	0.15	0.02	0.13	3.98	0.00	3.98	8.24	0.00
3	SJ0772D-010	TD 2	Lignite	0.43	0.05	0.38	11.69	0.00	11.69	8.27	0.00
4	SJ0772D-011	TD 2	Lignite	0.42	0.02	0.40	12.34	3.33	9.01	8.04	0.00
5	SJ0772D-014	TD 2	Lignite	0.65	0.03	0.62	18.92	0.00	18.92	8.77	0.00
6	SJ0727D-016	TD 2	Lignite	0.72	0.02	0.70	21.52	0.00	21.52	8.45	0.00
7	SJ0772D-020	TD 2	Lignite	0.13	0.01	0.12	3.67	0.00	3.67	8.65	0.00
8	SJ0772D-022	TD 2	Lignite	0.17	0.01	0.16	5.01	3.34	1.67	9.61	0.00
9	SJ0845RDT-008	TD 2	Lignite	0.13	0.06	0.07	2.25	0.00	2.25	4.75	1.94
10	SJ0845RDT-014	TD 2	Lignite	0.12	0.02	0.10	3.18	0.05	3.13	6.70	0.35
11	SJ0847D-025	MU	Black shale	0.40	0.03	0.36	11.1	12.71	-1.57	7.28	0.00
12	SJ0847D-026	MU	Black shale	0.13	0.00	0.13	3.86	49.25	-45.4	8.26	0.00
13	SJ0847D-027	MU	Black shale	0.31	0.01	0.30	9.21	48.14	-38.9	7.00	0.00
14	SJ0847D-028	MU	Black shale	0.16	0.00	0.15	4.63	6.98	-2.35	7.31	0.00
15	SJ0847D-031	MU	Black shale	2.29	0.02	2.27	69.5	85.02	-15.6	7.58	0.00
16	SJ0847D-034	MU	Black shale	1.53	0.03	1.50	46.0	55.13	-9.13	7.06	0.00
17	SJ0848D-021	MU	Black shale	0.1	0.00	0.10	2.99	70.93	-67.9	7.53	0.00

Furthermore, the correlation between NAG acidity and total sulphur shows a very strong coefficient, 0.99, for lignite samples of the Tertiary detrital sequence and black shale of the Undifferentiated Jeerinah Formation as shown in Figures 4.8. a and b. The slope of the line, 28, is close to the value of 30.6, used to calculate maximum potential acidities from wt % total sulphur. So this indicates good agreement between measured and calculated acidities, minus some neutralization that takes place.

To a lesser extent, black shale samples of the Nammuldi Member showed a lower correlation between their NAG acidity and total sulphur. This may be understood due to their moderate to high value of ANC neutralizing the sulphide generated acidity during the NAG testing. Whereas, mudstone and BIF samples having low total sulphur and neutralizing capacity resulted in very poor correlation between NAG acidity and total sulphur.

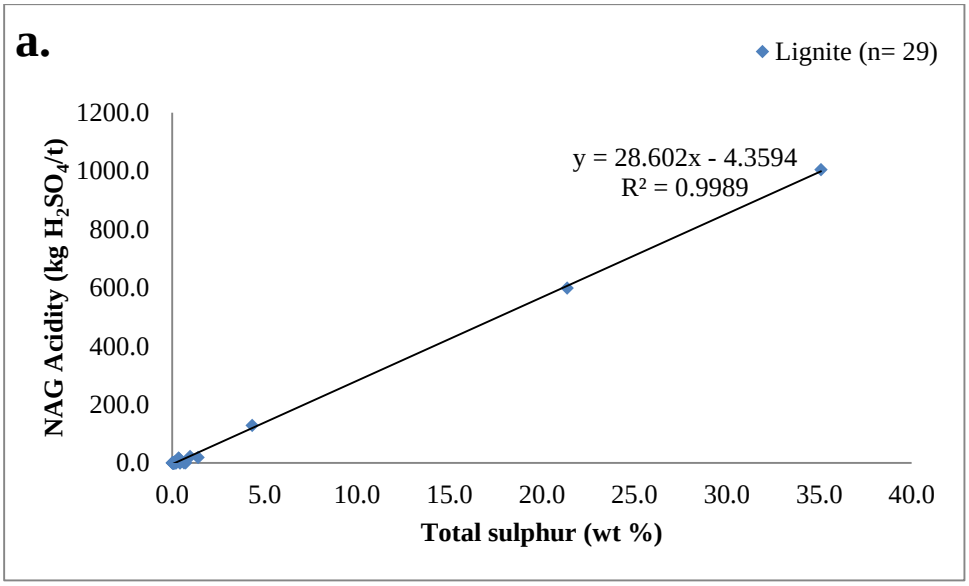

Figure 4.8. Correlation of $NAG_{pH\ 7.0}$ acidities and total sulphur for 144 samples of potential waste rock from the South Jimblebar prospect.

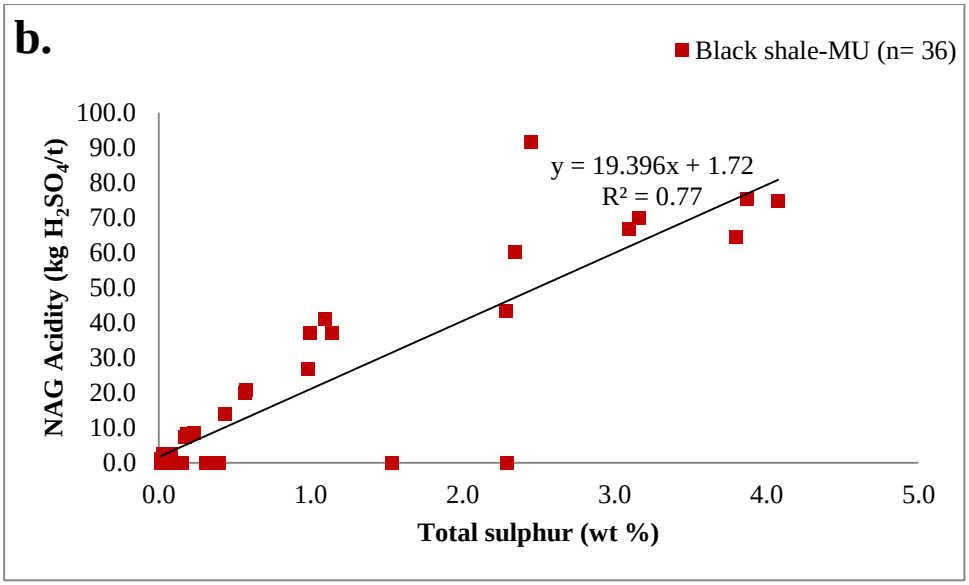

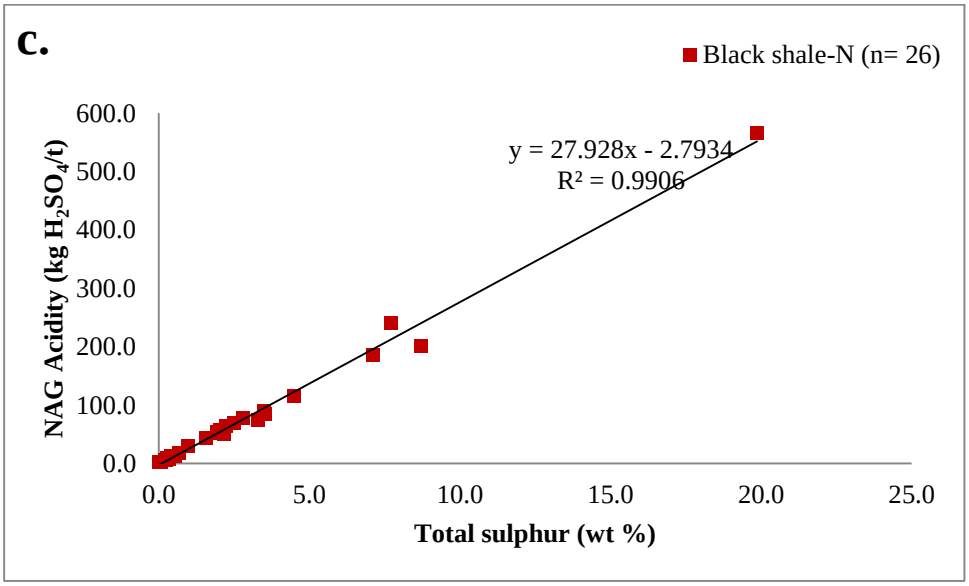

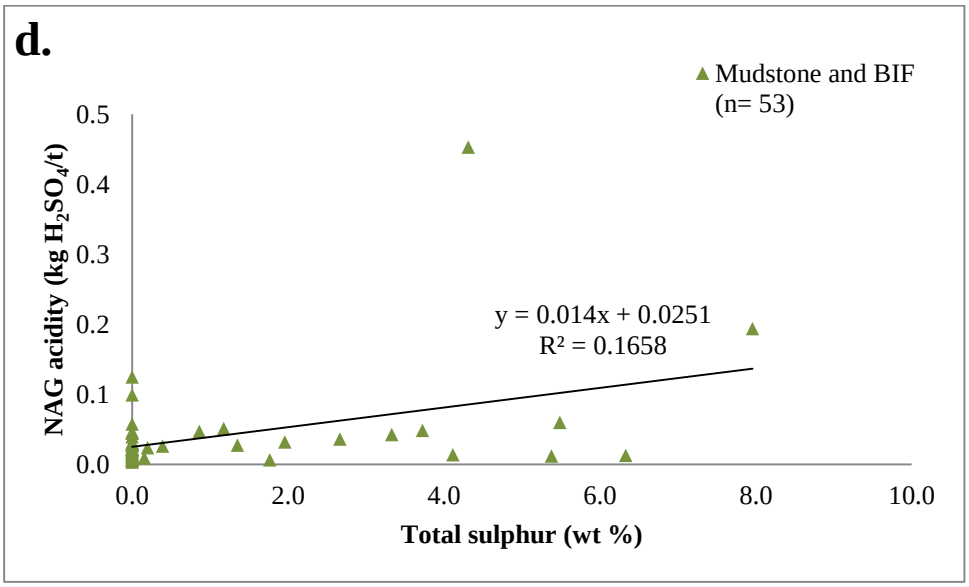

Figure 4.8. (Continued)

4.5. Geochemical Classification and Comparison of Static Techniques

4.5.1. Comparison Paste pH and NAG pH

The rock cores from which samples were sourced for the present study had been stored for more than 3 years after drilling before analysis. Therefore, there was opportunity for chemical weathering to occur, including oxidation of sulphide minerals. Framboidal and very fine-grained euhedral pyrite may be rapidly oxidized and produce sulphate salts, e.g. jarosite and melanterite, representing a source of sulphate acidity (Jambor and Blowes, 1998; White et al., 1999; Weber et al., 2004).

Since the secondary sulphates salts may be readily soluble in water and dissolution releases H^+ ions, their presence can be recognized by a low pH of powdered rock-water slurry. Figure 4.9 demonstrates the relation between paste pH and sulphate-sulphur of 144 waste rock samples. There is a general pattern of lower paste pH with increasing sulphate-sulphur.

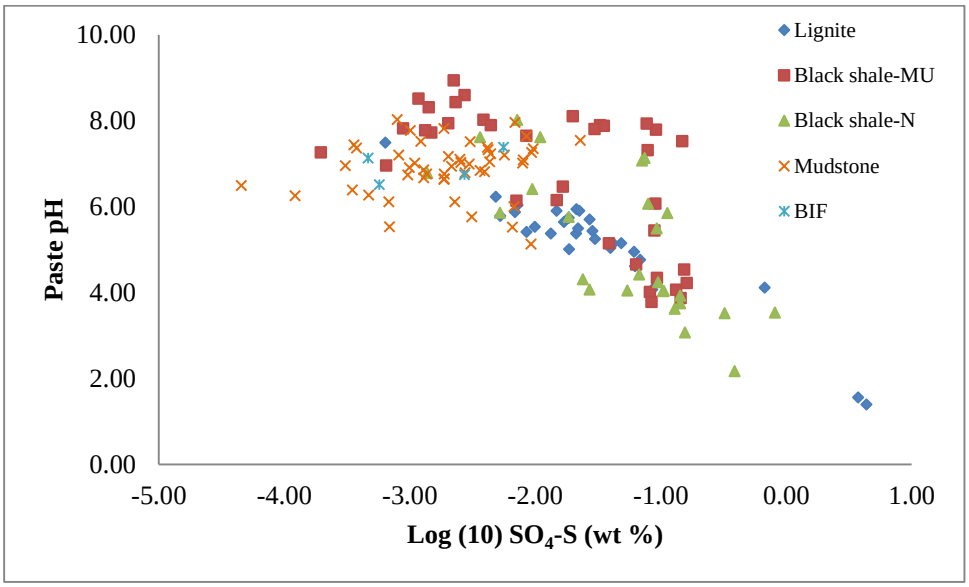

Figure 4.9. Correlation between paste pH and sulphate-sulphur recorded from 144 prospective waste rock samples from South Jimblebar.

Perry (1998) reported that sulphate minerals are usually present in significant quantities only in weathered spoil or refuse; and otherwise absent from fresh overburden in Pennsylvania's coal mines. Consequently, paste pH is indicative of the propensity to generate acid only in the case of weathered rock samples (Kania, 1998). A water-rock slurry (paste) with pH <4-5 indicates that the rock probably

contains sulphate acidity in the form of secondary mineral product of sulphide oxidation (Mohrin and Hutt, 1997; Weber 2003; and Stewart, 2005).

A comparison of paste pH and NAG pH (Fig. 4.10) reveals the true relationship of the inherent acidic condition (sulphate acidity) of the waste rock samples and their potential to produce acidity (AMD). If a NAG pH of <4.5 is taken to be indicative the presence of strong mineral acid, and a paste pH of < 5 is taken to be indicative of a propensity to generate AMD, then paste pH may correctly reflect a waste rock's acid generating capacity for dominant samples tested in this study.

In general, the correlation between paste pH and NAG pH for lignite and mudstone samples indicate a good agreement in distinguishing acid capacity of the samples. However, samples in the upper left quadrant, mainly black shale collected from Nammuldi Member and Undifferentiated Jeerinah Formation, show anomalous character where their slightly neutral to basic paste pH (>5) was in contrast to their low NAG pH (<4.5). Black shale samples of the Nammuldi Member (Figure 4.11) were enriched with not only pyrite but also carbonate minerals, such as calcite, dolomite and siderite, whereas black shale samples from Jeerinah Formation were high sulphur and low neutralizing capacity.

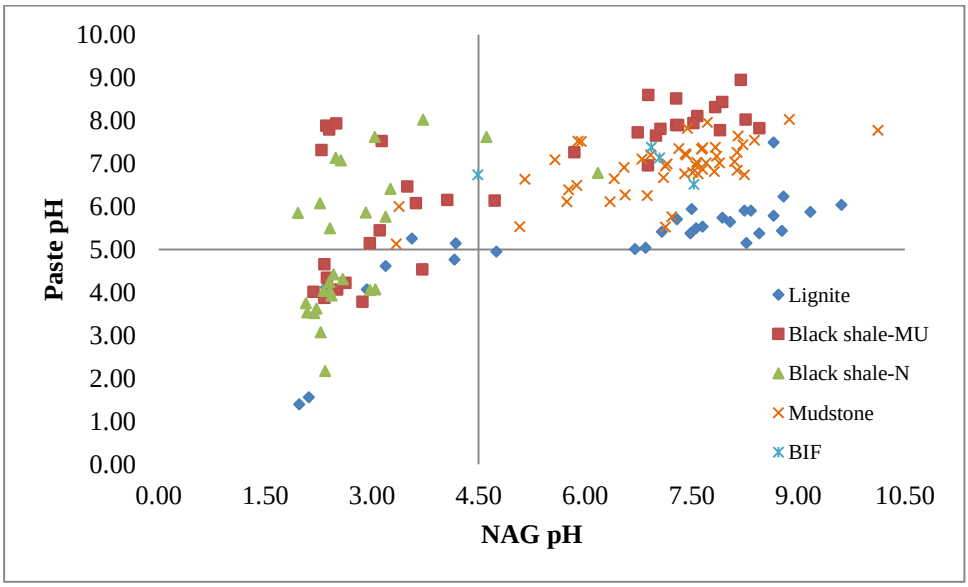

Figure 4.10. Comparison between paste pH and NAG pH of 144 prospective waste rock samples from South Jimblebar.

Figure 4.11. Black shales of the Nammuldi Member yielding conflicting neutral paste pH and low NAG pH. These samples have not only a significant sulphur content (3 wt %), but also an appreciable neutralizing capacity (16 kg H_2SO_4/t).

Fast reacting carbonate, such as calcite, probably initially reacted in the slurry producing neutral to basic paste pH. However, dolomite and siderite dissolution occurs more slowly in normal conditions (without strong oxidant at normal temperature), so that standing time for paste pH measurement (12 hours) is not enough to complete the reaction. Furthermore, strongly oxidizing conditions in the NAG test are designed to ensure complete oxidation of all chemically-reduced sulphur, which does not occur in the paste pH test. The weakly acid paste pH in samples from the Undifferentiated Jeerinah Formation probably was due to their sulphide minerals being in unweathered euhedral forms that are slow to oxidise. Conversely, lignite contained sulphide that may be in the form of fine grain framboidal pyrite has a greater specific surface area. Lignite bearing clay in South Jimblebar was formed from relatively young transported rock debris sedimented in a palaeovalley, so that some sulphide contents of its parent rock may have been

weathered producing secondary sulphate minerals in the subsequent sedimentary rock (lignite). Moreover, the formation of framboidal pyrite in the Tertiary detrital units is made possible through the abundance of iron and secondary sulphate occurring under anoxic conditions, as explained in previous research by Kolker (2012).

It may be concluded that paste pH has a limited capacity to project the tendency of rock to generate AMD for samples containing unoxidised sulphide and/ or fast reacting carbonate. Neutral to basic paste pH does not necessarily define the sample as non-acid forming. Weber (2003) suggested that samples having a paste pH greater than pH 7 and classified as potentially acid forming, will have an initial lag prior to acid formation in the kinetic NAG test and the column leach test. Moreover, Price (1997) recommends that rocks with sulphide-sulphur <0.3 wt % and a paste pH >5.5 require no further AMD testing and are considered safe to excavate if there is no concern for other metal leaching.

4.5.2. Comparison of NAG and NAPP Results

The use of final NAG pH in conjunction with calculated NAPP is widely used in initial classification of the acid generating potential of the rock (AMIRA, 2002; Pope *et al*, 2010). In a recent study by DoITR (2007), samples were classified according to the recommended scheme shown in Table 4.5. The combined use of NAPP and NAG pH reduces the risk of misclassifying material and, therefore, increases the reliability of AMD prediction. A plot of NAG pH and NAPP is presented at Fig.4.12 and Fig.4.13 for carbonaceous and non-carbonaceous rocks, respectively.

Table 4.5. Typical geochemical classification criteria based on NAPP and NAG pH (DoITR, 2007)

Primary Geochemical Material Type	NAPP (kg H_2SO_4/t)	NAG pH
Potentially Acid Forming (PAF)	> 5*	< 4.5
Potentially Acid Forming -Low Capacity (PAF-LC)	0 - 5*	< 4.5
Non Acid Forming (NAF)	Negative	≥ 4.5
Acid Consuming (ACM)	< -100	≥ 4.5
Uncertain	Positive	≥ 4.5
	Negative	< 4.5

*Site specific but typically in the range 5 – 20 kg H_2SO_4/t.

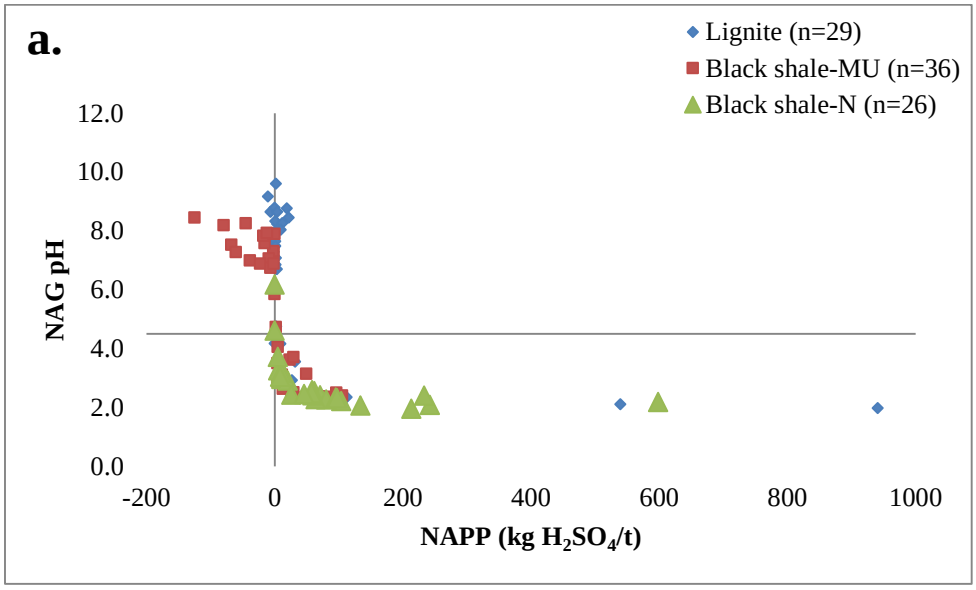

Figure 4.12. a. AMD classification plot of carbonaceous rocks; b. Enlarged view of NAPP axis region of Fig.4.10.a.

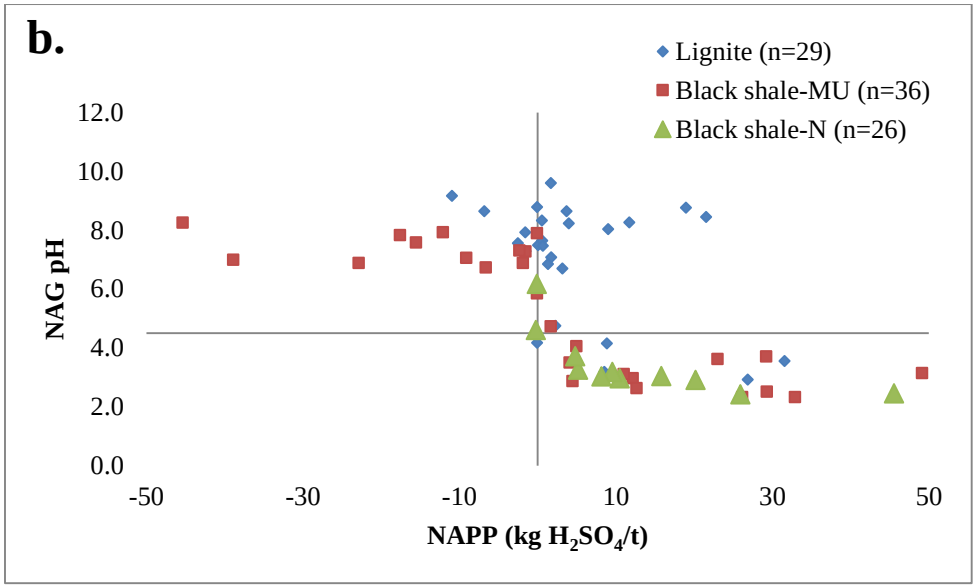

Figure 4.12. (Continued)

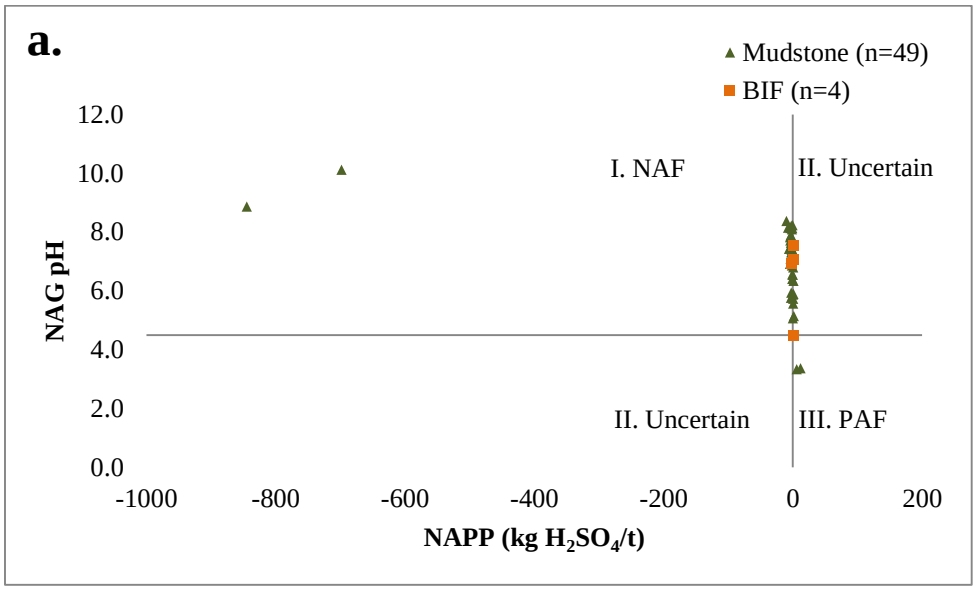

Figure 4.13. a. AMD classification plot of non-carbonaceous rocks; b. Enlarged view of NAPP axis region of Fig.4.10.a.

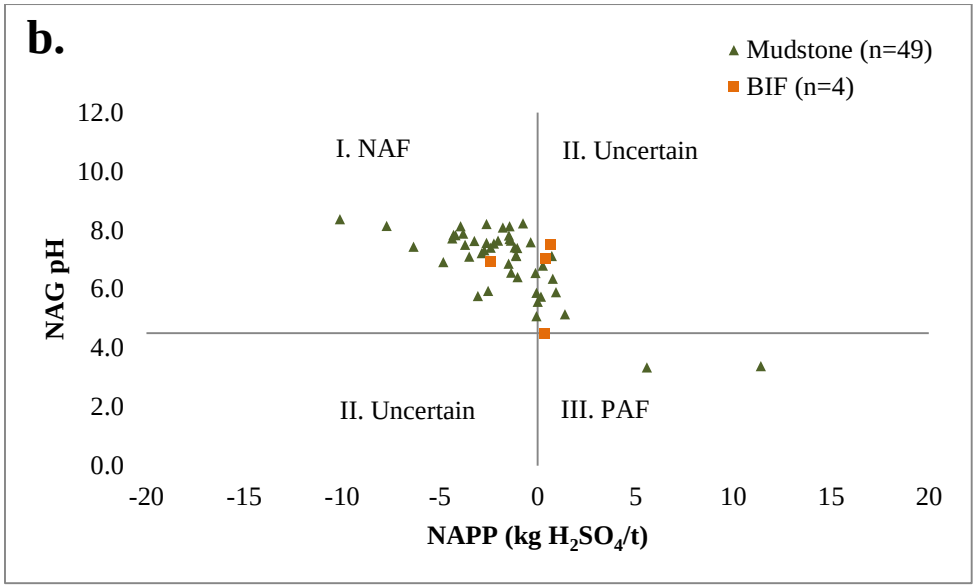

Figure 4.13. (Continued)

Figure 4.12 and Fig. 4.13 show that a comparison of NAG pH versus NAPP for 144 samples in the present study is generally consistent in plotting the samples within either the NAF or PAF domains. However, there are 24 samples which plotted as "uncertain". A total of 23 samples plotted in the upper right uncertain domain or quadrant II (indicating positive NAPP, but NAGpH >4.5), and another one plotted in the lower left uncertain domain or quadrant IV (negative NAPP, but NAGpH< 4.5). The proportion of the prospective waste rocks falling into each classification is given in Table 4.6.

Table 4.6. Summary of the results of waste rock classification according to the scheme of DoITR 2007

Rock Group	Rock Type	n	NAF	ACM	PAF	PAF-LC	UC (NAF)	UC (PAF)
Carbonaceous	Black Shale	62	19		37	5	1	
	Lignite	29	7		7		14	1
Non-carbonaceous	Mudstone	49	39	2	2		6	
	BIF	4	1			1	2	
Total (%)			46	1	32	4	16	1

Detailed geochemical characteristics of the 24 uncertain samples are presented in Table 4.7.

Table 4.7. Detail information of uncertain classified rocks

No	Sample ID	Stratigraphy	Rock Type	Total S	S-SO_4	S-Sulfide	TPA	ANC	NAPP	NAG Test Data			DoITR 2007, Classification
				wt %			(kg H_2SO_4/t)			NAG pH	NAG to pH 4.5	NAG to pH 7.00	
											(kg H_2SO_4/t)		
1	SJ0845RD-007	TD 2	Lignite	0.12	0.04	0.08	2.44	2.50	-0.07	4.18	0.10	2.45	UC (PAF-LC)
2	SJ0845RD-008	TD 2	Lignite	0.13	0.06	0.07	2.25	0.00	2.25	4.75	0.00	1.94	UC (NAF)
3	SJ0845RD-009	TD 2	Lignite	0.08	0.04	0.04	1.31	0.00	1.31	6.85	0.00	0.06	UC (NAF)
4	SJ0845RD-010	TD 2	Lignite	0.05	0.01	0.04	1.32	0.75	0.58	7.65	0.00	0.00	UC (NAF)
5	SJ0845RD-011	TD 2	Lignite	0.06	0.01	0.05	1.49	0.84	0.64	7.48	0.00	0.00	UC (NAF)
6	SJ0845RD-013	TD 2	Lignite	0.06	0.01	0.06	1.71	0.00	1.71	7.08	0.00	0.00	UC (NAF)
7	SJ0845RD-014	TD 2	Lignite	0.12	0.02	0.10	3.18	0.05	3.13	6.70	0.00	0.35	UC (NAF)
8	SJ1102D-004	TD 2	Lignite	0.15	0.02	0.13	3.98	0.00	3.98	8.24	0.00	0.00	UC (NAF)
9	SJ1102D-006	TD 2	Lignite	0.03	0.01	0.02	0.51	0.00	0.51	8.33	0.00	0.00	UC (NAF)
10	SJ0772D-010	TD 2	Lignite	0.43	0.05	0.38	11.69	0.00	11.69	8.27	0.00	0.00	UC (NAF)
11	SJ0772D-011	TD 2	Lignite	0.42	0.02	0.40	12.34	3.33	9.01	8.04	0.00	0.00	UC (NAF)
12	SJ0772D-014	TD 2	Lignite	0.65	0.03	0.62	18.92	0.00	18.92	8.77	0.00	0.00	UC (NAF)

Table 4.7. Continued

No	Sample ID	Stratigraphy	Rock Type	Total S	S-SO_4	S-Sulfide	TPA	ANC	NAPP	NAG Test Data			DoITR 2007, Classification
				wt %			(kg H_2SO_4/t)			NAG pH	NAG to pH 4.5	NAG to pH 7.00	
											(kg H_2SO_4/t)		
13	SJ0727D-016	TD 2	Lignite	0.72	0.02	0.70	21.52	0.00	21.52	8.45	0.00	0.00	UC (NAF)
14	SJ0772D-020	TD 2	Lignite	0.13	0.01	0.12	3.67	0.00	3.67	8.65	0.00	0.00	UC (NAF)
15	SJ0772D-022	TD 2	Lignite	0.17	0.01	0.16	5.01	3.34	1.67	9.61	0.00	0.00	UC (NAF)
16	SJ0845RD-017	TD 2	Mudstone	0.04	0.01	0.04	1.16	0.44	0.72	7.13	0.00	0.00	UC (NAF)
17	SJ 0848D-008	MN N3	Mudstone	0.02	0.00	0.02	0.66	0.39	0.27	6.80	0.00	0.20	UC (NAF)
18	SJ 0847 D-009	MN N2	BIF	0.01	0.00	0.01	0.43	0.00	0.43	7.05	0.00	0.00	UC (NAF)
19	SJ 0847 D-010	MN N1	BIF	0.02	0.00	0.02	0.64	0.00	0.64	7.53	0.00	0.00	UC (NAF)
20	SJ 0847 D-154.2	MM	Mudstone	0.03	0.00	0.02	0.76	0.00	0.76	6.35	0.00	1.35	UC (NAF)
21	SJ 0847 D-017	MU	Black Shale	0.08	0.01	0.07	2.19	0.52	1.67	4.73	0.00	2.70	UC (NAF)
22	SJ 0848D-017	MU	Mudstone	0.03	0.00	0.03	0.94	0.00	0.94	5.90	0.00	1.96	UC (NAF)
23	SJ 0848D-018	MU	Mudstone	0.01	0.00	0.01	0.17	0.00	0.17	5.74	0.00	1.76	UC (NAF)
24	SJ 0848D-051	MU	Mudstone	0.06	0.00	0.06	1.77	0.39	1.38	5.15	0.00	5.49	UC (NAF)

The uncertain classification recorded for 24 waste rock samples may be explained, as follows:

1. Mostly uncertain samples (16 of 24 samples) were Tertiary lignite from the CzD 2 sequence. Organic material is frequently associated with unreactive organic sulphur, so that the NAPP calculations overestimated the maximum acid potential (Schumann, 2012).
2. NAPP values of all the uncertain samples, except some lignite samples highlighted in grey color in Table 4.7, are very low (<5 kg H_2SO_4/t). The classification in such cases may be accounted for by the uncertainty in the measurement of total sulphur and ANC. It should be noted that duplication of total sulphur (40 of 144 samples) and ANC (41 of 144 samples) analyses resulted in relative percent difference at 3.04% and 3.11%, respectively.

Point 1 is consistent with the findings of section 4.3 which explained that 10 of 29 lignite samples with total sulphur up to 0.9 wt % and containing no or very low neutralizing capacity yielded NAG pH >4.5.This finding indicated that lignite may contain some degree of non sulphide-sulphur.

Chou (2012) reported that in low-sulphur coal (<1 % S), sulphur is derived primarily from parent plant material, whereas for higher sulphur coals there is additional sulphate derived from seawater that flooded peat swamp and was a major source of sulphide-sulphur. However, it is highly unlikely that seawater played any part in the sediments in South Jimblebar's Tertiary detrital unit. Therefore, the sulphur is probably derived from the breakdown of the high pyrite content of the black shales of the surrounding rocks (allogeneic sulphur) (R. C. Morris, personal communication, December 20, 2012). Moreover, sulphur in lignite rock may be in the form of secondary minerals, such as gypsum and jarosite. Authigenic pyrite formation may also have occurred in a reducing environment in the presence of secondary sulphate minerals and decomposable organic material.

Besides NAG pH, the result of NAG testing also was reported in NAG acidity. The NAG acidity describes net actual potential acidity of the rock. The linear regression between NAG acidity to pH 7.00 and calculated NAPP (Figures 4.14) indicates strong coefficient correlations, R^2 >0.9, for Tertiary detrital lignite and black shale of the Undifferentiated Jeerinah Formation. A lower value of the coefficient is showed for black shale of the Nammuldi Member with R^2 of 0.66,

while mudstone and BIF samples show very poor correlation between NAG acidity and calculated NAPP with R^2 of 0.28. Note that sample with NAG pH >7 was assumed produced 0.00 kg H_2SO_4/t acidity. In addition, two calcrete samples (SJ0772D-004 and SJ0772D-005) with very high ANC are excluded from the figure of mudstone (Fig.4.4.d).

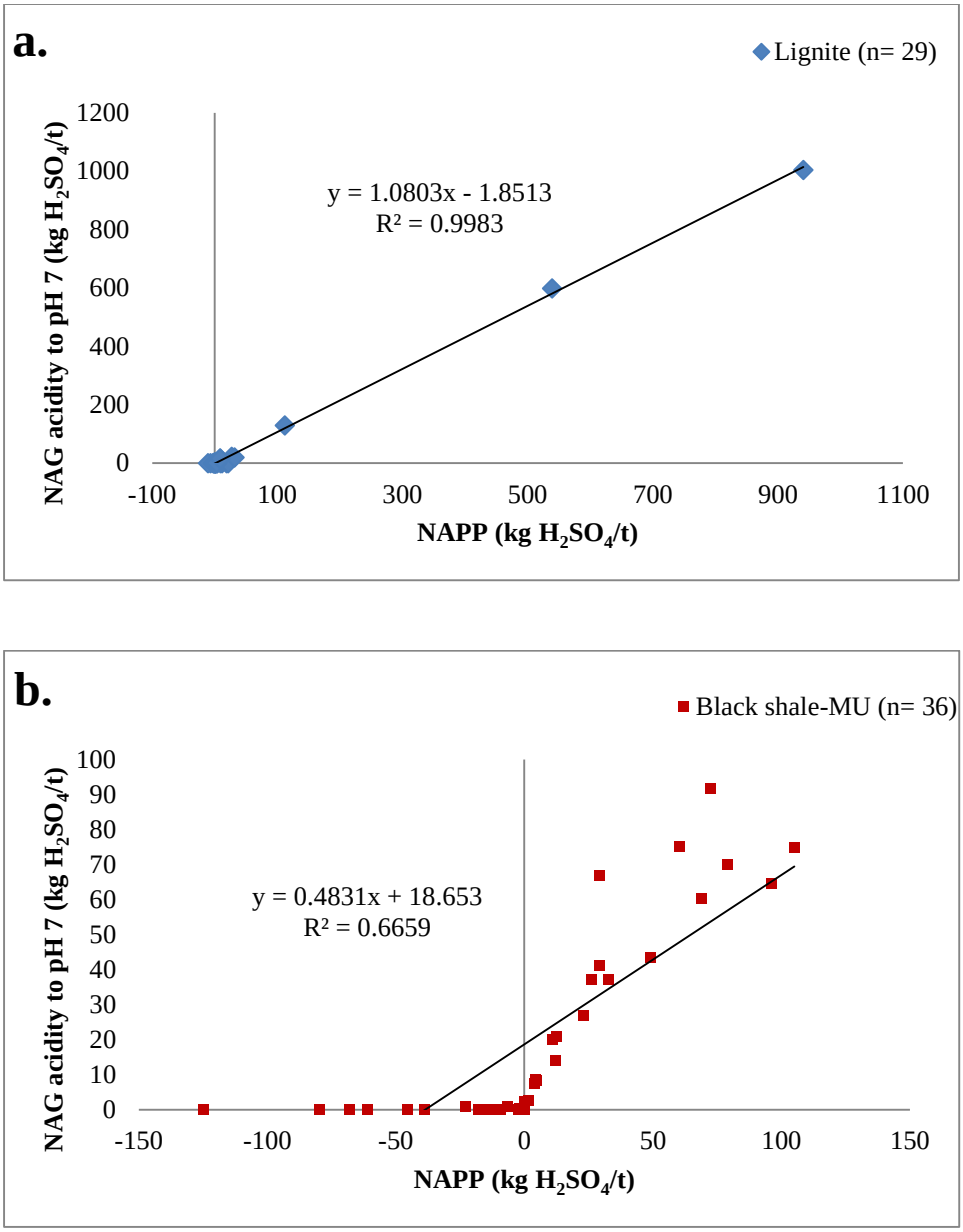

Figure 4.14. Correlation between $NAG_{pH\ 7.0}$ acidity and calculated NAPP for 142 of the 144 tested waste rock samples from South Jimblebar.

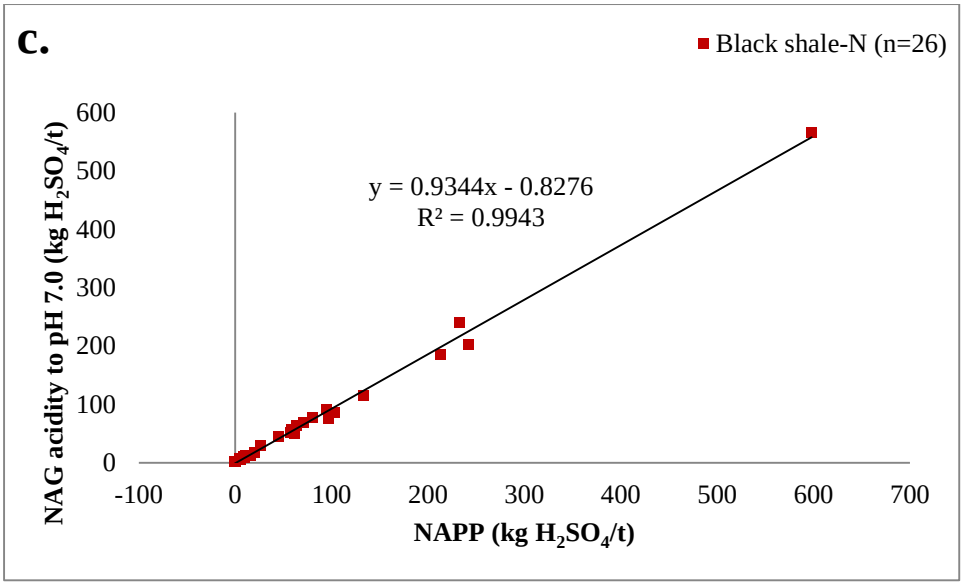

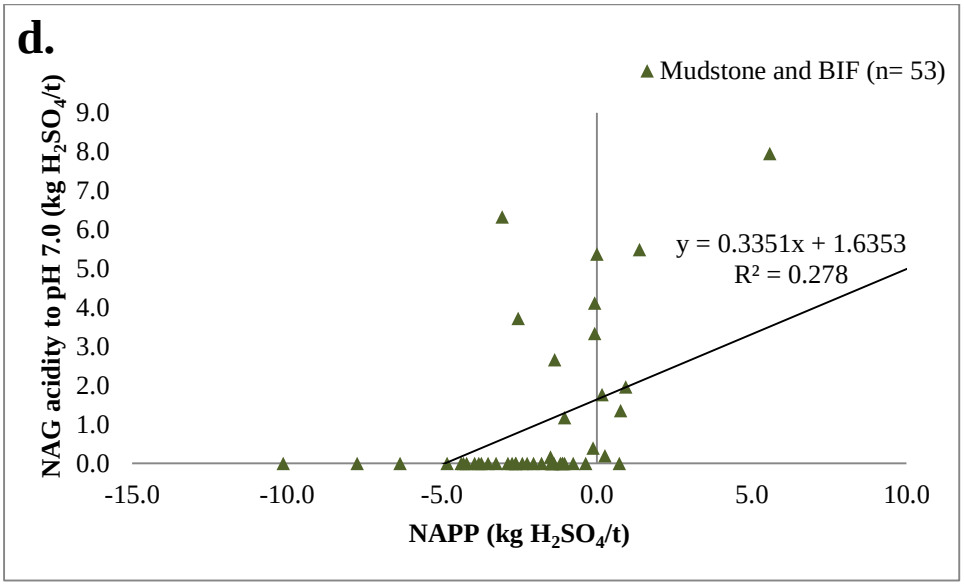

Figure 4.14. (Continued)

Generally, lignite and black shale of the Undifferentiated Jeerinah Formation were of high sulphur content and low neutralization capacity, while black shale of the Nammuldi Member showed enrichment in both sulphur and neutralizing capacity. In contrast, mudstone samples, except of calcareous rocks of CzD 2 unit, had very low sulphur and neutralizing capacity. From Figures 4.12, it can be seen that NAG testing can be valuable as a quantitative indicator of potential acidity for high sulphur samples with very low neutralizing capacity. Conversely, the NAG test cannot precisely reflect the neutralization capacity as determined by the ANC test as included in calculated NAPP value.

Nevertheless, a total of 67 of 144 samples having negative NAPP were correlated to their NAG pH as plotted in Figures 4.15. The figures display samples with negative NAPP mostly resulting in NAG pH >5.5. In other words, NAG pH >5.5 indicates that the rock sample contains excess neutralizing capacity. This value was lower than previous research (Pope *et al*., 2010) who suggested NAG pH >6.5 as a typical value.

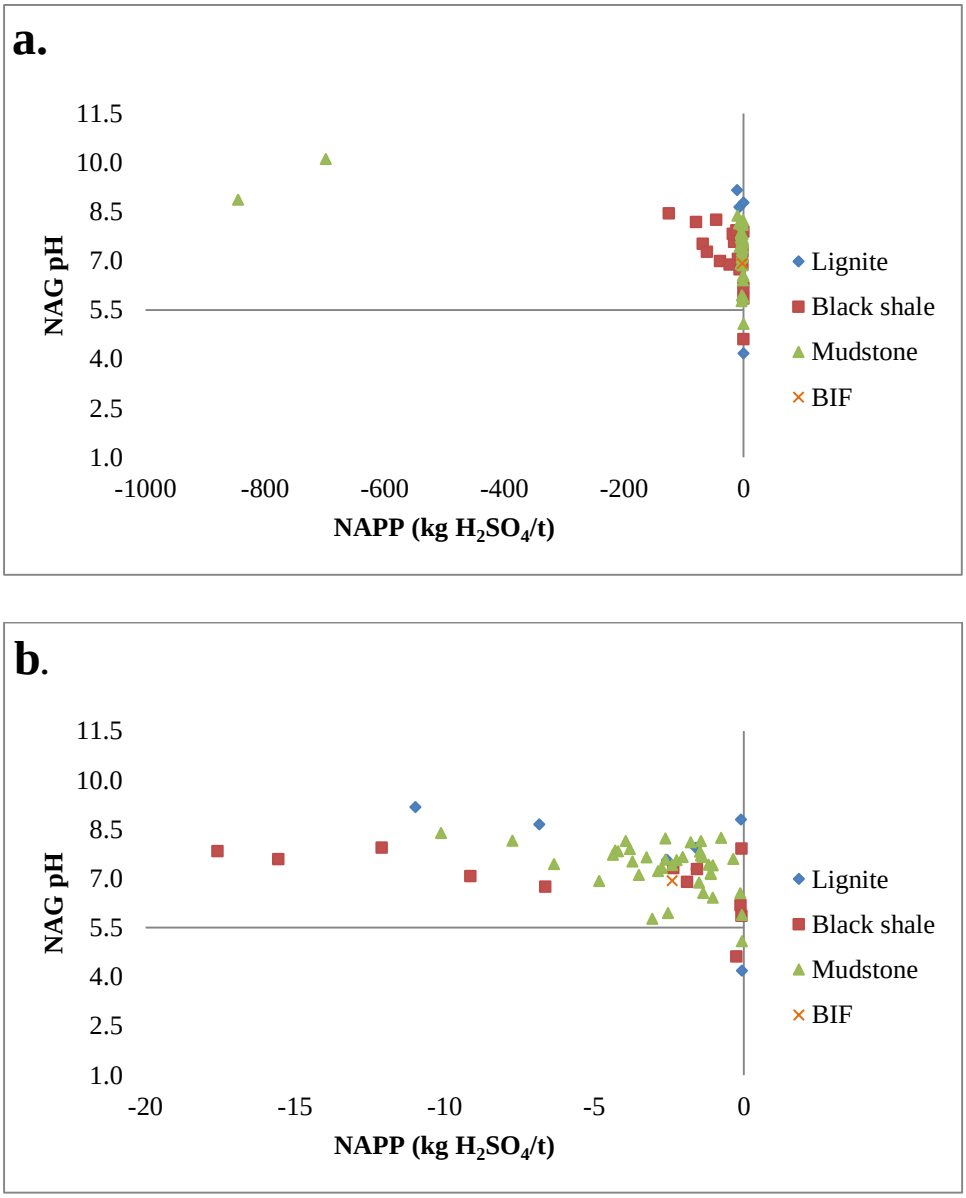

Figure 4.15. a. Correlation between negative NAPP and NAG pH for 67 of the 144 tested waste rock samples from South Jimblebar; b. Enlarged view of axis region of Fig. 4.15.a.

Overall, the results from the present study show that the acid base accounting and net acid generating (NAG) test are sufficient for initial screening for the acid generating potential of waste rocks at a future South Jimblebar mine.

4.6. Trace Elemental Abundance

Trace element analysis of selected prospective waste rock samples has been undertaken to identify the leachable concentrations of elements of environmental significance that may be released during mining and storage of waste rock. Partial digestion of powdered rock samples using a hot mixture of nitric (HNO_3) and perchloric acid ($HClO_4$) to decompose the minerals in the rock is considered to leach the maximum amount of each element that might be released under the most extreme degree of long-term natural weathering. It should be noted that highly resistant silicate and oxide minerals are not wholly digested in this process, and consequently the results are not equivalent to those of a whole rock analysis (Price, 2009; Watkins, 2012).

The average concentration of concerned trace metals and metalloids in this study, as well as median soil abundance for a comparison are given in Table 4.8. These include all 21 elements that are categorized as priority toxic elements to life forms by Siegel (2002); Sparks (2005); Allen (2010); Brown and Calas, (2011).

Lignite had the highest average concentration of various elements of environmental importance, namely Be, Sc, V, Cr, Co, Ni, As, Mo, Sb, Tl, Pb, and U. Black shale showed the highest concentration of leachable Cu, Zn, Se, Ag, and Cd, whereas mudstone indicated the most significant level in Ti, Mn, Hg, and Th.

The trace element enrichment in Tertiary detrital lignite can be explained by two mechanisms (E. Perry, personal communication, March 16, 2013). First is the presence of organic material that was once plant tissue. Since plants uptake numerous elements, those elements can be retained in the organic fraction that ends up in the rock. The elements may be chemically bound directly to organic compounds or held on clay minerals included in the rock.

Table 4.8. Average concentration of 21 potentially toxic elements and medians of elemental composition of soils.

No	Element	Median Soil Abundance (Bowen, 1979)	Black Shale		Lignite	Mudstone
			MU	N		
			(n=10)	(n=8)	(n = 7)	(n = 6)
		Average concentration (ppm)				
1	Be	0.3	0.57	0.53	5.86	1.22
2	Sc	7	4.80	3.05	11.3	8.59
3	Ti	5000	60.8	76.1	204	233
4	V	90	17.5	27.2	77.8	51.2
5	Cr	70	42.4	39.3	89.3	62.5
6	Mn	1000	295	44.2	102	2645
7	Co	8	16.7	20.2	35.7	13.5
8	Ni	50	34.4	40.2	137	31.0
9	Cu	30	134	102	45.4	45.3
10	Zn	90	190	581	73.2	45.4
11	As	6	4.12	14.5	127	10.9
12	Se	0.4	0.41	5.20	2.30	0.48
13	Ag	0.05	0.68	0.22	0.03	0.06
14	Mo	1.2	0.09	0.57	3.56	0.68
15	Cd	0.35	0.06	4.67	0.10	0.05
16	Sb	1	0.02	0.03	3.82	0.04
17	Hg	0.06	0.31	0.32	0.47	0.60
18	Tl	0.2	0.15	0.76	6.11	0.05
19	Pb	35	11.0	29.7	35.0	12.30
20	Th	9	5.21	2.31	6.56	6.70
21	U	2	0.69	1.47	6.80	1.73

Note:
- Numbers in red color indicate the highest average concentration among the rock sample types.
- MU : black shale of the Nammuldi Member of Marra Mamba Formation
- N : black shale of the Undifferentiated Jeerinah Formation

Second is the environment that the rock forms in. Tertiary lignite may form in swamps or lacustrine environment, which also receive transported sediment from surrounding land that has suffered weathering and erosion. The terrigenous material transported into the swamps can be the source of trace elements. Because materials

are not removed from the wetland after deposition, the trace elements accumulate there.

The concentrations of potentially toxic trace elements (Appendix C) were compared to the median soil abundance (Bowen, 1979) as given in Table 4.8 to highlight relative degrees of enrichment. The extent of enrichment is reported as the Geochemical Abundance Index (GAI) presented in Table 4.8, Table 4.9, and Table 4.10; respectively for lignite, mudstone, and black shale samples. It is generally considered that a GAI of 3 or greater (>12 fold enrichment) signifies that the element is likely to be environmental concern (Green and Borden, 2011).

The GAI results show that lignite samples display the most varied enrichment with As, Be, Co, Mo, Se, Sb, and Tl, enriched in the 3 to 7 GAI range in at least one sample. Also, Sc, Ni, Cu, and U indicated slight enrichment in more than one lignite sample. Arsenic, Se, and Tl consistently exhibited significant enrichment in the black shale samples from the Undifferentiated Jeerinah Formation. In addition, GAI values of 3-6 were also found for Ag, Cd and Zn in the black shale samples of the Undifferentiated Jeerinah Formation. In the case of black shale of the Nammuldi Member, appreciable enrichment is found in Zn and Ag, and slight enrichment in Be, Co, and Cu. In contrast, mudstone was only noticeably enriched in Be and Mn in a single sample.

Kolker (2012) reported iron disulphide in coal that mainly pyrite and marcasite are important carries of minor and trace elements of environmental interest. The elements present reflect substitution in the iron disulphide crystal structure, for either S or Fe (Abraitis *et al*., 2004). Based on favorable size and charge characteristics, As, Se and Sb can substitute for S in the pyrite structure. Co, Cu, Ni, Mo, Tl and Zn can substitute for Fe in the pyrite crystal because they are similar in ionic size and chemical properties to iron (Kolker, 2012). Trace elements can also occur as trace sulphide, such as sphalerite (ZnS), chalcopyrite ($CuFeS_2$), galena (PbS), and cinnabar (HgS). Thus, the high sulphur of lignite and black shale can also explain their enrichment of various toxic elements.

Table 4.9. Geochemical Abundance Index (GAI) of potentially toxic metals of lignite samples

No	Sample ID	Stratigraphy	Be	Sc	Ti	V	Cr	Mn	Co	Ni	Cu	Zn	As	Se	Ag	Mo	Cd	Sb	Hg	TI	Pb	Th	U
1	SJ0772D-016	TD 2	2											2									
2	SJ0772D-019	TD 2	1											1					1				
3	SJ0785D-005	TD 2	1						**3**	2			**6**	1		**3**		**4**		**7**			2
4	SJ0785D-003	TD 2	2						2	1			**5**	2		2		**3**		**6**			2
5	SJ1102D-002	TD 2	**4**	1					1					2									1
6	SJ1102D-006	TD 2	**6**	1					2	1	1			**3**							1		2
7	SJ0845RDT-015	TD 2	1	2		1	2		1		1			2									

Table 4.10. Geochemical Abundance Index (GAI) of potentially toxic metals of mudstone samples

No	Sample ID	Stratigraphy	Be	Sc	Ti	V	Cr	Mn	Co	Ni	Cu	Zn	As	Se	Ag	Mo	Cd	Sb	Hg	TI	Pb	Th	U
1	SJ0845RDT-024	WA	**3**					**3**	1		1												
2	SJ0848D-017	MU	1											1									
3	SJ0848D-018	MU													1				2				
4	SJ0848D-041	TD 3	1				1						1										
5	SJ0848D-043	WA	1										1										
6	SJ0849D-002	MN	2								1		1										

Table 4.11. Geochemical Abundance Index (GAI) of potentially toxic metals of black shale samples

No	Sample ID	Stratigraphy	Be	Sc	Ti	V	Cr	Mn	Co	Ni	Cu	Zn	As	Se	Ag	Mo	Cd	Sb	Hg	TI	Pb	Th	U
1	SJ0847D-035	MU	2					1	2			**3**			1					2			
2	SJ0848D-021	MU									2				2								
3	SJ0848D-023	MU									1				2								
4	SJ0848D-024	MU	1						2		2				**6**								
5	SJ0848D-025	MU									2		1		**3**								
6	SJ0848D-026	MU									2												
7	SJ0848D-027	MU							1		2												
8	SJ0848D-028	MU							1		1												
9	SJ0848D-029	MU	1								2	1			**3**								
10	SJ0848D-030B	MU	1									1											
11	SJ0847D-041	N	2						1		2	**3**		1	2		2			**3**			
12	SJ0848D-032	N									2			**3**	1								
13	SJ0848D-033	N									1			2	2								
14	SJ0848D-034	N									1			1	**3**								
15	SJ0848D-035	N											1	**6**			**6**						
16	SJ0848D-037	N									1			1	1								
17	SJ0848D-038	N							2		2		**3**	2	**3**					2	1		
18	SJ0848D-040	N	1						2			**5**		1			2			1			

Note: Values shown in red are elements with GAI ≥3.

4.7. Distribution of Potentially AMD Generating Rock Types and Implication for Waste Rock Management at South Jimblebar Mine

Geochemical characterization of 144 prospective waste rock samples from South Jimblebar suggests that non-acid forming material will dominate the waste rock to be stored at the South Jimblebar iron ore mine. Of the suite of potential waste rock studied, 63% of rocks samples were characterized as non-acid forming (NAF), while the remaining 37% were potentially acid forming (PAF) material. Nevertheless, the occurrence of PAF materials in significant quantities warrants appropriate strategies of waste rock management to prevent the generation of acid mine drainage and to minimize the risk of the dispersion of various potentially toxic elements into the broad environment.

Results from the present study broadly indicate that carbonaceous rocks have the greatest potential to generate acid. These are mainly found within three stratigraphic sequences at South Jimblebar, namely the Cenozoic Detrital (CzD) 2, Nammuldi Member (MU) of the Marra Mamba Formation and the Undifferentiated Jeerinah Formation (N). The extent of potential acid formation from individual waste rock types in each stratigraphic sequence is given in Table 4.12.

Table 4.12. Acid generating potential of major rock types in stratigraphic divisions at South Jimblebar

Stratigraphy	n	PAF	NAF	Rock Sample Type
		%		
Cenozoic Detrital 3 (CzD 3)	6	-	100	Mudstone
Cenozoic Detrital 2 (CzD 2)	44	23	77	Minor mudstone, major Lignite
West Angela Member Undifferentiated (OA)	7	-	100	Mudstone
West Angela Member (WA)	8	-	100	Mudstone
Mount Newman Member (MN)	9	-	100	Mudstone
MacLeod Member (MM)	3	-	100	Mudstone
Nammuldi Member (MU)	41	44	56	Minor mudstone, major black shale
Undifferentiated Jeerinah Formation (N)	26	92	8	Black shale

The main sequence in the South Jimblebar stratigraphy that potentially contributes acidity and may release various toxic elements is the Cenozoic Detrital (CzD) 2 sequence in the mining overburden. This sequence is mainly characterized by Tertiary lignite and lignite-bearing clays that typically contain elevated sulphur levels (Baker and Sike, 2010) and the highest concentration of a variety of elements that have environmental significance. Four of 7 drill cores made available for this study contained the CzD 2 sequence. The 29 lignite samples of 44 selected samples from the CzD 2 unit had highly variable total sulphur grade with an average 2.33 wt %. Sulphur is highly sporadic in distribution and is locally enriched in mineralized lignite rock up to 35.1 wt % sulphur. This is consistent with the observed presence of finely crystalline pyrite dispersed among region of the carbonaceous rocks during sampling. This gives difficulty in determining precisely the overall sulphur content and, thus, acid generating potential of the rock type.

Contrastingly, two mudstone samples collected from the CzD 2 sequence (SJ0772D-004 and SJ0772D-005) had very high acid neutralizing capacity up to 849 kg H_2SO_4/t. Baker and Sike (2010) have reported that the upper part of CzD 2 unit may or may not be capped by calcrete that is discontinues in the western extents and becomes thick and continues in the east. The calcrete also thins to the south and thickens to the north (the maximum thickness interpreted was 33 m). This rock unit clearly has potential use as a neutralizing cover material or for blending with PAF rocks during storage in waste rock piles.

Special overburden handling will also be necessary for the pyritic black shales of the Nammuldi Member. This lower part of early Proterozoic Marra Mamba Formation is enriched by sulphide minerals having an average total sulphur content of 1.02 wt % with minimum and maximum sulphur of 0.01 wt % and 4.08 wt %, respectively. The black shale of the Nammuldi Member also contains carbonate in the form of calcite, dolomite and siderite resulting in an average ANC value of 23.8 kg H_2SO_4/t. The balance between their potential acidity and neutralizing acidity yielded 39 black shale samples from the Nammuldi Member dominated by NAF material, with an overall average NAPP values were 5.98 kg H_2SO_4/t. This positive NAPP indicated that overall the black shale samples may potentially generate acid in low quantity.

A further source of PAF material at South Jimblebar is pyritic black shale within the Undifferentiated Jeerinah Formation. Almost all samples, 25 of 26,

indicated a high capacity for acid generation with an average NAPP 88.9 kg H_2SO_4/t. Sulphur in this unit is evenly distributed averaging 3.04 wt %. These rocks typically have very low acid neutralizing capacity, with average only 0.67 kg H_2SO_4/t.

It must be noted that the rock samples in this study were collected from exploration drill cores and the study conducted before optimization of the pit design. Consequently, rock sampling involved all stratigraphical units at South Jimblebar. Based on economic evaluation, final design of the open pit (Figures 4.2. a-c) will not extend wide and deep enough for the Undifferentiated Jeerinah Formation to be intersected. Only a small volume of overburden from the Jeerinah Formation will be removed in the Western Pit of the South Jimblebar Mine and will be dumped in overburden storage area (OSA) 1. Therefore, this unit should only be an environmental concern in waste rock storage pile of OSA 1. In addition, it may be an environmental factor as a result of mine dewatering.

The geochemical results of each lithology can be incorporated into an AMD geological block model as a reference in scheduling waste rock removal to a waste rock pile. Acid consuming material, such as calcareous mudstones at upper part of the CzD 2 unit, and non-acid forming rock in CzD 1, OA, WA, NM, and MM stratigraphy units can be considered as a cover material on waste rock piles to encapsulate the PAF material. Ideally, a cover system will minimize oxygen and water infiltration and also provide a medium for vegetation growth. Further research on mechanical rock behavior and waste rock pile design are necessary to develop eco-friendly waste rock pile.

5. CONCLUSIONS AND RECOMMENDATIONS

5.1. Conclusions

A total of 144 samples of prospective waste rock from the future South Jimblebar iron ore mine were collected from 7 exploration drill cores made available by BHP Billiton Iron Ore (BHPBIO). Eight stratigraphy units have been intercepted by drilling at the South Jimblebar prospect. According to BHPBIO's terminology, these units are, from youngest to oldest, Cenozoic Detrital 3 (CzD 3), Cenozoic Detrital 2 (CzD 2), Undifferentiated West Angela Member (OA), West Angela Member (WA), Mount Newman Member (MN), MacLeod Member (MM), Nammuldi Member (MU), and undifferentiated Jeerinah Formation (N).

Lignitic rocks are of particular interest at the South Jimblebar prospect since this is currently the only locality known to BHPBIO where substantial thickness (up to 169 m) of such deposits are present in the overburden. The lignite and lignite-bearing claystones occur within the Tertiary detrital sequence of CzD 2. The 29 lignite samples studied, collected from 4 drill cores, had low ANC (average 1.93 kg H_2SO_4/t) and sporadic sulphur enrichment up to 35.1 wt %. Lignite samples in this study were predominantly classified in the NAF category, however 28% (8 of 29) of samples had high positive NAPP, up to 941 kg H_2SO_4/t, that represents a potential acidification source if mixed with other rock types in the waste rock pile. In addition, lignite rocks showed a degree of relative enrichment in the potentially toxic elements, As, Be, Co, Mo, Se, Sb, and Tl.

Black shale of the Namuldi Member of the Marra Mamba Formation, in the main Proterozoic BIF sequence, was found to be moderately sulphur enriched with an average content of of 1.02 wt %. However, the acid potential from oxidation of this sulphide was balanced by carbonate mineral contents, as recognised by their moderate ANC (average 23.8 kg H_2SO_4/t). Eighteen of 39 (46%) black shale samples in this group are categorised as NAF, but overall their acid-base balance resulted in a small positive average NAPP of 5.98 kg H_2SO_4/t. Therefore they are classified as low PAF capacity. The trace elements, Ag and Zn were significantly enriched in the black shale samples relatively to median soil abundance.

Further concern for environmental impact arises from the mineralised black shale of the Undifferentiated Jeerinah Formation, which is the lowest stratigraphic

unit sampled in the current study. Geochemical characterisation of this unit indicated a well distributed high sulphur content (3.04 wt %) and negligible ANC. The balance between their acid and neutralizing capacity resulted in an average NAPP of 88.9 kg H_2SO_4/t, and most of the black shale samples considered as high PAF capacity. These samples also showed enrichment in Zn, As, Se, Ag, Cd, Tl, which are of environmental interest.

In contrast, the non-carbonaceous mudstones analysed in this study from all stratigraphic units, were dominantly categorized as NAF material with low neutralizing capacity (ANC <10 kg H_2SO_4/t). Regarding toxic metal contents, the mudstone was enriched only in Be and Mn, when compared to median soil abundance. Prospective waste rock having appreciable acid neutralizing capacity was identified from only two samples of micritic calcareous mudstone from the upper part of the CzD 2 unit.

Based on the geochemical characterisation of the future waste rock at the South Jimblebar Mine, 63% of the samples were classified as non-acid forming (NAF) and the remaining 37% as potentially acid forming (PAF) materials with enrichment of various potentially toxic elements. The occurrence of the PAF material suggests the need of implementation of a cover design system in future waste rock piles in the South Jimblebar prospect. Non-carbonaceous rocks that were mostly identified as NAF, particularly calcareous mudstone of the CzD 2 unit with its high neutralizing capacity, have the potential to be utilised as cover or blending material for the PAF (lignite and black shale) material.

The combination of acid base accounting (ABA) and net acid generation (NAG) testing in acid forming characterisation of the rock demonstrated the effectiveness of these static tests to produce more reliable results than either test alone. Overestimation of MPA capacity, that mainly occurred in lignite samples due to influence of unreactive sulphur, such as sulphate and organic sulphur, can be avoided in NAG testing. However, NAG testing cannot estimate the neutralizing capacity as provided by ABA.

Acid forming characterisations in this present study provide some possible screening criteria for identification of acid generation potential of the rock at the South Jimblebar mine, as follows:

- Paste pH <5.0 indicates the presence of acid sulphate salt and is evidence of prior acid-generating sulphide oxidation. It thus reflects generally that

the rock may be a source of AMD. However, it is crucial to note that neutral to basic (alkaline) paste pH cannot be used to assume the sample to be non-acid forming.

- A total sulphur content of 0.1 wt % is an appropriate reference point in the case of lignite and black shale rock to distinguish between NAF and PAF material. Lignite and black shale samples with total sulphur content > 0.1 wt % may potentially generate acid, and vice versa, while a cut-off of 0.2 wt % total sulphur is a criterion to separate NAF and PAF for non-carbonaceous rock.
- Samples with NAG pH >5.5 indicate an excess of neutralizing capacity of the rock associated with negative NAPP.

In the static geochemical testwork employed in this study, there were found to be two factors that may potentially lead to a misclassification of waste rocks with regard to their acid generating potential. These were the presence in the rock of organic acids and siderite (iron carbonate). Organic acids had an obvious effect on NAG testing for organic-rich rocks (lignite) with low sulphur content. Partial oxidation of organic carbon by H_2O_2 generates organic acid that causes overestimation of non-sulphate acidity. Incremental addition of H_2O_2 and extended boiling of the sample during the NAG test can resolve this uncertainty through complete breakdown of the organic acid.

A significant issue relating to ANC measurement of black shale samples of the Namuldi Member is the occurrence of the non-acid neutralizing iron carbonate mineral, siderite. Without modification of the test procedure, the presence of siderite can overestimate net ANC and surely underestimate NAPP resulting in incorrect classification of the waste rock sample. Application of a modified ANC test proposed by Stewart (2005) produces results with improved measurement of actual ANC.

5.2. Limitations of Present Study

The primary scope of the present investigation was the determination of the acid generating potential of the rock types that will report to waste rock piles during future iron ore mining at the South Jimblebar prospect. Particular questions were asked regarding the potential acidification risk arising from the unusual presence of

significant quantities of lignite in the future waste rock stream. Primary investigation of lignitic rocks in the CzD 2 sequence indicated their potential to generate AMD and to release a limited range of potentially toxic trace elements. However, many of the lignite samples were classified as "uncertain" acid potential due to the apparent conflict between the NAPP and NAG results. It is beyond the scope of the current study to investigate further the uncertainty, especially the mineralogical properties of lignite, that would elucidate the sulphur speciation and the presence of additional neutralizing potential minerals.

In addition, the current study only employed static tests to predict the geochemical characteristic of the rocks. Kinetic testing may usefully be employed to provide a better understanding of the mineral reactivity, oxidation kinetics, metal solubility and leaching behaviour of the rock.

5.3. Recommendations for Future Research

In the present study, 4 of the 7 exploration drill cores contained significant lignite. The highly variable development of lignite units between the exploration cores is indicative of a complex geometry of lignite deposition, presumably within a river channel. Final estimation of the volume of lignite that will be excavated and stored in waste rock piles at the future South Jimblebar mine will consequently require more detailed exploration and geological study.

A better understanding of the extent and spatial distribution of the PAF and NAF zones across the planned mined area should be developed in constructing an AMD block model in the South Jimblebar mine. Additional systematic testing of drill cores would assist in addressing this, especially the unusual lignite that potentially has a significant impact on environment. Furthermore, the distribution of pyrite mineralisation, and its origins, is of vital interest in any quantification of the extent of future AMD risk from the long term storage of lignite waste.

Detailed mineralogical analysis of the lignite is required, in particular the crystal habit and precise composition of sulphide minerals, as well as identification of acid neutralizing minerals. A combination of such mineral studies with appropriately designed kinetic testing will be most valuable in predicting the rates of acid formation and neutralization, and hence the scale and rates of possible AMD release to the environment during waste rock storage. Kinetic testing may also add to the knowledge of toxic metal solubilities and mobility in future waste rock piles.

Owing to lignite and black shale lithologies showing potential to generate acid and a degree of trace element enrichment, it is required to develop management protocols for the short-term handling of these waste rocks and their long term storage, in order to prevent AMD release during mining and after closure.

Open pit mining at South Jimblebar will result in a large scale excavation below the water table. The resulting void will potentially be infilled with ground water, as well as surface runoff after sporadic rainfall, on cessation of mining. Therefore, the location of lignite and potentially acid-generating black shale units relative to the final pit walls is an important consideration when planning for mine closure. The location and depth of exposed units relative to the final equilibrium water level has an important effect on the formation of AMD and its impact on the water quality in the future pit lake and also surrounding surface environment and groundwater system.

The coexistence of significant quantities of carbon and sulphide in lignite and black shale can potentially raise the risk of spontaneous combustion of rocks on the future waste rock piles. Consequently, it is required to investigate this potential risk and develop integrated strategies for the emplacement of the reactive lignite and black shale at waste rock piles at the South Jimblebar prospect to reduce the occurrences of AMD and spontaneous combustion.

REFERENCES

Abraitis, P. K., Pattrick, R. A. D., & Vaughan, D. J. (2004). Variations in the compositional, textural and electrochemical properties of natural pyrite: A review. *Intenational Journal of Mineral Processing, 74*, 41-59.

Allen, D. G. (2010, 29 September-1 October). *Geochemistry of thallium in lead-zinc tailings.* Paper presented at the First International Seminar on the Reduction of Risk in the Management of Tailings and Mine Waste, Perth, Australia

Australian Mineral Industries Research Association Limited (AMIRA). (2002). *Acid rock drainage test handbook* Project P387A, prediction and kinetic control of acid mine drainage[Unpublished report]. Ian Wark Research Institute, Environmental Geochemistry International Pty Ltd. Melbourne, Australia.

Australian Natural Resources Atlas (ANRA). (2012). Rangeland overview of Western Australia. Retrieved from http://www.anra.gov.au/topics/rangelands/overview/wa/ibra-pil.html

Benjamin, M. M. (2002). *Water chemistry* (First ed.). New York: McGraw Hill.

Bhat, U. M., & Khan, A. B. (2011). Heavy metals: An ambiguous category of inorganic contaminants, nutrients, and toxins. *Research Journal of Environmental Science, 5*, 682-690.

BHP Billiton Iron Ore Pty Ltd (BHPBIO). (2009). *Subterranean Fauna Habitat Review* Jimblebar Iron Ore Project[Unpublished report]. BHP Billiton Iron Ore Pty Ltd (BHPBIO). Perth, Western Australia.

BHP Billiton Iron Ore Pty Ltd (BHPBIO). (2011). *Resources model report of EPH Mindoona deposit* [Unpublished report]. Iron Ore Technical Services. Perth, Western Australia.

Biker, B., & Sike, P. (2010). *Mindoona infill drilling and modelling report 2009/10, South Jimblebar* [Unpublished report]. BHP Billiton Iron Ore Perth, Western Australia.

Birch, G. F. (1981). The Karbonat-Bombe: a precise, rapid and cheap instrument for determining calcium carbonate in sediments and rocks. *Trans. Geol. Soc. South Africa, 84*(3), 199-203.

Bowen, H. J. M. (1979). *Environmental chemistry of the elements*. New York: Academic Press.

Brown Jr, G. E., & Calas, G. (2011). Environmental mineralogy - Understanding element behaviour in ecosystem. *Comptes Rendus Geoscience, 343*, 90-112.

Bureau of Meteorology. (2012). Climate data online. Retrieved from http://www.bom.gov.au/climate/data/

Casagrande, D. J., Finkelman, R. B., & Caruccio, F. T. (1989). The nonparticipation of organic sulfur in acid mine drainage. *Environmental Geochemistry and Health*, 11(3-4), 187-192.

Chou, C. L. (2012). Sulfur in coals: A review of geochemistry and origins. *International Journal of Coal Geology, 100*, 1-13.

Department of Industry Tourism and Resources (DoITR). (2007). *Managing acid and metalliferous drainage*. Canberra, Australia: Department of Communications, Information Technology and the Arts, Australian Government.

Forstner, U., Ahlf, W., & Calmano, W. (1993). Sediment quality objectives and criteria development in Germany. *Water Science Technology, 28*(8-9), 307-316.

Garnett, K., & Bolton, E. (2004). *Jimblebar water supply installation of new bores: A report for BHP Billiton Iron Ore* [Unpublished report]. Aquattera Consulting Pty Ltd,. Perth, Western Australia.

Garrido-Ramírez, E. G., Theng, B. K. G., & M.L. Mora, M. L. (2010). Clays and oxide minerals as catalysts and nanocatalysts in Fenton-like reactions: A review. *Applied Clay Science, 47*, 182-192.

Garvie, A. M., & Taylor, G. F. (2000). *Manual of techniques to quantify processes associated with polluted effluent from sulfidic mine wastes*. Brisbane: Australian Centre for Mining Environmental Research.

Graeme Campbell & Associates Pty. Ltd (GCA). (1996). *Acid formation potential of waste rock from the weathered zone and fresh zone of the Mt. Whaleback Pit, implication for waste rock management : A report for BHP Billiton Iron Ore* [Unpublished report]. Perth, Western Australia.

Graeme Campbell & Associates Pty. Ltd (GCA). (2005). *Geochemical Characterisation of mine-waste samples of Cloud Break deposit and Implication for mine waste management: A report for Fortescue Metal Group Ltd* [Unpublished report]. Perth, Western Australia.

Green, R., & Borden, R. K. (2011). Geochemical Risk Assesment Process for Rio Tinto's Pilbara Iron Ore Mines. In S. Kumar (Ed.), In *Integrated Waste Management* (Vol. I: (InTech).

Jambor, J. L., & Blowes, D. W. (1998). Theory and application of mineralogy in environmental studies of sulfide-bearing mine waste. In L. J. Cabri & D. J.

Vaughan (Eds.), *Modern approaches to ore and environmental mineralogy* (pp. 367-401): Minerological Association of Canada.

Jennings, S. R., Dollhopf, D. J., & Inskeep, W. P. (2000). Acid production from sulfide minerals using hydrogen peroxide weathering. *Applied Geochemistry, 15*, 235-243.

Johnson, S. L., & Wright, A. H. (2001). *Central Pilbara groundwater study* (Report HG 8). Perth, Western Australia: Government of Western Australia.

Kania, T. (1998). Laboratory Methods for Acid-Base Accounting: An Update *Coal Mine Drainage Prediction and Pollution Prevention in Pennsylvania*. Harrisburgh, Pennysylvania: Pennsylvania Department of Environmental Protection.

Klein, C., & Gole, M. J. (1981). Mineralogy and petrology of parts of the Marra Mamba Iron Formation, Hamersley Basin, Western Australia. *American Mineralogist, 66*, 507-525.

Kneeshaw, M. (2008). *Guide to the geology of the Hamersley and Noth East Pilbara Iron ore province* [Unpublished internal report]. Resource Evaluation Group. BHP Billiton Iron Ore. Perth, Western Australia.

Kolker, A. (2012). Minor element dstrubution in iron disulfides in coal: A geochemical review. *Internatioanl Journal of Coal Geology, 94*, 32-43.

Lengke, M. F., Davis, A., & Bucknam, C. (2010). Improving management of potentially acid generating waste rock. *Mine Water and the Environment, 29*, 29-44.

Li, M. G. (2000). *Acid rock drainage prediction for low-sulphide, low-neutralisation potential mine wastes*. Paper presented at the 5th International Conference on Acid Rock Drainage (ICARD), Denver, USA

Macphail, M. K., & Stone, M. S. (2004). Age and paleoenvironmental constraints on the genesis of the Yandi channel iron deposits, Marillana Formation, Pilbara, northwestern Australia. *Australian Journal of Earth Sciences: An Australian Geoscience Journal of the Geological Society of Australia, 51*(4), 497-520.

Miller, S. D., Jeffery, J. J., & Wong, J. W. C. (1991). *Use and misuse of the acid-base account for AMD prediction.* Paper presented at the 2nd International Conference on the Abatement of Acidic Drainage Montreal, Canada

Moncur, M. C., Jambor, J. L., Ptacek, C. J., & Blowes, D. W. (2009). Mine drainage from the weathering of sulfide minerals and magnetite. *Applied Geochemistry, 24*, 2362-2373.

Morin, K. A., & Hutt, N. M. (1997). *Environmental geochemistry of minesite drainage: Practical theory and case studies*. Vancouver, Canada: Minesite Drainage Assesment Group.

Morris, R. C. (1994). *Detrital Iron Deposits of the Hamersley Province* [Unpublished report]. Division of Exploration and Mining. Commonwealth Scientific and Industrial Research Organisation (CSIRO). Perth, Western Australia.

Morris, R. C., & Kneeshaw, M. (2011). Genesis modelling for the Hamersley BIF-hosted iron ores of Western Australia: a crtital review. *Australian Journal of Earth Sciences, 58*(5), 417-451.

Morris, R. C., & Ramanaidou, E. R. (2007). Genesis of the channel iron deposit (CID) of the Pilbara region, Western Australia. *Australian Journal of Earth Sciences: An Australian Geoscience Journal of the Geological Society of Australia, 54*(5), 733-756.

Muller, G., & Gastner, M. (1971). The "Karbonate Bombe", a simple device for the determination of the calcium carbonate content in sediments, soils, and other minerals. *N. Jb. Mineral, 10*(3), 466-469.

Nichols, G. (2009). *Sedimentology and stratigraphy* (Second ed.). Hoboken, N.J: Willey-Blackwell.

Paktunc, A. D. (1999). Mineralogical Constraints on the determination of neutralization potential and prediction of acid mine drainage. *Environmental Geology 39*(2), 103-112.

Patridge, M. A., Golding, S. D., Baublys, K. A., & Young, E. (2008). Pyrite paragenesis and multiple sulfur isotope dstribution in late Archean and early Paleoproterozic Hamersley Basin sediments. *Earth and Planetary Science Letters, 272*, 41-49.

Perry, E. (1998). Interpretation of Acid-Base Accounting *Coal Mine Drainage Prediction and Pollution Prevention in Pennsylvania*. Harrisburgh, Pennysylvania: Pennysylvania Department of Environmental Protection.

Pickard, A. L., Barley, M. E., & Krapez, B. (2004). Deep-marine depositional setting of banded iron formation: sedimentological evidence from interbedded clastic sedimentary rocks in the early Palaeoproterozoic Dales Gorge Member of Western Australia. *Sedimentary Geology, 170*(1-2), 37-62.

Pope, J., Weber, P. A., Mackenzie, A., Newman, N., & Rait, R. (2010). Correlation of acid base accounting characteristic with the geology of commonly mined coal measures, West Coast and Southland, New Zealand. *New Zealkand Journal of Geology and Geophysics, 53*(2-3), 153-156.

Price, W. A. (2009). *Prediction manual for drainage chemistry from sulphidic geologic materials: A report for mine environment neutral drainage (MEND) program* (Report 1.20.1). British Colombia, Canada: Natural Resources Canada.

Price, W. A., Morin, K. A., & Hutt, N. M. (1997). *Guidlines for the prediction of acid rock drainage and metal leaching for mines in British Colombia: Part II. Recomended procedure for static and kinetic testing*. Paper presented at the 4th International Conference on Acid Rock Drainage, Vancouver, B.C. Canada

Ramanaidou, E. R., Horwitz, R. C., & Morris, R. C. (1991). *Channel Iron Deposits* [Unpublished report]. Division of Exploration Geoscience. Commonwealth Scientific and Industrial Research Organisation (CSIRO). Perth, Western Australia.

Schumann, R., Stewart, W., Miller, S., Kawashima, N., Li, J., & Smart, R. (2012). Acid–base accounting assessment of mine wastes using the chromium reducible sulfur method. *Science of the Total Environment*, 424, 289–296.

Siegel, F. R. (2002). *Environmental geochemistry of potentially toxic metals*. Berlin: Springer.

Siesser, W. G., & Rogers, J. (1971). An investigation of the suitability of four methods used in routine carbonate analysis of marine sediments. *Deep Sea Research and Oceanographic Abstracts*, *18*(1), 135-139.

Sinclair Knight Merz (SKM). (2009). *Air quality and greenhouse gas impact assessment of Jimblebar Iron Ore Project : A report for BHPBIO* [Unpublished report].

Skousen, J., Brown, R. H., Evans, P., Leavitt, B., Brady, K., Cohen, L., & Ziekiewicz, P. (1997). Neutralization potential of overburden samples containing siderite. *Journal of Environmental Quality*, *26*(3), 673-681.

Sparks, D. L. (2005). Toxic metals in the environment: The role of surface. *Elements*, *1*, 193-197.

Stewart, W. (2005). Development of acid rock drainage prediction methodologies for coal mine wastes (Doctoral dissertation, University of South Australia) Retrieved from http://ura.unisa.edu.au/R/?func=dbin-jump-full&object_id=unisa24976.

Stewart, W. A., Miller, S. D., & Smart, R. (2006, 26-30 March). *Advances in acid rock drainage (ARD) characterisation of mine wastes.* Paper presented at the 7th International Conference on Acid Rock Drainage (ICARD), St. Louis, Missouri

Stone, M. S. (2004). Depositional history and mineralisation of Tertiary channel iron deposits at Yandi, Eastern Pilbara, Australia (Doctoral dissertation, University of Western Australia) Retrieved from http://repository.uwa.edu.au:80/R/-?func=dbin-jump-full&object_id=7976&silo_library=GEN01.

Stow, D. A. V. (2005). *Sedimentary rocks in the field (a colour guide)*. London: Manson Publishing.

Strong, S., & Hall, J. (2009). *Hydrogeological assesment for Jimblebar Iron Ore Project: A report for BHP Billiton Iron Ore Pty Ltd* [Unpublished report]. Aquaterra consulting Pty Ltd. Perth, Western Australia.

Stumm, W., & Morgan, J. J. (1981). *Aquatic Chemistry - An Introduction Emphasizing Chemical Equilibria in Natural Waters*. New York: John Wiley & Sons, Inc.

Thomas, & Evans. (1998). *Hedges gold mine: Geochemical study of process amd residue and implication for long-term management of the residue storage facility* [Unpublished report].

Tucker, M. E. (1981). *Sedimentary petrology : An introduction* (Vol. 3). London: Blackwell Scientific Publications.

Watkins, R. (2011). *Environmental geochemistry of minesite pollution: An Introduction* [Short course proceedings]. Australian Centre for Geomechanics, University of Western Australia. Perth, Western Australia.

Watkins, R. (2012). *Geochemical characterisation of 52 rock samples (prospective waste rock types and some non-waste types) from site of Pit 5, Premier Mine, Collie, Western Australia* [Unpublished report]. Environmental Inorganic Geochemistry Group, Department of Applied Geology. Curtin University.

Weber, P. A. (2003). Geochemical investigations of neutralising reactions associated with acid rock drainage : prediction, mechanisms, and improved tools for management (Doctoral dissertation, University of South Australia) Retrieved from http://ura.unisa.edu.au/R/?func=dbin-jump-full&object_id=unisa43767.

Weber, P. A., Stewart, W. A., Skinner, W. M., Weisener, C. G., Thomas, J. E., & Smart, R. S. C. (2004). Geochemical effects of oxidation products and framboidal pyrite oxidation in acid mine drainage prediction techniques. *Applied Geochemistry*, *19*, 1953-1974.

White III, W. W., Lapakko, K. A., & Cox, R. L. (1999). Static test methods most commonly used to predict acid-mine drainage: Practical guidlines for use and interpretations. In G. S. Plumlee & M. J. Logsdon (Eds.), *Reviews in*

economic geology (Vol. 6A, pp. 325-338). Littleton, CO: Society of Economic Geologist.

APPENDIX A

A.1. Rock sample description of drill core SJ0772D from the South Jimblebar prospect, BHPBIO.

No	Sample ID	Depth (m)	Stratigraphy	Rock Type	Grain Size*	Colour**
1	SJ0772D-001	5.2	CzD 3	Mudstone	Medium Sand	Yellowish grey 5Y 8/1
2	SJ0772D-002	19.3	CzD 3	Mudstone	Very fine	Pale greenish yellow 10Y 8/2
3	SJ0772D-003	39.3	CzD 2	Mudstone	Fine	Greyish yellow 5Y 8/4
4	SJ0772D-004	56.6	CzD 2	Calcareous Mudstone	Fine	Greyish yellow 5Y 8/4
5	SJ0772D-005	71.6	CzD 2	Calcareous Mudstone	Very fine	Yellowish grey 5Y 8/1
6	SJ0772D-006	83.6	CzD 2	Mudstone	Very fine	Pinkish grey 5YR
7	SJ0772D-007	93.7	CzD 2	Mudstone	Fine	Moderate reddish brown 10R 4/6
8	SJ0772D-008	96.9	CzD 2	Mudstone	Fine	Yellowish grey 5Y 8/1
9	SJ0772D-009	101.3	CzD 2	Lignite	Very fine	Medium dark grey N6
10	SJ0772D-010	107.9	CzD 2	Lignite	Very fine	Dark grey N3
11	SJ0772D-011	112.5	CzD 2	Lignite	Very fine	Medium dark grey N4
12	SJ0772D-012	113.2	CzD 2	Lignite	Very fine	Light grey N7
13	SJ0772D-013	119.9	CzD 2	Mudstone	Very fine	Moderate pink 5R 7/4
14	SJ0772D-014	125.5	CzD 2	Lignite	Very fine	Dark grey N3
15	SJ0772D-015	134,5	CzD 2	Lignite	Very fine	Greyish black N3

Note
*Grain size classification of the rock particles is referred to Stow (2011); **Rock colour classification is referred to the Munsell colour system

A.1. (Continued).

No	Sample ID	Depth (m)	Stratigraphy	Rock Type	Grain Size*	Colour**
16	SJ0727D-016	142	CzD 2	Lignite	Very fine	Dark grey N3
17	SJ0772D-017	158.5	CzD 2	Mudstone	Very fine	Yellowish grey 5Y 8/1
18	SJ0772D-018	164.5	CzD 2	Lignite	Very fine	Medium grey N5
19	SJ0727D-019	180.6	CzD 2	Lignite	Very fine	Black N1
20	SJ0772D-020	197.9	CzD 2	Lignite	Very fine	Dark grey N3
21	SJ0772D-021	206.9	CzD 2	Mudstone	Very fine	Light brownish grey 5YR 6/1
22	SJ0772D-022	214.15	CzD 2	Lignite	Very fine	Dark grey N3

A.2. Rock sample description of drill core SJ0785D from the South Jimblebar prospect, BHPBIO.

No	Sample ID	Depth (m)	Stratigraphy	Rock Type	Grain Size*	Colour**
1	SJ0785D-003	105.7	CzD 2	Lignite	Very fine	Medium grey N5
2	SJ0785D-005	107.6	CzD 2	Lignite	Very fine	Dark grey N3
3	SJ0785D-010	114.7	CzD 2	Lignite	Very fine	Medium grey N5

A.3. Rock sample description of drill core SJ0845RDT from the South Jimblebar prospect, BHPBIO.

No	Sample ID	Deep (m)	Stratigraphy	Rock Type	Grain Size*	Colour**
1	SJ0845RDT-002	92.5	CzD 2	Mudstone	Coarse	White N9
2	SJ0845RDT-003	100.0	CzD 2	Mudstone	Very fine	Pinkish grey 5YR 8/1
3	SJ0845RDT-004	108.6	CzD 2	Lignite	Fine	Light grey N7
4	SJ0845RDT-005	112.0	CzD 2	Lignite	Fine	Light grey N7
5	SJ0845RDT-006	115.0	CzD 2	Lignite	Fine	Light grey N7
6	SJ0845RDT-007	118.0	CzD 2	Lignite	Fine	Light grey N7
7	SJ0845RDT-008	121.0	CzD 2	Lignite	Fine	Light grey N7
8	SJ0845RDT-009	123.5	CzD 2	Lignite	Medium sand	Medium grey N5
9	SJ0845RDT-010	126.0	CzD 2	Lignite	Medium sand	Medium grey N5
10	SJ0845RDT-011	128.4	CzD 2	Lignite	Medium sand	Medium grey N5
11	SJ0845RDT-012	134.3	CzD 2	Mudstone	Very fine	Very light grey N8
12	SJ0845RDT-013	139.0	CzD 2	Lignite	Fine	Medium grey N5
13	SJ0845RDT-014	142.8	CzD 2	Lignite	Fine	Medium grey N5
14	SJ0845RDT-015	146.0	CzD 2	Lignite	Fine	Medium grey N5
15	SJ0845RDT-016	147.4	CzD 2	Lignite	Fine	Medium grey N5

A.3. (Continued)

No	Sample ID	Deep (m)	Stratigraphy	Rock Type	Grain Size*	Colour**
16	SJ0845RDT-017	150.0	CzD 2	Mudstone	Very fine	Very light grey N8
17	SJ0845RDT-018	154.9	CzD 2	Mudstone	Very fine	Pinkish grey 5YR 8/1
18	SJ0845RDT-021	176.2	WA 1	Mudstone	Very fine	Pale red 5R 6/2
19	SJ0845RDT-023	184.0	WA 1	Mudstone	Very fine	Pale red 5R 6/2
20	SJ0845RDT-024	190.0	WA 1	Mudstone	Very fine	Pale red 5R 6/2
21	SJ0845RDT-025	193.0	WA 1	Mudstone	Very fine	Pale red 5R 6/2
22	SJ0845RDT-026	196.7	WA 1	Mudstone	Very fine	Moderate red 5R 5/4
23	SJ0845RDT-028	202.7	WA 1	Mudstone	Very fine	Light brownish grey 5YR 6/1
24	SJ0845RDT-031	211.8	WA 1	Mudstone	Very fine	Pinkish grey 5YR 8/1
25	SJ0845RDT-033	217.6	WA 1	Mudstone	Very fine	Pinkish grey 5YR 8/1
26	SJ0845RDT-043	262.6	MN 2	Mudstone	Very fine	Dusky yellowish brown 10YR 2/2
27	SJ0845RDT-044	269.6	MN 1	Mudstone	Very fine	Pinkish grey 5YR 8/1

A.4. Rock sample description of drill core SJ0847D from the South Jimblebar prospect, BHPBIO.

No	Sample ID	Deep (m)	Stratigraphy	Rock Type	Grain Size*	Colour**
1	SJ0847 D-001	4.9	CzD 3	Mudstone	Fine	Moderate reddish brown 10R 4/6
2	SJ0847 D-002	12.8	CzD 3	Mudstone	Fine	Moderate reddish brown 10R 4/6
3	SJ0847 D-003	26.4	CzD 2	Mudstone	Fine	Moderate reddish brown 10R 4/6
4	SJ0847 D-004	34.8	OA	Mudstone	Very Fine	Pale greenish yellow 10Y 8/2
5	SJ0847 D-005	46.9	OA	Mudstone	Very Fine	Dark yellowish orange
6	SJ0847 D-006	52.3	OA	Mudstone	Very Fine	Dark grey N3
7	SJ0847 D-007	54.3	OA	Mudstone	Very Fine	Greyish black N2
8	SJ0847 D-008	62.0	OA	BIF	Very Fine	Dusky brown 5YR 2/2
9	SJ0847 D-009	96.7	MN 2	BIF	Very Fine	Blackish red 5R 2/2
10	SJ0847 D-010	116.3	MN 1	BIF	Very Fine	Moderate brown 5YR 3/9
11	SJ0847 D-154.2	154.2	MM	Mudstone	Very Fine	Pinkish grey 5YR 8/1
12	SJ0847 D-011	163.9	MU	Mudstone	Very Fine	Greyish orange pink 10R 8/2
13	SJ0847 D-012	174.2	MU	Black shale	Very Fine	Dark grey N3
14	SJ0847 D-013	175.2	MU	Black shale	Very Fine	Dark grey N3
15	SJ 0847 D-014	179.5	MU	Black shale	Very Fine	Medium Dark grey N4

A.4. (Continued)

No	Sample ID	Deep (m)	Stratigraphy	Rock Type	Grain Size*	Colour**
16	SJ0847 D-015	183.8	MU	Black shale	Very Fine	Dark grey N3
17	SJ0847 D-016	185.1	MU	Black shale	Very Fine	Greyish black N2
18	SJ0847 D-017	186.7	MU	Black shale	Very Fine	Greyish black N2
19	SJ0847 D-018	190.3	MU	Black shale	Very Fine	Dark grey N3
20	SJ0847 D-019	191.8	MU	Black shale	Very Fine	Dark grey N3
21	SJ0847 D-020	194.7	MU	BIF	Fine	Medium grey N5
22	SJ0847 D-021	196.0	MU	Black shale	Very Fine	Medium dark grey N4
23	SJ0847 D-022	200.1	MU	Black shale	Very Fine	Dark grey N3
24	SJ0847 D-023	203.7	MU	Black shale	Very Fine	Medium dark grey N4
25	SJ0847 D-024	206.4	MU	Black shale	Very Fine	Medium dark grey N4
26	SJ0847 D-025	209.9	MU	Black shale	Very Fine	Medium dark grey N4
27	SJ0847 D-026	212.9	MU	Black shale	Very Fine	Medium dark grey N4
28	SJ0847 D-027	215.7	MU	Black shale	Very Fine	Dark grey N3
29	SJ0847 D-028	218.8	MU	Black shale	Very Fine	Dark grey N3
30	SJ0847 D-029	221.8	MU	Black shale	Very Fine	Greyish black N2

A.4. (Continued)

No	Sample ID	Deep (m)	Stratigraphy	Rock Type	Grain Size*	Colour**
31	SJ0847 D-030	225.5	MU	Black shale	Very Fine	Dark grey N3
32	SJ0847 D-031	227.5	MU	Black shale	Very Fine	Dark grey N3
33	SJ0847 D-032	229.4	MU	Black shale	Very Fine	Dark grey N3
34	SJ0847 D-033	232.2	MU	Black shale	Very Fine	Dark grey N3
35	SJ0847 D-034	235.5	MU	Black shale	Very Fine	Medium dark grey N4
36	SJ0847 D-035	238.9	MU	Black shale	Very Fine	Dark grey N3
37	SJ0847 D-036	241.8	MU	Black shale	Very Fine	Medium dark grey N4
38	SJ0847 D-037	243.4	MU	Black shale	Very Fine	Medium dark grey N4
39	SJ0847 D-038	247.7	N	Black shale	Very Fine	Medium dark grey N4
40	SJ0847 D-039	249.9	N	Black shale	Very Fine	Dark grey N3
41	SJ0847 D-040	253.8	N	Black shale	Very Fine	Dark grey N3
42	SJ0847 D-041	255.5	N	Black shale	Very Fine	Dark grey N3
43	SJ0847 D-042	258.5	N	Black shale	Very Fine	Dark grey N3
44	SJ0847 D-043	260.7	N	Black shale	Very Fine	Dark grey N3
45	SJ0847 D-044	264.5	N	Black shale	Very Fine	Dark grey N3
46	SJ0847 D-045	266.6	N	Black shale	Very Fine	Dark grey N3

A.5. Rock sample description of drill core SJ0848D from the South Jimblebar prospect, BHPBIO.

No	Sample ID	Depth (m)	Stratigraphy	Rock Type	Grain Size*	Colour**
1	SJ0848D-041	8.95	TD 3	Mudstone	Fine	Moderate reddish orange 10R 6/6
2	SJ0848D-043	21.00	OA	Mudstone	Fine	Moderate reddish orange 10R 6/7
3	SJ0848D-044	27.38	MN 3	Mudstone	Fine	Dark yellowish orange 10 YR 6/6
4	SJ0848D-001	32.80	MN 3	Mudstone	Very fine	Dark yellowish orange 10 YR 6/6
5	SJ0848D-004	52.70	MN 1	Mudstone	Fine	Medium light grey N6
6	SJ0848D-008	65.10	MN 3	Mudstone	Fine	Greyish brown 5YR 3/2
7	SJ0848D-017	120.40	MU	Mudstone	Very fine	Moderate reddish orange 10R 6/6
8	SJ0848D-018	133.95	MU	Mudstone	Very fine	Medium grey
9	SJ0848D-021	150.30	MU	Black shale	Very fine	Medium dark grey N3
10	SJ0848D-023	151.50	MU	Black shale	Very fine	Medium dark grey N3
11	SJ0848D-024	152.20	MU	Black shale	Very fine	Greyish black N2
12	SJ0848D-025	157.90	MU	Black shale	Very fine	Greyish black N2
13	SJ0848D-026	165.10	MU	Black shale	Fine	Medium light grey N6
14	SJ0848D-027	165.98	MU	Black shale	Fine	Medium light grey N7
15	SJ0848D-028	166.60	MU	Black shale	Fine	Medium light grey N6

A.5. (Continued).

No	Sample ID	Depth (m)	Stratigraphy	Rock Type	Grain Size*	Colour**
16	SJ0848D-029	167.50	MU	Black shale	Very fine	Medium light grey N6
17	SJ0848D-030A	179.18	MU	Black shale	Very fine	Medium dark grey N3
18	SJ0848D-030B	179.18	MU	Black shale	Very fine	Greyish Black N2
19	SJ0848D-031	181.65	MU	Black shale	Very fine	Medium light grey N6
20	SJ0848D-032	184.43	N	Black shale	Very fine	Greyish black N2
21	SJ0848D-033	187.00	N	Black shale	Very fine	Medium dark grey
22	SJ0848D-034	188.48	N	Black shale	Very fine	Greyish black N2
23	SJ0848D-035	191.68	N	Black shale	Very fine	Medium dark grey
24	SJ0848D-036	194.55	N	Black shale	Very fine	Medium grey N5
25	SJ0848D-037	199.20	N	Black shale	Very fine	Greyish black N2
26	SJ0848D-038	208.35	N	Black shale	Very fine	Greyish Black N2
27	SJ0848D-039	214.25	N	Black shale	Very fine	Medium light grey N6
28	SJ0848D-040	215.55	N	Black shale	Very fine	Medium dark grey N3
29	SJ0848D-048	78.00	MM	Mudstone	Very fine	White N9
30	SJ0848D-051	122.45	MU	Mudstone	Very fine	Light grey N7
31	SJ0848D-055	183.18	N	Black shale	Very fine	Greyish black N2

A.6. Rock sample description of drill core SJ0849D from the South Jimblebar prospect, BHPBIO.

No	Sample ID	Depth (m)	Stratigraphy	Rock Type	Grain Size*	Colour**
1	SJ0849D-001	9.50	TD 3	Mudstone	Fine	Moderate reddish brown 10R 4/6
2	SJ0849D-002	65.75	MN 2	Mudstone	Very fine	Bluish white 5B 9/1
3	SJ0849D-003	97.95	MM	Mudstone	Very fine	Pale purple 5P 6/2
4	SJ0849D-004	155.7	MU	Mudstone	Very fine	Bluish white 5B 9/1
5	SJ0849D-005	157.6	N	Black shale	Very fine	Medium grey N5
6	SJ0849D-006	160.0	N	Black shale	Very fine	Greyish black N2
7	SJ0849D-007	161.25	N	Black shale	Very fine	Dark grey N3
8	SJ0849D-008	164.25	N	Black shale	Very fine	Medium dark grey N4
9	SJ0849D-009	165.0	N	Black shale	Very fine	Medium dark grey N4
10	SJ0849D-010	165.4	N	Black shale	Very fine	Medium dark grey N4
11	SJ0849D-011	165.7	N	Black shale	Very fine	Medium dark grey N4
12	SJ0849D-012	166.1	N	Black shale	Very fine	Medium dark grey N4

A.7. Rock sample description of drill core SJ1102D from the South Jimblebar prospect, BHPBIO.

No	Sample ID	Depth (m)	Stratigraphy	Rock Type	Grain Size*	Colour**
1	SJ1102D-002	114.0	CzD 2	Lignite	Very fine	Dark grey N3
2	SJ1102D-004	115.6	CzD 2	Lignite	Very fine	Dark grey N3
3	SJ1102D-006	117.1	CzD 2	Lignite	Very fine	Dark grey N3

Appendix B

B.1. Acid forming characteristics of 29 lignite samples from the South Jimblebar prospect, BHPBIO.

No	Sample ID	Stratigraphy	Acid-Base Data								NAG Test Data			DoITR 2007, Classification
			Paste pH	Total C	Total S	S-SO_4	S-Sulfide	MPA	ANC	NAPP	NAGpH	NAG to pH 4.5	NAG to pH 7.00	
				(%)				(kg H_2SO_4/t)				(kg H_2SO_4/t)		
1	SJ1102D-002	CzD 2	5.94	22.0	0.22	0.02	0.20	6.18	6.13	0.05	7.50	0.00	0.00	NAF
2	SJ1102D-004	CzD 2	5.90	30.3	0.15	0.02	0.13	3.98	0.00	3.98	8.24	0.00	0.00	UC (NAF)
3	SJ1102D-006	CzD 2	5.90	18.6	0.03	0.01	0.02	0.51	0.00	0.51	8.33	0.00	0.00	UC (NAF)
4	SJ0772D-009	CzD 2	7.49	6.50	0.00	0.00	0.00	0.02	6.86	-6.84	8.65	0.00	0.00	NAF
5	SJ0772D-010	CzD 2	5.15	20.7	0.43	0.05	0.38	11.7	0.00	11.7	8.27	0.00	0.00	UC (NAF)
6	SJ0772D-011	CzD 2	5.64	17.5	0.42	0.02	0.40	12.3	3.33	9.01	8.04	0.00	0.00	UC (NAF)
7	SJ0772D-012	CzD 2	4.07	5.22	0.96	0.09	0.88	26.8	0.00	26.8	2.93	14.2	21.6	PAF
8	SJ0772D-014	CzD 2	5.43	29.2	0.65	0.03	0.62	18.9	0.00	18.9	8.77	0.00	0.00	UC (NAF)
9	SJ0772D-015	CzD 2	6.23	17.2	0.05	0.00	0.05	1.50	1.59	-0.10	8.79	0.00	0.00	NAF
10	SJ0727D-016	CzD 2	5.37	36.0	0.72	0.02	0.70	21.52	0.00	21.5	8.45	0.00	0.00	UC (NAF)
11	SJ0772D-018	CzD 2	5.87	13.4	0.05	0.01	0.04	1.37	12.3	-11.0	9.17	0.00	0.00	NAF
12	SJ0727D-019	CzD 2	5.25	35.8	1.41	0.03	1.38	42.1	10.6	31.6	3.56	8.51	18.95	PAF
13	SJ0772D-020	CzD 2	5.78	22.0	0.13	0.01	0.12	3.67	0.00	3.67	8.65	0.00	0.00	UC (NAF)
14	SJ0772D-022	CzD 2	6.04	25.2	0.17	0.01	0.16	5.01	3.34	1.67	9.61	0.00	0.00	UC (NAF)
15	SJ0785D-003	CzD 2	1.56	27.7	21.4	3.75	17.62	539	0.00	539	2.11	565	599	PAF
16	SJ0785D-005	CzD 2	1.39	13.9	35.1	4.36	30.74	941	0.00	941	1.98	934	1004	PAF
17	SJ0785D-010	CzD 2	4.11	29.1	4.33	0.67	3.66	112	0.00	112	2.35	53.8	129	PAF
18	SJ0845RD-004	CzD 2	5.74	3.09	0.04	0.02	0.02	0.75	2.35	-1.61	7.93	0.00	0.00	NAF
19	SJ0845RD-005	CzD 2	5.49	4.05	0.05	0.02	0.03	0.77	3.33	-2.56	7.56	0.00	0.00	NAF
20	SJ0845RD-006	CzD 2	5.70	2.06	0.04	0.03	0.02	0.49	2.07	-1.58	7.29	0.00	0.00	NAF

B.1. (Continued).

No	Sample ID	Stratigraphy	Acid-Base Data								NAG Test Data			DoITR 2007, Classification
			Paste pH	Total C	Total S	S-SO_4	S-Sulfide	MPA	ANC	NAPP	NAGpH	NAG to pH 4.5	NAG to pH 7.00	
				(%)				(kg H_2SO_4/t)				(kg H_2SO_4/t)		
21	SJ0845RD-007	CzD 2	5.14	0.93	0.12	0.04	0.08	2.44	2.50	-0.07	4.18	0.10	2.45	UC (PAF-LC)
22	SJ0845RD-008	CzD 2	4.95	1.69	0.13	0.06	0.07	2.25	0.00	2.25	4.75	0.00	1.94	UC (NAF)
23	SJ0845RD-009	CzD 2	5.04	2.98	0.08	0.04	0.04	1.31	0.00	1.31	6.85	0.00	0.06	UC (NAF)
24	SJ0845RD-010	CzD 2	5.53	4.79	0.05	0.01	0.04	1.32	0.75	0.58	7.65	0.00	0.00	UC (NAF)
25	SJ0845RD-011	CzD 2	5.37	5.21	0.06	0.01	0.05	1.49	0.84	0.64	7.48	0.00	0.00	UC (NAF)
26	SJ0845RD-013	CzD 2	5.41	4.05	0.06	0.01	0.06	1.71	0.00	1.71	7.08	0.00	0.00	UC (NAF)
27	SJ0845RD-014	CzD 2	5.01	5.72	0.12	0.02	0.10	3.18	0.05	3.13	6.70	0.00	0.35	UC (NAF)
28	SJ0845RD-015	CzD 2	4.61	3.75	0.34	0.06	0.28	8.51	0.00	8.51	3.19	5.08	16.19	PAF
29	SJ0845RD-016	CzD 2	4.76	4.58	0.36	0.07	0.29	8.82	0.00	8.82	4.16	1.12	15.37	PAF

B.2. Acid forming characteristic of 62 black shale samples from the South Jimblebar prospect, BHPBIO.

No	Sample ID	Stratigraphy	Acid-Base Data								NAG Test Data			DoITR 2007, Classification
			Paste pH	Total C	Total S	S- SO_4	S-Sulfide	TPA	ANC	NAPP	NAGpH	NAG to pH 4.5	NAG to pH 7.00	
				(%)				(kg H2SO4/t)				(kg H2SO4/t)		
1	SJ 0847 D-012	MU	6.46	5.04	0.17	0.02	0.16	4.77	0.67	4.10	3.50	3.12	7.47	PAF LC
2	SJ 0847 D-013	MU	3.87	1.17	1.00	0.14	0.85	26.1	0.00	26.1	2.33	31.2	37.2	PAF
3	SJ 0847 D-014	MU	5.14	1.10	0.44	0.04	0.40	12.1	0.00	12.1	2.97	9.11	14.1	PAF
4	SJ 0847 D-015	MU	4.65	3.93	1.14	0.06	1.07	32.9	0.00	32.9	2.33	30.7	37.3	PAF
5	SJ 0847 D-016	MU	6.15	4.41	0.19	0.01	0.17	5.24	0.30	4.94	4.06	1.98	8.23	PAF LC
6	SJ 0847 D-017	MU	6.13	2.97	0.08	0.01	0.07	2.19	0.52	1.67	4.73	0.00	2.70	UC (NAF)
7	SJ 0847 D-018	MU	4.06	2.80	1.09	0.13	0.96	29.3	0.00	29.3	2.51	31.4	41.2	PAF
8	SJ 0847 D-019	MU	4.01	1.25	2.45	0.08	2.37	72.4	0.00	72.4	2.18	85.8	91.5	PAF
9	SJ 0847 D-021	MU	3.78	0.22	0.23	0.08	0.15	4.46	0.00	4.46	2.87	7.02	8.47	PAF LC
10	SJ 0847 D-022	MU	5.44	1.39	0.57	0.09	0.48	14.6	3.65	11.0	3.11	10.2	20.0	PAF
11	SJ 0847 D-023	MU	6.07	3.92	0.98	0.09	0.89	27.2	4.20	23.0	3.62	4.74	26.9	PAF
12	SJ 0847 D-024	MU	7.31	4.04	3.87	0.08	3.80	116	55.7	60.5	2.29	65.2	75.2	PAF
13	SJ 0847 D-025	MU	7.89	5.77	0.40	0.03	0.36	11.1	12.7	-1.57	7.28	0.00	0.00	NAF
14	SJ 0847 D-026	MU	8.02	3.56	0.13	0.00	0.13	3.86	49.2	-45.4	8.26	0.00	0.00	NAF
15	SJ 0847 D-027	MU	7.65	3.55	0.31	0.01	0.30	9.21	48.1	-38.9	7.00	0.00	0.00	NAF
16	SJ 0847 D-028	MU	7.89	6.86	0.16	0.00	0.15	4.63	6.98	-2.35	7.31	0.00	0.00	NAF
17	SJ 0847 D-029	MU	7.52	4.58	2.29	0.15	2.14	65.5	16.3	49.1	3.14	16.4	43.4	PAF
18	SJ 0847 D-030	MU	7.88	2.04	3.16	0.04	3.12	95.6	16.5	79.1	2.36	56.6	69.9	PAF
19	SJ 0847 D-031	MU	8.10	7.25	2.29	0.02	2.27	69.5	85.0	-15.6	7.58	0.00	0.00	NAF
20	SJ 0847 D-032	MU	7.79	3.18	4.08	0.09	3.99	122	16.9	105	2.40	62.0	74.7	PAF

B.2. (Continued).

No	Sample ID	Stratigraphy	Acid-Base Data								NAG Test Data			DoITR 2007, Classification
			Paste pH	Total C	Total S	S- SO_4	S- Sulfide	TPA	ANC	NAPP	NAGpH	NAG to pH 4.5	NAG to pH 7.00	
				(%)				(kg H_2SO_4/t)				(kg H_2SO_4/t)		
21	SJ 0847 D-033	MU	7.93	3.59	3.80	0.08	3.72	114	17.8	96.1	2.50	52.8	64.6	PAF
22	SJ 0847 D-034	MU	7.80	4.77	1.53	0.03	1.50	46.0	55.1	-9.13	7.06	0.00	0.00	NAF
23	SJ 0847 D-035	MU	4.53	9.47	3.10	0.15	2.94	90.1	60.9	29.2	3.71	5.12	66.8	PAF
24	SJ 0847 D-036	MU	4.22	0.05	0.58	0.16	0.41	12.6	0.00	12.6	2.63	14.2	20.9	PAF
25	SJ 0847 D-037	MU	4.34	0.19	2.35	0.09	2.25	69.0	0.00	69.0	2.37	51.8	60.4	PAF
26	SJ 0847 D-038	N	3.53	1.70	8.72	0.81	7.90	242	0.00	242	2.09	157	202	PAF
27	SJ 0847 D-039	N	3.62	3.12	3.52	0.13	3.39	104	0.00	104	2.22	75.9	85.5	PAF
28	SJ 0847 D-040	N	3.52	3.19	19.9	0.32	19.5	598	0.00	598	2.19	530.5	566	PAF
29	SJ 0847 D-041	N	7.07	4.46	2.17	0.07	2.10	64.4	2.93	61.4	2.56	38.1	50.2	PAF
30	SJ 0847 D-042	N	4.24	4.87	7.71	0.10	7.62	233	0.00	233	2.40	228	241	PAF
31	SJ 0847 D-043	N	5.85	4.53	7.12	0.11	7.00	214	1.48	213	1.96	163	185	PAF
32	SJ 0847 D-044	N	5.49	4.88	2.48	0.09	2.39	73.1	2.20	70.9	2.41	57.8	69.0	PAF
33	SJ 0847 D-045	N	6.07	3.12	2.79	0.08	2.71	82.8	2.47	80.4	2.27	63.6	77.8	PAF
34	SJ 0848D-021	MU	7.94	3.37	0.10	0.00	0.10	2.99	70.9	-67.9	7.53	0.00	0.00	NAF
35	SJ 0848D-023	MU	7.72	1.20	0.01	0.00	0.01	0.32	6.96	-6.63	6.74	0.00	0.98	NAF
36	SJ 0848D-024	MU	8.31	3.69	0.06	0.00	0.06	1.71	19.3	-17.6	7.83	0.00	0.00	NAF
37	SJ 0848D-025	MU	7.77	1.73	0.06	0.00	0.06	1.78	1.86	-0.08	7.90	0.00	0.00	NAF
38	SJ 0848D-026	MU	7.26	3.16	0.03	0.00	0.03	0.90	0.98	-0.08	5.85	0.00	2.35	NAF
39	SJ 0848D-027	MU	6.95	2.26	0.02	0.00	0.02	0.56	2.45	-1.89	6.89	0.00	0.39	NAF
40	SJ 0848D-028	MU	8.51	1.82	0.01	0.00	0.01	0.35	61.2	-60.8	7.28	0.00	0.00	NAF

B.2. (Continued).

No	Sample ID	Stratigraphy	Acid-Base Data								NAG Test Data			DoITR 2007, Classification
			Paste pH	Total C	Total S	S- SO_4	S- Sulfide	TPA	ANC	NAPP	NAGpH	NAG to pH 4.5	NAG to pH 7.00	
				(%)				(kg H_2SO_4/t)				(kg H_2SO_4/t)		
41	SJ 0848D-029	MU	7.82	5.41	0.06	0.00	0.06	1.89	127	-125	8.46	0.00	0.00	NAF
42	SJ 0848D-030A	MU	8.94	1.37	0.02	0.00	0.02	0.61	80.1	-79.5	8.19	0.00	0.00	NAF
43	SJ 0848D-030B	MU	8.59	3.81	0.04	0.00	0.04	1.23	24.1	-22.9	6.89	0.00	0.98	NAF
44	SJ 0848D-031	MU	8.43	0.74	0.02	0.00	0.01	0.39	12.5	-12.1	7.93	0.00	0.00	NAF
45	SJ 0848D-032	N	6.41	7.74	0.20	0.01	0.19	5.95	0.78	5.16	3.26	3.92	5.68	PAF LC
46	SJ 0848D-033	N	4.05	4.16	0.40	0.05	0.34	10.5	0.00	10.5	2.97	9.51	12.4	PAF
47	SJ 0848D-034	N	3.07	6.53	2.24	0.16	2.08	63.7	0.00	63.7	2.28	57.0	63.9	PAF
48	SJ 0848D-035	N	5.86	2.27	0.67	0.01	0.67	20.4	0.20	20.2	2.92	11.5	17.8	PAF
49	SJ 0848D-036	N	3.93	2.83	0.99	0.14	0.85	25.9	0.00	25.9	2.43	27.0	30.2	PAF
50	SJ 0848D-037	N	4.07	5.18	0.54	0.03	0.52	15.8	0.00	15.8	3.05	7.25	12.2	PAF
51	SJ 0848D-038	N	2.17	7.26	3.50	0.39	3.11	95.2	0.00	95.2	2.34	83.7	90.9	PAF
52	SJ 0848D-039	N	3.75	2.52	4.51	0.14	4.36	134	0.00	134	2.07	110	116	PAF
53	SJ 0848D-040	N	4.31	2.06	1.93	0.02	1.91	58.4	0.39	58.0	2.59	35.6	54.5	PAF
54	SJ 0848D-055	N	6.78	0.94	0.02	0.00	0.02	0.48	0.59	-0.11	6.18	0.00	1.76	NAF
55	SJ 0849D-005	N	5.76	0.78	0.33	0.02	0.31	9.53	0.00	9.53	3.19	4.80	8.41	PAF
56	SJ 0849D-006	N	4.04	6.17	2.03	0.11	1.92	58.8	0.00	58.8	2.41	50.2	56.7	PAF
57	SJ 0849D-007	N	4.03	7.78	3.28	0.10	3.18	97.2	0.00	97.2	2.32	68.5	75.4	PAF
58	SJ 0849D-008	N	8.02	3.10	0.25	0.01	0.24	7.49	2.70	4.80	3.72	2.18	6.74	PAF LC
59	SJ 0849D-009	N	7.62	3.73	0.07	0.00	0.07	1.99	2.24	-0.25	4.61	0.00	1.76	NAF
60	SJ 0849D-010	N	7.13	0.60	1.99	0.07	1.92	58.8	1.40	57.4	2.49	43.4	52.2	PAF
61	SJ 0849D-011	N	7.62	3.11	0.28	0.01	0.27	8.14	0.00	8.14	3.04	5.17	9.74	PAF
62	SJ 0849D-012	N	4.42	4.01	1.55	0.07	1.49	45.5	0.00	45.5	2.46	38.5	44.6	PAF

B.3. Acid forming characteristics of 49 mudstone samples from the South Jimblebar prospect, BHPBIO.

No	Sample ID	Stratigraphy	Acid-Base Accounting								NAG Test Data			DoITR 2007, Classification
			Paste pH	Total C	Total S	S-SO4	S-Sulfide	TPA	ANC	NAPP	NAG pH	NAG to pH 4.5	NAG to pH 7.00	
				(%)				(kg H2SO4/t)				(kg H2SO4/t)		
1	SJ0772D-001	TD 3	7.17	0.08	0.02	0.00	0.02	0.58	4.88	-4.30	7.85	0.00	0.00	NAF
2	SJ0772D-002	TD 3	7.23	0.12	0.01	0.00	0.00	0.03	2.43	-2.40	7.41	0.00	0.00	NAF
3	SJ0772D-003	TD 2	7.03	0.02	0.01	0.00	0.01	0.22	2.84	-2.62	7.57	0.00	0.00	NAF
4	SJ0772D-004	TD 2	7.77	10.43	0.10	0.00	0.10	3.00	701	-698	10.1	0.00	0.00	ACM
5	SJ0772D-005	TD 2	8.03	12.55	0.12	0.00	0.12	3.79	849	-845	8.87	0.00	0.00	ACM
6	SJ0772D-006	TD 2	6.76	0.17	0.01	0.00	0.01	0.31	0.67	-0.36	7.59	0.00	0.00	NAF
7	SJ0772D-007	TD 2	6.74	0.04	0.01	0.00	0.01	0.20	0.96	-0.76	8.24	0.00	0.00	NAF
8	SJ0772D-008	TD 2	6.95	0.32	0.01	0.00	0.01	0.40	2.65	-2.25	7.56	0.00	0.00	NAF
9	SJ0772D-013	TD 2	6.00	2.50	0.45	0.01	0.45	13.7	2.25	11.4	3.38	2.06	4.31	PAF
10	SJ0772D-017	TD 2	6.27	0.48	0.04	0.00	0.04	1.09	2.45	-1.36	6.56	0.00	2.67	NAF
11	SJ0772D-021	TD 2	6.25	0.24	0.01	0.00	0.01	0.27	1.76	-1.49	6.87	0.00	0.16	NAF
12	SJ0845RD-002	TD 2	7.09	0.01	0.01	0.01	0.00	0.11	0.11	0.01	5.58	0.00	5.38	NAF
13	SJ0845RD-003	TD 2	7.01	0.24	0.00	0.00	0.00	0.06	1.50	-1.44	7.70	0.00	0.00	NAF
14	SJ0845RD-012	TD 2	5.13	0.07	0.19	0.01	0.18	5.64	0.06	5.59	3.34	3.90	7.96	PAF
15	SJ0845RD-017	TD 2	5.52	0.66	0.04	0.01	0.04	1.16	0.44	0.72	7.13	0.00	0.00	UC (NAF)
16	SJ0845RD-018	TD 2	5.53	0.09	0.04	0.00	0.04	1.28	1.35	-0.07	5.08	0.00	3.33	NAF
17	SJ0845RD-021	WA1	6.79	0.06	0.02	0.00	0.02	0.61	4.33	-3.72	7.51	0.00	0.00	NAF
18	SJ0845RD-023	WA1	6.99	0.04	0.03	0.00	0.03	0.85	1.96	-1.11	7.15	0.00	0.00	NAF
19	SJ0845RD-024	WA1	6.67	0.02	0.03	0.00	0.03	0.84	4.35	-3.51	7.10	0.00	0.00	NAF
20	SJ0845RD-025	WA1	6.84	0.04	0.01	0.00	0.00	0.10	1.54	-1.44	8.14	0.00	0.00	NAF

B.3. (Continued).

No	Sample ID	Stratigraphy	Acid-Base Data								NAG Test Data			DoITR 2007, Classification
			Paste pH	Total C	Total S	S- SO4	S- Sulfide	TPA	ANC	NAPP	NAG pH	NAG to pH 4.5	NAG to pH 7.00	
				(%)				(kg H2SO4/t)				(kg H2SO4/t)		
21	SJ0845RD-026	WA1	6.94	0.03	0.02	0.00	0.01	0.46	1.56	-1.10	7.13	0.00	0.00	NAF
22	SJ0845RD-028	WA1	6.86	0.02	0.01	0.00	0.01	0.20	1.58	-1.38	7.65	0.00	0.00	NAF
23	SJ0845RD-031	WA1	7.04	0.03	0.01	0.00	0.00	0.03	1.81	-1.78	8.10	0.00	0.00	NAF
24	SJ0845RD-033	WA1	7.01	0.03	0.01	0.01	0.00	0.13	3.94	-3.81	7.89	0.00	0.00	NAF
25	SJ0845RD-043	MN 2	7.38	0.06	0.01	0.00	0.01	0.22	4.42	-4.20	7.83	0.00	0.00	NAF
26	SJ0845RD-044	MN 1	7.33	0.04	0.02	0.00	0.01	0.36	3.61	-3.25	7.64	0.00	0.00	NAF
27	SJ 0847 D-001	TD 3	7.96	0.10	0.06	0.01	0.05	1.56	5.93	-4.37	7.72	0.00	0.00	NAF
28	SJ 0847 D-002	TD 3	7.20	0.06	0.02	0.01	0.01	0.44	5.27	-4.84	6.92	0.00	0.00	NAF
29	SJ 0847 D-003	TD 2	7.64	0.04	0.02	0.01	0.01	0.39	8.12	-7.73	8.15	0.00	0.00	NAF
30	SJ 0847 D-004	OA	7.26	0.05	0.03	0.01	0.02	0.67	4.62	-3.94	8.14	0.00	0.00	NAF
31	SJ 0847 D-005	OA	7.35	0.03	0.02	0.01	0.01	0.38	3.12	-2.74	7.32	0.00	0.00	NAF
32	SJ 0847 D-006	OA	7.44	0.05	0.03	0.00	0.03	0.79	3.41	-2.62	8.22	0.00	0.00	NAF
33	SJ 0847 D-007	OA	7.54	0.06	0.03	0.02	0.00	0.14	10.3	-10.1	8.38	0.00	0.00	NAF
34	SJ 0847 D-011	MU	6.39	0.00	0.01	0.00	0.01	0.39	3.44	-3.06	5.77	0.00	6.33	NAF
35	SJ 0847 D-154.2	MM	6.11	0.01	0.03	0.00	0.02	0.76	0.00	0.76	6.35	0.00	1.35	UC (NAF)
36	SJ 0848D-001	MN N3	6.81	0.08	0.04	0.00	0.04	1.08	2.55	-1.47	7.82	0.00	0.00	NAF
37	SJ 0848D-004	MN N1	6.76	0.08	0.01	0.00	0.00	0.13	1.18	-1.04	7.40	0.00	0.00	NAF
38	SJ 0848D-008	MN N3	7.10	0.07	0.02	0.00	0.02	0.66	0.39	0.27	6.80	0.00	0.20	UC (NAF)
39	SJ 0848D-017	MU	7.52	0.04	0.03	0.00	0.03	0.94	0.00	0.94	5.90	0.00	1.96	UC (NAF)
40	SJ 0848D-018	MU	6.11	0.06	0.01	0.00	0.01	0.17	0.00	0.17	5.74	0.00	1.76	UC (NAF)

B.3. (Continued).

No	Sample ID	Stratigraphy	Acid-Base Data								NAG Test Data			DoITR 2007, Classification
			Paste pH	Total C	Total S	S- SO4	S-Sulfide	TPA	ANC	NAPP	NAG pH	NAG to pH 4.5	NAG to pH 7.00	
				(%)				(kg H2SO4/t)				(kg H2SO4/t)		
41	SJ 0848D-041	TD 3	7.51	0.07	0.05	0.00	0.05	1.39	3.92	-2.53	5.95	0.00	3.72	NAF
42	SJ 0848D-043	OA	6.65	0.12	0.05	0.00	0.05	1.51	2.55	-1.04	6.41	0.00	1.18	NAF
43	SJ 0848D-044	MN N3	6.91	0.08	0.03	0.00	0.03	0.77	0.88	-0.12	6.55	0.00	0.39	NAF
44	SJ 0848D-048	MM	6.49	0.02	0.01	0.00	0.01	0.42	0.49	-0.07	5.88	0.00	4.12	NAF
45	SJ 0848D-051	MU	6.63	0.07	0.06	0.00	0.06	1.77	0.39	1.38	5.15	0.00	5.49	UC (NAF)
46	SJ 0849D-001	TD 3	7.36	0.02	0.05	0.00	0.05	1.41	3.45	-2.04	7.65	0.00	0.00	NAF
47	SJ 0849D-002	MN N2	5.76	0.03	0.04	0.00	0.04	1.27	4.14	-2.87	7.22	0.00	0.00	NAF
48	SJ 0849D-003	MM	7.20	0.01	0.03	0.00	0.03	0.88	2.06	-1.18	7.42	0.00	0.00	NAF
49	SJ 0849D-004	MU	7.82	0.00	0.03	0.00	0.03	0.80	7.14	-6.35	7.44	0.00	0.00	NAF

B.4. Acid-base accounting of 4 Banded Iron Formation (BIF) samples from the South Jimblebar prospect, BHPBIO.

No	Sample Code	Stratigraphy	Acid-Base Accounting								NAG Test Data			DoITR 2007, Classification
			Paste pH	Total C	Total S	$S\text{-}SO_4$	S-Sulfide	TPA	ANC	NAPP	NAG pH	NAG to pH 4.5	NAG to pH 7.00	
				%				(kg H2SO4/t)				(kg H2SO4/t)		
1	SJ 0847 D-008	OA	7.38	0.07	0.02	0.01	0.01	0.40	2.79	-2.39	6.93	0.00	0.00	NAF
2	SJ 0847 D-009	MN N2	7.13	0.02	0.01	0.00	0.01	0.43	0.00	0.43	7.05	0.00	0.00	UC (NAF)
3	SJ 0847 D-010	MN N1	6.51	0.00	0.02	0.00	0.02	0.64	0.00	0.64	7.53	0.00	0.00	UC (NAF)
4	SJ 0847 D-020	MU	6.74	0.24	0.05	0.00	0.04	1.35	0.98	0.37	4.49	0.00	0.86	PAF-LC

Appendix C

Appendix C.1. Concentration of hot acid (HNO_3: $HClO_4$) leachable major elements in 31 rock samples from the South Jimblebar prospect, BHBIO.

No	Sample ID	Litho Type	Stratigraphy	Mg	Na	Al	Si	K	P	Ca	S	Fe
				ppm								
1	SJ 0847D-035	Black Shale	MU	4,790	8.71	14,500	18.2	<0.1	<0.1	2,390	5,490	311,000
2	SJ 0847D-041	Black Shale	N	8,280	136	36,600	59.1	21,900	61.8	939	7,420	22,400
3	SJ0848D-021	Black Shale	MU	3,750	202	6,500	290	28.8	37.6	24,800	346	2,510
4	SJ0848D-023	Black Shale	MU	843	182	6,750	273	28.0	20.9	1,660	57.1	523
5	SJ0848D-024	Black Shale	MU	2,960	200	6,800	336	18.7	101	6,790	150	23,000
6	SJ0848D-025	Black Shale	MU	370	95.1	4,150	82.0	10.6	78.5	282	31.2	9,890
7	SJ0848D-026	Black Shale	MU	315	111	6,700	301	12.1	80.0	236	35.0	8,190
8	SJ0848D-027	Black Shale	MU	345	188	6,400	168	9.40	91.5	317	65.1	9,490
9	SJ0848D-028	Black Shale	MU	1,060	62.6	3,610	166	18.5	28.5	22,800	298	4,280
10	SJ0848D-029	Black Shale	MU	2,900	191	6,850	268	25.5	20.9	43,400	574	2,980
11	SJ0848D-030B	Black Shale	MU	14,500	210	6,800	309	8.40	94.0	4,150	111	618
12	SJ0848D-032	Black Shale	N	158	127	5,320	281	27.8	26.1	176	1,670	13,400
13	SJ0848D-033	Black Shale	N	106	110	5,200	90.0	15.0	9.25	131	3,340	10,100
14	SJ0848D-034	Black Shale	N	127	149	6,500	160	<0.1	16.3	172	12,190	16,200
15	SJ0848D-035	Black Shale	N	71.0	76.1	5,700	185	<0.1	29.9	98.6	4,980	19,400
16	SJ0848D-037	Black Shale	N	257	82.6	6,050	145	1,360	103	77.6	4,340	3,580
17	SJ0848D-038	Black Shale	N	583	81.6	5,700	148	3,900	50.0	70.6	16,600	9,390
18	SJ0848D-040	Black Shale	N	50.5	90.6	7,800	485	71.0	166	80.6	12,700	6,840

Appendix C.1. (Continued)

No	Sample ID	Litho Type	Stratigraphy	Mg	Na	Al	Si	K	P	Ca	S	Fe
				ppm								
1	SJ 0772D-019	Lignite	CzD 2	2,550	346	26,600	142	707	<0.1	5,250	11,700	9,090
2	SJ 0785D-005	Lignite	CzD 2	1,230	124	1,070	<0.1	<0.1	<0.1	3,170	192,000	166,000
3	SJ 0785D-003	Lignite	CzD 2	2,640	306	1,530	<0.1	219	<0.1	6,940	130,000	108,000
4	SJ 1102D-002	Lignite	CzD 2	5,140	509	93,300	179	1,670	<0.1	5,440	1,620	22,400
5	SJ 1102D-006	Lignite	CzD 2	5,200	578	114,000	232	983	<0.1	6,330	526	3,760
6	SJ 0845RDT-015	Lignite	CzD 2	852	433	139,000	128	1,530	<0.1	1,350	4,130	7,760

No	Sample ID	Litho Type	Stratigraphy	Mg	Na	Al	Si	K	P	Ca	S	Fe
				ppm								
1	SJ0848D-017	Mudstone	MU	101	97.6	4,420	149	20.6	74.0	88.1	21.8	72,000
2	SJ0848D-018	Mudstone	MU	47.0	20.5	1,190	23.3	<0.1	33.9	46.1	14.2	36,300
3	SJ0848D-041	Mudstone	CzD 3	1,120	392	6,850	274	738	132	976	78.1	204,000
4	SJ0848D-043	Mudstone	WA	763	236	6,950	108	150	317	464	125	273,000
5	SJ 0849D-002	Mudstone	MN	1,520	154	55,400	252	<0.1	1,520	424	<0.1	284,000

Appendix C.2. Concentration of hot acid (HNO_3: $HClO_4$) leachable potentially toxic elements in 31 rock samples from the South Jimblebar prospect, BHBIO.

No	Sample ID	Litho Type	Stratigraphy	Be	Sc	Ti	V	Cr	Mn	Co	Ni	Cu	Zn
				(ppm)									
1	SJ 0847D-035	Black Shale	MU	1.58	3.79	74	27.4	32.5	2,930	34.0	90.3	42.9	935
2	SJ 0847D-041	Black Shale	N	1.51	8.25	274	42.6	86.9	346	29.8	65.3	186	787
3	SJ0848D-021	Black Shale	MU	0.32	9.38	86	20.7	75.9	0.65	4.37	22.1	165	58.8
4	SJ0848D-023	Black Shale	MU	0.39	5.13	125	15.8	55.9	0.28	6.03	8.67	74.5	25.1
5	SJ0848D-024	Black Shale	MU	0.78	3.95	59.5	23.9	78.6	5.52	43.0	24.3	196	82.0
6	SJ0848D-025	Black Shale	MU	0.19	2.79	2.15	18.3	21.8	1.30	14.9	22.8	207	79.8
7	SJ0848D-026	Black Shale	MU	0.39	4.67	11.3	14.1	43.3	0.16	11.8	30.4	185	83.8
8	SJ0848D-027	Black Shale	MU	0.45	3.12	18.0	14.3	34.1	1.13	18.3	31.5	179	75.3
9	SJ0848D-028	Black Shale	MU	0.10	2.94	3.61	9.68	10.5	11.0	19.0	25.0	108	110
10	SJ0848D-029	Black Shale	MU	0.75	5.73	147	21.7	52.4	2.94	8.08	50.0	173	229
11	SJ0848D-030B	Black Shale	MU	0.74	6.48	80.7	9.48	19.4	0.39	7.68	39.2	8.39	226
12	SJ0848D-032	Black Shale	N	0.23	3.94	65.5	33.3	28.4	1.33	4.56	15.4	135	47.8
13	SJ0848D-033	Black Shale	N	0.26	2.71	75.2	28.1	34.2	0.56	12.1	11.8	105	29.4
14	SJ0848D-034	Black Shale	N	0.36	3.57	113	34.5	58.9	0.91	16.5	25.2	104	44.9
15	SJ0848D-035	Black Shale	N	0.23	1.21	15.7	25.7	17.5	0.91	11.7	16.7	39.0	25.7
16	SJ0848D-037	Black Shale	N	0.58	1.54	14.6	15.9	28.4	0.67	8.18	42.4	67.5	16.4
17	SJ0848D-038	Black Shale	N	0.41	0.94	42.8	13.2	29.3	2.44	42.2	74.0	129	24.0
18	SJ0848D-040	Black Shale	N	0.66	2.22	8.14	24.6	31.0	0.81	36.4	70.5	52.0	3,670

Appendix C.2. (Continued)

No	Sample ID	Litho Type	Stratigraphy	As	Se	Ag	Mo	Cd	Sb	Hg	Tl	Pb	Th	U
				(ppm)										
1	SJ 0847D-035	Black Shale	MU	0.71	0.47	0.19	0.63	0.24	0.04	0.15	1.29	7.03	1.63	0.31
2	SJ 0847D-041	Black Shale	N	5.53	1.08	0.25	1.41	1.80	0.02	0.40	3.05	16.3	4.13	0.84
3	SJ0848D-021	Black Shale	MU	3.05	0.37	0.25	0.01	0.02	0.02	0.14	0.03	8.15	11.9	0.70
4	SJ0848D-023	Black Shale	MU	<0.0001	0.14	0.26	<0.0001	0.01	0.01	0.05	0.01	10.4	8.28	0.37
5	SJ0848D-024	Black Shale	MU	4.33	0.36	4.52	0.08	0.03	0.05	1.07	0.02	23.3	7.26	0.97
6	SJ0848D-025	Black Shale	MU	14.3	0.42	0.55	0.05	0.03	0.00	0.31	0.01	24.3	3.66	0.59
7	SJ0848D-026	Black Shale	MU	5.95	0.32	0.06	0.04	0.05	0.01	0.06	0.01	7.25	2.85	0.99
8	SJ0848D-027	Black Shale	MU	5.95	0.57	0.06	0.03	0.06	0.01	0.28	0.01	7.50	3.16	0.78
9	SJ0848D-028	Black Shale	MU	4.19	0.49	0.01	0.03	0.15	0.01	0.91	0.00	2.59	1.60	0.30
10	SJ0848D-029	Black Shale	MU	2.73	0.41	0.84	0.01	0.03	0.02	0.15	0.04	2.65	9.48	0.92
11	SJ0848D-030B	Black Shale	MU	<0.0001	0.61	0.06	0.00	0.02	0.02	0.02	0.05	16.4	2.21	1.01
12	SJ0848D-032	Black Shale	N	5.57	4.75	0.15	0.29	0.14	0.03	0.04	0.15	8.47	2.08	1.73
13	SJ0848D-033	Black Shale	N	4.88	1.84	0.21	0.17	0.10	0.03	0.17	0.27	13.1	2.29	1.69
14	SJ0848D-034	Black Shale	N	9.85	1.64	0.48	0.34	0.13	0.04	0.15	0.29	18.2	2.44	2.75
15	SJ0848D-035	Black Shale	N	13.7	28.5	0.06	0.59	32.3	0.02	0.89	0.05	8.65	1.04	2.28
16	SJ0848D-037	Black Shale	N	1.53	1.01	0.16	0.73	0.18	0.00	0.09	0.17	68.0	2.89	0.55
17	SJ0848D-038	Black Shale	N	72.5	1.74	0.45	0.85	0.15	0.06	0.18	1.51	84.0	1.66	0.88
18	SJ0848D-040	Black Shale	N	2.52	1.03	0.04	0.22	2.60	0.02	0.66	0.58	20.3	1.97	0.99

Appendix C.2. (Continued)

No	Sample ID	Litho Type	Stratigraphy	Be	Sc	Ti	V	Cr	Mn	Co	Ni	Cu	Zn
				(ppm)									
1	SJ 0772D-016	Lignite	CzD 2	1.63	5.88	342	47.7	88.6	25.9	9.66	46.3	48.2	175
2	SJ 0772D-019	Lignite	CzD 2	0.85	4.48	314	41.2	48.5	8.47	11.2	26.8	21.5	62.0
3	SJ 0785D-005	Lignite	CzD 2	1.20	0.48	40.6	0.08	0.86	34.3	83.5	392	2.15	9.70
4	SJ 0785D-003	Lignite	CzD 2	1.71	0.32	49.9	0.49	0.82	56.6	49.0	185	3.06	<0.0001
5	SJ 1102D-002	Lignite	CzD 2	9.58	17.3	173	67.3	76.9	468	27.9	87.4	42.7	165
6	SJ 1102D-006	Lignite	CzD 2	25.0	19.8	263	136	106	101	35.4	121	83.6	88.5
7	SJ 0845RDT-015	Lignite	CzD 2	1.03	30.6	244	252	304	17.43	32.9	102	117	12.3

No	Sample ID	Litho Type	Stratigraphy	As	Se	Ag	Mo	Cd	Sb	Hg	Tl	Pb	Th	U
				(ppm)										
1	SJ 0772D-016	Lignite	CzD 2	8.19	2.24	0.06	0.79	0.20	0.13	0.14	0.19	26.1	5.12	1.79
2	SJ 0772D-019	Lignite	CzD 2	6.93	1.40	0.04	0.56	0.09	0.06	1.79	0.22	14.1	3.01	0.49
3	SJ 0785D-005	Lignite	CzD 2	558	1.14	0.00	14.5	0.03	17.3	0.47	27.9	0.16	0.17	9.46
4	SJ 0785D-003	Lignite	CzD 2	305	1.95	0.01	8.58	0.05	9.20	0.81	14.1	0.30	0.19	10.3
5	SJ 1102D-002	Lignite	CzD 2	2.70	2.82	0.04	0.12	0.26	0.02	0.05	0.19	65.2	10.1	7.06
6	SJ 1102D-006	Lignite	CzD 2	2.04	4.76	0.03	0.10	0.05	0.01	0.03	0.08	126	13.2	16.6
7	SJ 0845RDT-015	Lignite	CzD 2	5.39	1.77	0.04	0.31	0.02	<0.0001	0.03	0.14	13.8	14.2	1.93

Appendix C.2. (Continued)

No	Sample ID	Litho Type	Stratigraphy	Be	Sc	Ti	V	Cr	Mn	Co	Ni	Cu	Zn
				(ppm)									
1	SJ 0845RDT-024	Mudstone	WA	2.81	12.5	78.3	2.73	3.92	12,300	21.6	101	90.1	102
2	SJ0848D-017	Mudstone	MU	0.68	6.68	34.3	68.1	30.2	12.6	4.08	8.72	38.6	27.7
3	SJ0848D-018	Mudstone	MU	0.44	1.73	21.4	13.1	11.5	2.62	34.8	1.74	4.46	2.97
4	SJ0848D-041	Mudstone	CzD 3	0.70	10.5	131	131	221	42.3	4.98	11.6	12.8	23.8
5	SJ0848D-043	Mudstone	WA	0.82	9.33	455	26.1	28.0	1,780	8.83	21.0	49.4	25.6
6	SJ 0849D-002	Mudstone	MN	1.84	10.8	679	65.8	80.7	1,740	6.89	41.6	76.6	90.7

No	Sample ID	Litho Type	Stratigraphy	As	Se	Ag	Mo	Cd	Sb	Hg	Tl	Pb	Th	U
				(ppm)										
1	SJ 0845RDT-024	Mudstone	WA	0.80	0.72	<0.0001	0.02	<0.0001	<0.0001	0.01	0.11	0.79	8.96	1.84
2	SJ0848D-017	Mudstone	MU	7.80	0.87	0.03	0.50	0.01	0.06	0.13	0.01	16.5	3.04	0.47
3	SJ0848D-018	Mudstone	MU	2.60	0.12	0.14	0.25	0.01	0.08	3.17	0.00	14.5	0.32	0.07
4	SJ0848D-041	Mudstone	CzD 3	23.2	0.31	0.04	0.93	0.07	0.03	0.14	0.10	26.1	13.9	1.60
5	SJ0848D-043	Mudstone	WA	13.5	0.59	0.07	0.32	0.07	0.02	0.14	0.04	11.1	5.68	2.31
6	SJ 0849D-002	Mudstone	MN	17.2	0.29	0.01	2.04	0.13	0.02	0.03	0.00	4.81	8.35	4.10

Appendix C.3. Concentration of hot acid (HNO_3: $HClO_4$) leachable non-toxic elements in 31 rock samples from the South Jimblebar prospect, BHBIO.

No	Sample ID	Litho Type	Stratigraphy	Li	B	Sc	Ga	Ge	Rb	Sr	Y	Zr	Nb	Ru	Pd
				(ppm)											
1	SJ 0847D-035	Black shale	MU	1.72	<0.0001	3.79	4.01	0.70	0.17	0.33	11.1	6.31	0.12	<0.0001	0.21
2	SJ 0847D-041	Black shale	N	15.2	<0.0001	8.25	11.6	0.12	129	1.30	8.64	29.5	0.03	<0.0001	1.08
3	SJ0848D-021	Black shale	MU	2.83	5.65	9.38	7.49	0.27	0.18	27.1	5.64	4.64	0.03	0.01	0.04
4	SJ0848D-023	Black shale	MU	5.59	3.20	5.13	4.10	0.11	0.10	14.1	3.65	7.66	0.02	<0.0001	0.05
5	SJ0848D-024	Black shale	MU	2.94	3.55	3.95	5.46	0.26	0.13	18.4	5.84	10.8	0.06	<0.0001	0.08
6	SJ0848D-025	Black shale	MU	1.34	4.49	2.79	1.82	0.16	0.15	7.87	4.00	1.84	0.01	<0.0001	0.01
7	SJ0848D-026	Black shale	MU	1.41	0.55	4.67	3.66	0.15	0.12	11.52	6.44	4.57	0.02	<0.0001	0.04
8	SJ0848D-027	Black shale	MU	2.17	1.50	3.12	4.48	0.27	0.04	9.22	6.44	6.76	0.03	<0.0001	0.05
9	SJ0848D-028	Black shale	MU	1.23	1.10	2.94	1.51	0.06	0.12	6.77	6.49	1.31	0.02	<0.0001	0.01
10	SJ0848D-029	Black shale	MU	4.47	2.70	5.73	6.34	0.06	0.12	40.6	3.82	9.96	0.15	<0.0001	0.08
11	SJ0848D-030B	Black shale	MU	6.59	5.45	6.48	3.63	0.22	0.08	24.9	13.0	6.56	0.02	<0.0001	0.05
12	SJ0848D-032	Black shale	N	1.19	3.15	3.94	2.45	0.12	0.17	5.25	5.97	4.86	0.16	<0.0001	0.04
13	SJ0848D-033	Black shale	N	0.69	0.80	2.71	2.38	0.07	0.13	3.28	2.81	4.82	0.11	<0.0001	0.04
14	SJ0848D-034	Black shale	N	0.95	4.12	3.57	3.69	0.10	0.14	4.65	2.64	6.16	0.19	<0.0001	0.05
15	SJ0848D-035	Black shale	N	2.36	5.95	1.21	1.62	0.20	0.10	3.98	1.67	2.94	0.01	<0.0001	0.74
16	SJ0848D-037	Black shale	N	3.23	2.93	1.54	3.55	0.08	8.44	10.6	3.73	5.61	0.00	<0.0001	0.04
17	SJ0848D-038	Black shale	N	2.27	4.19	0.94	3.59	0.05	21.5	9.52	1.15	3.29	0.01	<0.0001	0.03
18	SJ0848D-040	Black shale	N	101	4.90	2.22	3.55	0.11	0.13	23.4	8.34	7.46	0.01	<0.0001	0.13

Appendix C.3. (Continued)

No	Sample ID	Litho Type	Stratigraphy	In	Sn	Sb	Te	Cs	Ba	La	Ce	Pr	Nd
				(ppm)									
1	SJ 0847D-035	Black shale	MU	0.04	0.18	0.04	0.13	0.05	16.9	7.15	15.1	1.73	6.98
2	SJ 0847D-041	Black shale	N	0.26	0.95	0.02	0.28	6.54	13.9	15.2	28.9	3.28	12.8
3	SJ0848D-021	Black shale	MU	0.07	0.01	0.02	0.02	0.02	5.38	70.0	135	16.0	59.5
4	SJ0848D-023	Black shale	MU	0.03	0.04	0.01	<0.0001	0.05	4.82	23.4	45.1	5.40	20.5
5	SJ0848D-024	Black shale	MU	0.08	0.08	0.05	0.04	0.03	8.03	31.7	60.2	7.22	27.6
6	SJ0848D-025	Black shale	MU	0.02	0.01	0.00	0.03	0.03	6.18	19.2	45.1	5.40	21.2
7	SJ0848D-026	Black shale	MU	0.04	0.02	0.01	0.08	0.03	6.53	20.6	43.6	5.75	23.7
8	SJ0848D-027	Black shale	MU	0.04	0.07	0.01	0.05	0.01	8.03	47.3	98.5	13.0	54.5
9	SJ0848D-028	Black shale	MU	0.01	0.00	0.01	0.03	0.02	1.86	10.2	20.3	2.57	9.94
10	SJ0848D-029	Black shale	MU	0.04	0.06	0.02	0.01	0.02	5.53	2.08	4.60	0.58	2.51
11	SJ0848D-030B	Black shale	MU	0.01	0.04	0.02	0.01	0.01	25.7	30.6	61.5	8.45	42.9
12	SJ0848D-032	Black shale	N	0.06	0.04	0.03	0.05	0.04	4.75	4.23	9.51	1.33	6.67
13	SJ0848D-033	Black shale	N	0.05	0.04	0.03	0.09	0.06	2.55	1.83	5.04	0.70	3.57
14	SJ0848D-034	Black shale	N	0.08	0.20	0.04	0.15	0.06	1.99	2.70	7.44	1.01	4.50
15	SJ0848D-035	Black shale	N	0.05	0.01	0.02	0.27	0.02	8.08	6.94	15.7	1.92	9.04
16	SJ0848D-037	Black shale	N	0.07	0.05	0.00	0.08	0.27	75.4	19.7	37.0	4.32	16.4
17	SJ0848D-038	Black shale	N	0.05	0.16	0.06	0.93	0.81	35.4	9.64	17.9	1.61	5.79
18	SJ0848D-040	Black shale	N	0.06	0.08	0.02	0.12	0.02	97.9	9.09	26.6	2.66	9.99

Appendix C.3. (Continued)

No	Sample ID	Litho Type	Stratigraphy	Dy	Ho	Er	Tm	Yb	Lu	Hf	Ta	W	Bi
				(ppm)									
1	SJ 0847D-035	Black shale	MU	1.48	0.33	0.99	0.15	0.87	0.17	0.21	0.01	5.43	0.14
2	SJ 0847D-041	Black shale	N	1.62	0.33	0.96	0.13	0.79	0.14	0.87	0.00	11.7	0.28
3	SJ0848D-021	Black shale	MU	2.14	0.23	0.82	0.09	0.60	0.09	0.15	<0.0001	0.94	0.20
4	SJ0848D-023	Black shale	MU	1.00	0.14	0.50	0.07	0.49	0.07	0.28	<0.0001	0.74	0.04
5	SJ0848D-024	Black shale	MU	1.41	0.21	0.73	0.10	0.72	0.11	0.39	<0.0001	57.8	0.35
6	SJ0848D-025	Black shale	MU	1.28	0.17	0.57	0.07	0.53	0.08	0.06	<0.0001	17.2	0.11
7	SJ0848D-026	Black shale	MU	1.69	0.24	0.72	0.08	0.57	0.08	0.14	<0.0001	3.30	0.26
8	SJ0848D-027	Black shale	MU	2.32	0.26	0.83	0.09	0.60	0.08	0.24	<0.0001	16.7	0.17
9	SJ0848D-028	Black shale	MU	1.34	0.22	0.69	0.09	0.60	0.08	0.04	<0.0001	51.3	0.09
10	SJ0848D-029	Black shale	MU	0.83	0.16	0.57	0.08	0.62	0.09	0.31	<0.0001	0.51	0.05
11	SJ0848D-030B	Black shale	MU	3.41	0.52	1.78	0.23	1.58	0.22	0.28	0.01	0.42	0.14
12	SJ0848D-032	Black shale	N	1.23	0.21	0.67	0.09	0.62	0.09	0.13	<0.0001	0.60	0.18
13	SJ0848D-033	Black shale	N	0.71	0.12	0.40	0.05	0.40	0.06	0.16	<0.0001	8.55	0.35
14	SJ0848D-034	Black shale	N	0.62	0.10	0.31	0.04	0.26	0.04	0.22	<0.0001	8.55	0.60
15	SJ0848D-035	Black shale	N	0.65	0.08	0.21	0.02	0.13	0.02	0.09	<0.0001	59.8	0.24
16	SJ0848D-037	Black shale	N	1.44	0.17	0.40	0.03	0.19	0.02	0.26	<0.0001	5.40	0.18
17	SJ0848D-038	Black shale	N	0.47	0.05	0.14	0.01	0.08	0.01	0.15	<0.0001	2.52	0.53
18	SJ0848D-040	Black shale	N	1.77	0.34	0.98	0.11	0.64	0.08	0.28	0.004	47.2	0.19

Appendix C.3. (Continued)

No	Sample ID	Litho Type	Stratigraphy	Li	B	Sc	Ga	Ge	Rb	Sr	Y	Zr	Nb	Ru	Pd
				(ppm)											
1	SJ 0772D-016	Lignite	CZD 2	3.76	<0.0001	5.88	9.20	0.18	0.96	37.1	30.4	23.1	0.25	<0.0001	0.83
2	SJ 0772D-019	Lignite	CZD 2	1.81	<0.0001	4.48	7.16	0.14	0.60	22.8	16.0	16.3	0.70	<0.0001	0.60
3	SJ 0785D-005	Lignite	CZD 2	<0.0001	<0.0001	0.48	0.58	26.9	0.13	5.14	5.36	1.82	0.04	<0.0001	0.07
4	SJ 0785D-003	Lignite	CZD 2	<0.0001	<0.0001	0.32	0.96	55.5	0.20	16.4	7.53	0.89	0.09	<0.0001	0.03
5	SJ 1102D-002	Lignite	CZD 2	14.4	<0.0001	17.3	13.8	0.36	8.51	31.8	78.1	25.8	<0.0001	<0.0001	0.86
6	SJ 1102D-006	Lignite	CZD 2	19.1	11.9	19.8	16.3	0.67	5.19	38.1	183	30.1	0.01	<0.0001	0.98
7	SJ 0845RDT-015	Lignite	CZD 2	23.6	<0.0001	30.6	31.4	0.13	0.66	7.55	22.3	37.3	0.01	<0.0001	1.26

No	Sample ID	Litho Type	Stratigraphy	In	Sn	Sb	Te	Cs	Ba	La	Ce	Pr	Nd
				(ppm)									
1	SJ 0772D-016	Lignite	CZD 2	0.08	0.61	0.13	0.01	0.17	4.06	43.5	109	6.97	23.70
2	SJ 0772D-019	Lignite	CZD 2	0.06	0.58	0.06	0.03	0.19	3.81	21.6	50.9	3.19	10.91
3	SJ 0785D-005	Lignite	CZD 2	<0.0001	<0.0001	17.33	<0.0001	0.19	0.59	1.56	3.01	0.29	1.29
4	SJ 0785D-003	Lignite	CZD 2	<0.0001	<0.0001	9.20	0.01	0.15	3.12	5.57	12.6	0.88	3.33
5	SJ 1102D-002	Lignite	CZD 2	0.06	0.33	0.02	0.01	3.26	98.8	157	290	29.4	104
6	SJ 1102D-006	Lignite	CZD 2	0.08	0.32	0.01	0.03	2.02	131	321	601	62.0	216
7	SJ 0845RDT-015	Lignite	CZD 2	0.24	0.28	<0.0001	0.00	0.06	7.02	22.1	57.3	5.55	20.5

Appendix C.3. (Continued)

No	Sample ID	Litho Type	Stratigraphy	Dy	Ho	Er	Tm	Yb	Lu	Hf	Ta	W	Bi
				(ppm)									
1	SJ 0772D-016	Lignite	CZD 2	4.31	0.96	2.74	0.38	1.99	0.32	0.87	0.01	0.84	0.32
2	SJ 0772D-019	Lignite	CZD 2	2.04	0.46	1.32	0.18	0.93	0.16	0.61	0.01	93.8	0.19
3	SJ 0785D-005	Lignite	CZD 2	0.36	0.10	0.31	0.04	0.24	0.05	0.05	0.05	16.0	0.01
4	SJ 0785D-003	Lignite	CZD 2	0.46	0.12	0.39	0.05	0.27	0.05	0.05	0.03	33.3	0.01
5	SJ 1102D-002	Lignite	CZD 2	16.1	3.10	8.40	1.11	6.08	0.93	1.04	0.05	1.08	0.37
6	SJ 1102D-006	Lignite	CZD 2	35.5	7.17	19.5	2.47	13.5	2.09	1.28	0.12	0.87	0.53
7	SJ 0845RDT-015	Lignite	CZD 2	4.72	0.96	2.55	0.33	1.75	0.25	1.29	0.02	<0.0001	0.44

No	Sample ID	Litho Type	Stratigraphy	Li	B	Sc	Ga	Ge	Rb	Sr	Y	Zr	Nb	Ru	Pd
				(ppm)											
1	SJ 0845RDT-024	Mudstone	WA	222	<0.0001	12.5	14.5	0.66	1.14	31.3	68.8	3.47	0.01	<0.0001	0.12
2	SJ0848D-017	Mudstone	MU	1.78	3.80	6.68	2.89	0.21	0.11	1.41	4.55	2.56	0.06	<0.0001	0.02
3	SJ0848D-018	Mudstone	MU	0.15	2.40	1.73	0.84	0.13	0.09	0.68	2.05	2.14	0.01	<0.0001	0.02
4	SJ0848D-041	Mudstone	CZD 3	2.98	6.10	10.5	19.6	0.40	6.44	17.0	3.56	29.8	0.08	<0.0001	0.24
5	SJ0848D-043	Mudstone	WA	3.00	2.20	9.33	6.44	0.63	1.77	7.62	9.29	24.8	0.15	0.004	0.19
6	SJ 0849D-002	Mudstone	MN	7.14	<0.0001	10.8	17.1	0.73	0.19	4.02	6.51	15.2	0.16	<0.0001	0.52

Appendix C.3. (Continued)

No	Sample ID	Litho Type	Stratigraphy	In	Sn	Sb	Te	Cs	Ba	La	Ce	Pr	Nd
				(ppm)									
1	SJ 0845RDT-024	Mudstone	WA	0.06	<0.0001	<0.0001	<0.0001	0.22	12.91	50.9	78.9	8.34	32.0
2	SJ0848D-017	Mudstone	MU	0.04	0.01	0.06	0.06	0.02	1.20	11.6	21.8	2.86	11.0
3	SJ0848D-018	Mudstone	MU	0.01	0.01	0.08	0.04	0.02	1.84	1.29	4.34	0.49	1.99
4	SJ0848D-041	Mudstone	CZD 3	0.29	0.06	0.03	0.27	0.80	48.9	4.57	11.1	1.36	5.74
5	SJ0848D-043	Mudstone	WA	0.05	0.09	0.02	0.05	0.19	9.13	6.19	17.6	1.82	7.69
6	SJ 0849D-002	Mudstone	MN	0.05	0.21	0.02	0.11	0.10	2.45	4.01	12.7	1.14	4.42

No	Sample ID	Litho Type	Stratigraphy	Dy	Ho	Er	Tm	Yb	Lu	Hf	Ta	W	Bi
				(ppm)									
1	SJ 0845RDT-024	Mudstone	WA	7.03	1.68	4.93	0.71	3.92	0.71	0.27	0.04	0.13	0.03
2	SJ0848D-017	Mudstone	MU	1.51	0.25	0.83	0.12	0.89	0.13	0.11	0.00	5.75	0.20
3	SJ0848D-018	Mudstone	MU	0.53	0.09	0.34	0.05	0.38	0.05	0.06	<0.0001	169	0.02
4	SJ0848D-041	Mudstone	CZD 3	1.05	0.18	0.56	0.08	0.51	0.07	1.28	0.01	7.15	0.86
5	SJ0848D-043	Mudstone	WA	1.85	0.36	1.21	0.17	1.18	0.17	1.07	0.01	5.40	0.30
6	SJ 0849D-002	Mudstone	MN	1.14	0.24	0.73	0.11	0.71	0.13	0.50	0.01	1.01	0.37

Appendix D

Appendix D.1. Relative percent difference of total carbon from 40 duplications of 144 rock samples of the South Jimblebar prospect, BHPBIO.

No	Sample ID	Mesurement of the total carbon (wt %)		Relative percent difference (%)
		1	2	
1	SJ0772D-003	0.0223	0.0182	5.02
2	SJ0772D-006	0.1013	0.1138	2.91
3	SJ0772D-007	0.0423	0.0355	4.35
4	SJ0772D-010	21.0464	20.2916	0.91
5	SJ0772D-011	17.7382	17.2227	0.74
6	SJ0772D-012	5.2186	5.2260	0.04
7	SJ0772D-014	28.8931	29.5543	0.57
8	SJ0772D-015	17.1115	17.3034	0.28
9	SJ0727D-016	35.4316	35.3775	0.04
10	SJ0772D-017	0.4749	0.4798	0.26
11	SJ0727D-019	36.5039	36.0852	0.29
12	SJ0772D-020	20.9544	20.2089	0.91
13	SJ0772D-022	25.7404	24.6139	1.12
14	SJ0845RDT-002	0.0134	0.0131	0.66
15	SJ0845RDT-007	0.7532	0.7205	1.11
16	SJ0845RDT-008	1.6851	1.7028	0.26
17	SJ0845RDT-009	3.0501	3.1224	0.59
18	SJ0845RDT-010	4.7888	4.7935	0.02
19	SJ0845RDT-013	4.3049	4.2365	0.40
20	SJ0845RDT-014	5.8573	5.7980	0.25
21	SJ0845RDT-017	0.6885	0.6870	0.05
22	SJ0845RDT-021	0.0414	0.0549	7.00
23	SJ0845RDT-026	0.0216	0.0306	8.57
24	SJ0845RDT-033	0.0302	0.0284	1.51
25	SJ 0847 D-001	0.0980	0.0962	0.46
26	SJ 0847 D-004	0.0540	0.0501	1.87
27	SJ 0847 D-005	0.0313	0.0320	0.59
28	SJ 0847 D-006	0.0553	0.0473	3.86
29	SJ 0847 D-007	0.0537	0.0672	5.58
30	SJ 0847 D-012	4.6713	5.4005	3.62
31	SJ 0847 D-024	4.1144	4.2229	0.65
32	SJ 0847 D-035	9.4189	9.4533	0.09
33	SJ 0848D-033	4.3354	4.4023	0.38
34	SJ 0848D-034	6.4600	6.5940	0.51
35	SJ 0848D-038	7.1944	7.3220	0.44
36	SJ 0848D-039	2.4600	2.5861	1.25
37	SJ 0848D-040	2.0030	2.1154	1.36
38	SJ 0849D-004	0.0000	0.0000	0.00
39	SJ 0849D-007	7.7637	7.7968	0.11
40	SJ 0849D-009	3.6830	3.6766	0.04
Average of relative percent difference (%)				1.47

Appendix D.2. Relative percent difference of total sulphur from 40 duplications of 144 rock samples of the South Jimblebar prospect, BHPBIO.

No	Sample ID	Measurement of the total sulphur (wt %)		Relative percent difference (%)
		1	2	
1	SJ0772D-003	0.0104	0.0093	2.64
2	SJ0772D-006	0.0121	0.0132	2.23
3	SJ0772D-007	0.0080	0.0069	3.97
4	SJ0772D-010	0.4322	0.4283	0.23
5	SJ0772D-011	0.3391	0.5000	9.59
6	SJ0772D-012	0.9527	0.9724	0.51
7	SJ0772D-014	0.6720	0.6221	1.93
8	SJ0772D-015	0.0523	0.0553	1.42
9	SJ0727D-016	0.7587	0.7260	1.10
10	SJ0772D-017	0.0483	0.0239	16.90
11	SJ0727D-019	1.4739	1.4104	1.10
12	SJ0772D-020	0.1552	0.1176	6.89
13	SJ0772D-022	0.1482	0.1937	6.65
14	SJ0845RDT-002	0.0150	0.0166	2.60
15	SJ0845RDT-007	0.1074	0.1168	2.10
16	SJ0845RDT-008	0.1392	0.1303	1.65
17	SJ0845RDT-009	0.0890	0.0911	0.59
18	SJ0845RDT-010	0.0542	0.0523	0.86
19	SJ0845RDT-013	0.0739	0.0768	0.99
20	SJ0845RDT-014	0.1242	0.1285	0.85
21	SJ0845RDT-017	0.0431	0.0412	1.12
22	SJ0845RDT-021	0.0262	0.0225	3.85
23	SJ0845RDT-026	0.0214	0.0127	12.68
24	SJ0845RDT-033	0.0116	0.0127	2.30
25	SJ 0847 D-001	0.0496	0.0549	2.50
26	SJ 0847 D-004	0.0359	0.0441	5.14
27	SJ 0847 D-005	0.0196	0.0179	2.30
28	SJ 0847 D-006	0.0220	0.0306	8.13
29	SJ 0847 D-007	0.0232	0.0259	2.76
30	SJ 0847 D-012	0.1650	0.1799	2.16
31	SJ 0847 D-024	4.1305	4.2313	0.60
32	SJ 0847 D-035	3.1923	3.1098	0.65
33	SJ 0848D-033	0.3870	0.3683	1.24
34	SJ 0848D-034	2.2168	2.2601	0.48
35	SJ 0848D-038	3.3582	3.6403	2.02
36	SJ 0848D-039	4.3395	4.6751	1.86
37	SJ 0848D-040	1.7683	2.0939	4.22
38	SJ 0849D-004	0.0228	0.0225	0.33
39	SJ 0849D-007	3.3267	3.2344	0.70
40	SJ 0849D-009	0.0582	0.0625	1.76
Average of relative percent difference (%)				**3.04**

Appendix D.3. Relative percent difference of ANC from 40 duplications of 144 rock samples of the South Jimblebar prospect, BHPBIO.

No	Sample ID	Measurement of ANC (kg H_2SO_4/t)		Relative Percent Difference (%)
		1	2	
1	SJ0772D-004	691.39	711.48	0.72
2	SJ0772D-005	847.21	850.89	0.11
3	SJ0772D-006	0.65	0.69	1.47
4	SJ0772D-007	0.95	1.44	10.25
5	SJ0772D-010	0.00	0.00	0.00
6	SJ0772D-011	3.33	3.43	0.72
7	SJ0772D-014	0.00	0.00	0.00
8	SJ0772D-015	1.37	1.46	1.56
9	SJ0727D-016	0.00	0.00	0.00
10	SJ0772D-020	0.00	0.00	0.00
11	SJ0772D-021	1.76	1.76	0.00
12	SJ0772D-022	3.82	3.17	4.70
13	SJ0845RD-002	0.07	0.09	6.25
14	SJ0845RD-007	2.60	2.41	1.86
15	SJ0845RD-010	0.78	0.72	2.29
16	SJ0845RD-013	0.00	0.00	0.00
17	SJ0845RD-014	0.00	0.00	0.00
18	SJ0845RD-015	0.00	0.00	0.00
19	SJ0845RD-017	0.28	0.60	17.78
20	SJ0847 D-011	3.46	3.43	0.21
21	SJ0847 D-012	0.67	0.05	43.15
22	SJ0847 D-019	0.00	0.00	0.00
23	SJ0847 D-021	0.00	0.00	0.00
24	SJ0847 D-024	56.84	54.51	1.05
25	SJ0847 D-025	12.81	12.61	0.39
26	SJ0847 D-028	7.35	6.61	2.63
27	SJ0847 D-032	16.14	17.63	2.21
28	SJ0847 D-033	18.50	17.05	2.04
29	SJ0847 D-035	62.35	59.41	1.21
30	SJ0847 D-038	0.00	0.00	0.00
31	SJ0847 D-045	2.73	2.21	5.36
32	SJ0848D-021	70.32	70.93	0.22
33	SJ0848D-024	19.70	18.91	1.02
34	SJ0848D-028	60.88	61.50	0.25
35	SJ0848D-029	127.40	126.18	0.24
36	SJ0848D-030B	24.11	21.66	2.68
37	SJ0848D-032	0.59	0.98	12.50
38	SJ0848D-033	0.00	0.00	0.00
39	SJ0848D-038	0.00	0.00	0.00
40	SJ0849D-007	0.00	0.00	0.00
41	SJ0849D-009	2.64	2.20	4.56
Average of relative percent difference (%)				**3.11**

Appendix D.4. Relative percent difference of NAG testing from 58 duplications of 144 rock samples of the South Jimblebar prospect, BHPBIO.

No	Sampel ID	Measurement of NAG pH		Relative percent difference of NAG pH (%)	Measurement of NAG acidity pH 7.0 (kg H_2SO_4/t)		Relative percent difference of NAG Acidity (%)
		1	2		1	2	
1	SJ077D2-004	10.51	9.73	1.93			
2	SJ0772D-005	8.93	8.81	0.34			
3	SJ0772D-007	8.29	8.19	0.30			
4	SJ0772D-008	7.00	8.11	3.67			
5	SJ0772D-010	8.27	8.29	0.06			
6	SJ0772D-011	8.29	7.79	1.55			
7	SJ0772D-012	2.98	2.87	0.94	20.07	23.13	3.54
8	SJ0772D-013	3.38	3.68	2.12	5.49	3.14	13.64
9	SJ0772D-014	8.77	8.83	0.17			
10	SJ0772D-015	8.79	8.65	0.40			
11	SJ0772D-016	8.39	8.51	0.36			
12	SJ0772D-017	6.56	6.64	0.30	2.82	2.51	2.94
13	SJ0772D-018	9.17	8.26	2.61			
14	SJ0772D-019	3.56	3.20	2.66	16.07	21.83	7.60
15	SJ0772D-020	8.65	8.67	0.06			
16	SJ0772D-022	9.84	9.37	1.22			
17	SJ0785D-003	1.89	2.33	5.21	603.48	594.37	0.38
18	SJ0785D-005	1.82	2.13	3.92	1011.95	996.66	0.38
19	SJ0845RDT-002	5.44	5.71	1.21	5.61	5.15	2.09
20	SJ0845RDT-008	4.75	4.72	0.16	1.94	1.94	0.00

Appendix D.4. (Continued)

No	Sampel ID	Measurement of NAG pH		Relative Percent Difference (%)	Measurement of NAG Acidity pH 7.0 (kg H_2SO_4/t)		Relative Percent Difference (%)
		1	2		1	2	
21	SJ0845RDT-013	7.01	7.15	0.49			
22	SJ0845RDT-014	6.70	6.60	0.38	0.39	0.31	5.56
23	SJ0845RDT-015	3.19	3.12	0.55	16.23	16.15	0.12
24	SJ0845RDT-017	7.01	7.25	0.84			
25	SJ0845RDT-028	7.65	7.55	0.33			
26	SJ0845RDT-031	8.10	8.07	0.09			
27	SJ 0847D-019	2.18	2.08	1.17	92.12	90.94	0.32
28	SJ 0847D-024	2.29	2.31	0.22	74.56	75.89	0.44
29	SJ0847D-029	3.14	3.07	0.56	44.37	42.38	1.15
30	SJ0847D-030	2.36	2.44	0.83	71.23	68.52	0.97
31	SJ0847D-031	7.58	7.59	0.03			
32	SJ0847D-032	2.40	2.41	0.10	74.99	74.48	0.17
33	SJ0847D-033	2.5	2.5	0.00	64.64	64.48	0.06
34	SJ0847D-034	7.06	7.15	0.32			
35	SJ0847D-035	3.73	3.75	0.13	67.74	65.90	0.69
36	SJ0847D-037	2.50	2.37	1.33	51.35	60.37	4.04
37	SJ0847D-038	2.09	2.06	0.36	203.06	200.55	0.31
38	SJ0847D-039	2.21	2.23	0.23	85.61	85.46	0.05
39	SJ0847D-040	2.19	2.20	0.11	562.03	570.65	0.38
40	SJ0847D-041	2.56	2.55	0.10	49.98	50.41	0.21

Appendix D.4. (Continued)

No	Sampel ID	Measurement of NAG pH		Relative Percent Difference (%)	Measurement of NAG Acidity pH 7.0 (kg H_2SO_4/t)		Relative Percent Difference (%)
		1	2		1	2	
41	SJ0847D-042	2.4	2.4	0.00	239.61	242.45	0.29
42	SJ0847D-043	1.96	1.96	0.00	184.63	186.20	0.21
43	SJ0847D-044	2.41	2.41	0.00	68.68	69.23	0.20
44	SJ0847D-045	2.27	2.26	0.11	77.69	77.93	0.08
45	SJ0848D-021	7.28	7.77	1.63			
46	SJ0848D-024	8.01	7.65	1.15			
47	SJ0848D-027	7.15	6.62	1.92	0.00	0.78	50.0
48	SJ0848D-029	8.41	8.50	0.27			
49	SJ0848D-033	3.01	2.93	0.67	12.35	12.54	0.39
50	SJ0848D-035	2.97	2.86	0.94	17.64	18.03	0.55
51	SJ0848D-036	2.46	2.40	0.62	29.99	30.38	0.32
52	SJ0848D-039	2.06	2.08	0.24	118.07	113.92	0.90
53	SJ0848D-041	5.74	6.15	1.72	4.90	2.55	15.8
54	SJ0849D-006	2.41	2.39	0.21	55.39	57.98	1.14
55	SJ0849D-007	2.32	2.31	0.11	75.26	75.62	0.12
56	SJ0849D-010	2.49	2.49	0.00	53.31	51.16	1.03
57	SJ0849D-012	2.46	2.47	0.10	44.81	44.34	0.26
58	SJ1102D-002	7.51	7.49	0.07			
Average of relative percent difference (%)				0.81	Average of relative percent difference (%)		3.23

Note : Sample with NAG pH >7.0 is considered having NAG acidity 0.00 kg H_2SO_4/t.

Appendix D.5. Relative percent difference of element concentrations from 3 duplications of 31 rock samples of the South Jimblebar prospect, BHPBIO

No	Elements	Element Concentration of sample SJ0848D-024 (ppm)		Relative percent difference (%)	Element Concentration of sample SJ0848D-024 (ppm)		Relative percent difference (%)	Element Concentration of sample SJ0848D-024 (ppm)		Relative percent difference (%)
		1	2		1	2		1	2	
1	Li	3.12	2.77	2.97	1.06	1.32	5.57	210	235	2.86
2	Be	0.82	0.74	2.56	0.21	0.25	4.98	2.68	2.93	2.23
3	B	4.05	3.05	7.04	0.05	6.25	49.2	<0.0001	<0.0001	0.00
4	Mg	3198	2723	4.01	154	162	1.27	2415	2450	0.36
5	Na	215	185	3.69	120	134	2.76	276	286	0.81
6	Al	6895	6695	0.74	4945	5695	3.52	57568	60256	1.14
7	Si	460	212	18.5	290	273	1.51	580	211	23.4
8	K	20.0	17.5	3.27	34.2	21.5	11.4	674	721	1.69
9	P	109	94.0	3.58	24.2	28.0	3.60	889	967	2.10
10	Ca	7341	6241	4.05	174	179	0.64	847	864	0.50
11	S	162.60	138.10	4.07	1189	2154	14.4	<0.0001	<0.0001	0.00
12	Sc	4.26	3.64	3.92	3.92	3.97	0.35	12.4	12.6	0.25
13	Ti	64.2	54.7	3.99	57.2	73.7	6.30	81.0	75.6	1.70
14	V	25.8	22.0	4.03	31.1	35.6	3.37	3.16	2.31	7.81
15	Cr	83.87	73.37	3.34	25.7	31.2	4.79	4.46	3.37	7.01
16	Mn	6.05	5.00	4.76	1.38	1.28	1.88	12214	12366	0.31
17	Fe	24938	21138	4.12	12588	14138	2.90	259611	260184	0.06
18	Co	46.5	39.5	4.04	4.09	5.03	5.13	21.11	22.12	1.16
19	Ni	26.2	22.3	4.02	13.7	17.2	5.75	98.7	103	1.18
20	Cu	211	181	3.82	94.0	177	15.3	89.0	91.2	0.59
21	Zn	88.8	75.3	4.12	46.5	49.1	1.33	100	103	0.67
22	Ga	5.79	5.14	2.97	2.09	2.82	7.38	14.1	14.9	1.32

Appendix D.5. (Continued)

No	Elements	Element Concentration of sample SJ0848D-024 (ppm)		Relative percent difference (%)	Element Concentration of sample SJ0848D-024 (ppm)		Relative percent difference (%)	Element Concentration of sample SJ0848D-024 (ppm)		Relative percent difference (%)
		1	2		1	2		1	2	
23	Ge	0.28	0.24	4.14	0.10	0.13	7.23	0.66	0.66	0.13
24	As	4.65	4.01	3.70	5.35	5.80	2.02	0.85	0.75	3.08
25	Se	0.35	0.37	1.31	3.20	6.31	16.3	0.71	0.74	1.13
26	Rb	0.16	0.10	11.3	0.15	0.18	3.96	1.13	1.15	0.46
27	Sr	19.8	17.0	3.87	4.87	5.62	3.57	30.9	31.6	0.58
28	Y	6.24	5.44	3.42	5.79	6.14	1.47	68.6	68.9	0.13
29	Zr	11.4	10.2	2.90	4.72	5.01	1.49	2.31	4.64	16.7
30	Nb	0.07	0.05	11.5	0.17	0.15	3.42	0.01	0.01	4.30
31	Mo	0.10	0.07	9.88	0.28	0.30	1.74	0.02	0.01	17.2
32	Ru	<0.0001	<0.0001	0.00	<0.0001	<0.0001	0.00	<0.0001	<0.0001	0.00
33	Pd	0.09	0.08	4.22	0.04	0.04	0.77	0.08	0.17	17.5
34	Ag	4.96	4.09	4.81	0.11	0.18	12.8	<0.0001	<0.0001	0.00
35	Cd	0.04	0.03	4.29	0.14	0.15	3.21	0.11	0.13	3.61
36	In	0.08	0.07	3.92	0.05	0.06	3.25	0.06	0.06	0.30
37	Sn	0.08	0.07	3.51	0.04	0.05	6.30	<0.0001	<0.0001	0.00
38	Sb	0.07	0.04	15.2	0.03	0.03	2.34	<0.0001	<0.0001	0.00
39	Te	0.04	0.03	6.23	0.05	0.06	4.67	<0.0001	<0.0001	0.00
40	Cs	0.04	0.02	9.39	0.03	0.04	4.68	0.21	0.22	1.24
41	Ba	8.68	7.38	4.05	4.28	5.23	4.97	12.8	13.0	0.47
42	La	33.8	29.5	3.36	3.86	4.59	4.35	50.2	51.6	0.68
43	Ce	64.5	56.0	3.53	8.54	10.5	5.12	76.6	81.2	1.45
44	Pr	7.75	6.70	3.63	1.18	1.48	5.65	8.11	8.57	1.38

Appendix D.5. (Continued)

No	Elements	Element Concentration of sample SJ0848D-024 (ppm)		Relative percent difference (%)	Element Concentration of sample SJ0848D-024 (ppm)		Relative percent difference (%)	Element Concentration of sample SJ0848D-024 (ppm)		Relative percent difference (%)
		1	2		1	2		1	2	
45	Nd	29.5	25.6	3.53	5.84	7.49	6.19	31.4	32.6	0.91
46	Eu	1.02	0.89	3.27	0.61	0.75	4.96	2.08	2.16	0.91
47	Sm	4.35	3.70	4.01	1.68	2.05	4.95	5.93	6.21	1.18
48	Gd	3.67	3.13	3.93	1.81	2.15	4.29	6.11	6.37	1.04
49	Tb	0.29	0.25	3.52	0.20	0.23	2.89	1.28	1.34	1.10
50	Dy	1.52	1.30	3.81	1.16	1.30	2.84	6.95	7.10	0.56
51	Ho	0.22	0.20	2.78	0.20	0.22	2.84	1.65	1.71	0.92
52	Er	0.78	0.68	3.41	0.64	0.70	2.23	4.80	5.05	1.28
53	Tm	0.10	0.09	3.61	0.09	0.09	0.97	0.69	0.72	0.99
54	Yb	0.77	0.67	3.48	0.60	0.64	1.62	3.84	4.00	1.03
55	Lu	0.11	0.10	3.66	0.09	0.09	1.93	0.70	0.73	1.05
56	Hf	0.40	0.37	1.78	0.12	0.14	3.09	0.20	0.34	13.4
57	Ta	<0.0001	<0.0001	0.00	<0.0001	<0.0001	0.00	0.04	0.04	0.87
58	W	63.30	52.30	4.76	0.53	0.68	6.01	0.11	0.15	8.15
59	Hg	1.19	0.94	5.75	0.04	0.05	8.62	0.02	0.01	20.1
60	TI	0.03	0.02	8.78	0.11	0.19	12.4	0.10	0.12	2.95
61	Pb	24.6	22.0	2.73	7.35	9.60	6.64	0.70	0.88	5.54
62	Bi	0.37	0.33	3.16	0.19	0.18	1.63	0.03	0.04	11.7
63	Th	7.83	6.68	3.96	2.01	2.15	1.68	8.74	9.17	1.22
64	U	1.04	0.89	4.02	1.69	1.77	1.15	1.80	1.89	1.22
Average of each sample				**4.53**			**5.15**			**3.18**
Average of all the samples				**4.29**						